

IDENTIFICATION OF COMPONENTS REQUIRED FOR MITOPHAGY AND MITOCHONDRIAL INHERITANCE BY GENETIC SCREENS IN YEAST

Dissertation

zur Erlangung des akademischen Grades

eines Doktors der Naturwissenschaften

- Dr. rer. nat. -

an der Bayreuther Graduiertenschule für Mathematik und

Naturwissenschaften (BayNAT) der Universität Bayreuth

vorgelegt von

Stefan Böckler

aus Feuchtwangen

Bayreuth, 2015

Die vorliegende Arbeit wurde in der Zeit von März 2011 bis Februar 2015 in Bayreuth am Institut für Zellbiologie unter Betreuung von Herrn Professor Dr. Benedikt Westermann angefertigt.

Vollständiger Abdruck der von der Bayreuther Graduiertenschule für Mathematik und Naturwissenschaften (BayNAT) der Universität Bayreuth genehmigten Dissertation zur Erlangung des akademischen Grades eines Doktors der Naturwissenschaften (Dr. rer. nat.).

Dissertation eingereicht am: 17.02.2015

Zulassung durch das Leitungsgremium: 03.03.2015

Wissenschaftliches Kolloquium: 27.07.2015

Amtierender Direktor: Prof. Dr. Franz Xaver Schmid

Prüfungsausschuss:

Prof. Dr. Benedikt Westermann	(Erstgutachter)
Prof. Dr. Olaf Stemmann	(Zweitgutachter)
Prof. Dr. Stephan Clemens	(Vorsitz)
Prof. Dr. Matthias Weiss	
(Drittgutachter: Prof. Dr. Johannes Herrmann)	

Table of contents

Table of contents	III
Abbreviations.....	VI
Summary	VIII
Zusammenfassung.....	IX
Introduction.....	1
The mitochondrial life cycle	1
Mitochondrial contacts with other organelles	3
Mitochondrial transport and partitioning	7
Autophagy.....	11
The selective degradation of mitochondria by mitophagy	13
Functional genetics in yeast	16
Aim of this thesis.....	19
Results	20
Mitochondrial ER contacts are the sites of mitophagosome biogenesis	20
Respiratory activity is not necessary for mitophagy	20
Screening of respiratory-deficient mutants for altered mitophagy	22
Mutants lacking the ER-mitochondria tetherERMES have a mitophagy defect.....	24
ERMES mutants show no defect in bulk autophagy and the Cvt pathway	26
Altered mitochondrial mass or membrane biogenesis are not the cause of aberrant mitophagy in ERMES mutants	28
Mitophagy in ERMES mutants is not compromised due to misshapen mitochondria	29
Deletion of <i>DNM1</i> in an ERMES mutant background has no additional influence on mitophagy	31
Artificial mitochondrial ER tethering promotes mitophagy in the absence of ERMES	33
Mitophagosomes form at ER-mitochondria contact sites	35
Mmm1 interacts with Atg8 in vivo independent of Atg8 lipidation.....	36
ERMES is dispensable for mitochondrial localization of Atg8	39
Mitochondrial ER contacts are important for the formation of the mitophagophore	40

Mitophagophore biogenesis is rescued by artificial ER-mitochondria tethering but not by restoring normal mitochondrial morphology.....	42
ERMES is important for the localization of Atg9 to mitochondria	44
Artificial mitochondrial localization of a peroxisome-specific autophagy receptor complements the mitophagy defect in ERMES mutants.....	45
Mapping the genetic interactome of the mitochondrial inheritance mutant <i>myo2(LQ)</i>	48
Genomic integration of the <i>myo2(LQ)</i> mutations leads to reduced growth, diminished mitochondrial inheritance and synthetic lethality with <i>Δypt11</i>	48
Synthetic genetic array analysis with <i>myo2(LQ)</i>	50
<i>myo2(LQ) Δnum1</i> mutants are synthetic sick	53
The growth phenotype of <i>myo2(LQ) Δnum1</i> is caused by a nuclear migration defect rather than a mitochondrial deficit	54
Mutants with disturbed mitochondrial dynamics genetically interact with <i>myo2(LQ)</i>	57
Dnm1 depletion alleviates the mitochondrial inheritance defect of <i>myo2(LQ)</i>	59
Mitochondrial inheritance is blocked in <i>myo2(LQ) fzo1</i> mutants.....	60
Fragmentation of mitochondria leads to impaired mitochondrial inheritance	62
Discussion and outlook.....	64
The role of mitochondrial ER contacts in mitophagy	64
ERMES-mediated mitophagophore biogenesis.....	64
ER-assisted mitochondrial division and mitophagy.....	66
ER association as a prerequisite for organellophagy	68
Genetic interactions of <i>myo2(LQ)</i>	70
Organelle specificity of <i>myo2(LQ)</i>	70
Significance of genetic interactions between components of mitochondrial dynamics and <i>myo2(LQ)</i>	71
Materials and methods.....	74
Molecular biology.....	74
Plasmids and primers	74
Yeast genetics and cell biology	78
Yeast strains.....	78
Culturing and media	79
Transformation of plasmids	80

Drop dilution assay	80
Construction of diploid cells and tetrad dissection	81
Quantification of colony size	81
Synthetic genetic array	81
SGA data acquisition.....	82
Functional enrichment analysis of GO terms	82
Fluorescence microscopy	82
Staining of cellular structures.....	83
Protein biochemistry	83
Preparation of cell extracts	83
SDS-PAGE, Western blotting, immuno-detection and antibodies	83
Shock-freezing of cells and cryo-grinding.....	84
Immuno-precipitation	85
References	86
Acknowledgments.....	103
Appendix	104
The <i>pet</i> library	104
Genetic interactors of <i>myo2(LQ)</i>.....	107
List of publications.....	110
DVD	111
Erklärung.....	112

Abbreviations

AIM	Atg8-family interacting motif	MDV	Mitochondrion-derived vesicle
ALS	Amyotrophic lateral sclerosis	MECA	Mitochondria–ER–cortex anchor
AP	Autophagosome	MIM	Mitochondrial inner membrane
Atg	Autophagy related	MOM	Mitochondrial outer membrane
BiFC	Bimolecular fluorescence complementation	MSG	Mono-sodium glutamate
CBD	Cargo binding domain	mtDNA	Mitochondrial DNA
cER	Cortical endoplasmic reticulum	mtGFP	Mitochondria-targeted green fluorescent protein
chiMERA	Construct in helping mitochondrion-ER association	mtRFP	Mitochondria-targeted red fluorescent protein
Co-IP	Co-immunoprecipitation	MTS	Mitochondria-targeting sequence
Cvt	Cytoplasm-to-vacuole targeting	n.s.	Not significant
D	Dextrose	OE	Overexpression
DAPI	4',6-Diamidin-2-phenylindol	ORF	Open reading frame
DIC	Differential interference contrast	PAP	Peroxidase Anti-Peroxidase
EM	Electron microscopy	PAS	Phagophore assembly site
EMC	ER membrane complex	PCA	Protein-fragment complementation assay
ERES	ER exit site	PD	Parkinson's Disease
(E)RFP	(Enhanced) red fluorescent protein	PDB	Protein data base
ERMD	ER-assisted mitochondrial division	PE	Phosphatidylethanolamine
ERMES	ER-mitochondria encounter structure	PH	Pleckstrin homology
Gal	Galactose	PI3K	Phosphatidylinositol-3-kinase
HDA	High-density array	PM	Plasma membrane
IM	Isolation membrane	ProtA	Protein A
IMS	Intermembrane space	PtdIns3P	Phosphatidylinositol-3- phosphate
LIR	LC3 interacting region	PtdIns(4,5)P₂	Phosphatidylinositol 4,5- bisphosphate
MAPK	Mitogen-activated protein kinase	R	Raffinose
		rcf	Relative centrifugal force

ROS	Reactive oxygen species
SAGA	Spt-Ada-Gcn5-acetyltransferase
SC	Synthetic complete
SD	Standard deviation
SD-N	Synthetic dextrose medium without nitrogen
SGA	Synthetic genetic array
SGD	Saccharomyces genome database
SM	Synthetic minimal
SNARE	Soluble N-ethylmaleimide-sensitive-factor attachment receptor
TOM	Translocase of the outer membrane
TOR	Target of rapamycin
TULIP	Tubular lipid-binding
VICS	Vacuole-isolation membrane contact site
Y_C	C-terminal fragment of YFP
YFG	Your favourite gene
YFP	Yellow fluorescent protein
YKO	Yeast knock-out
Y_N	N-terminal fragment of YFP
YNB	Yeast nitrogen base
YPD	Yeast peptone dextrose
YPG	Yeast peptone glycerol

Summary

Mitochondria are membrane-bounded organelles, which are important for diverse cellular and physiological processes such as energy production by oxidative phosphorylation. Loss of functional mitochondria can lead to cell death and is associated with neurodegenerative diseases like Parkinson's disease and amyotrophic lateral sclerosis. In order to execute their tasks, mitochondria have to communicate and interact with different cellular structures including other organelles and the cytoskeleton.

In the first part of this study, it is shown that the contacts between the endoplasmic reticulum (ER) and mitochondria are important for the mitochondrial turnover by autophagy, also called mitophagy. Mitophagy is a process ensuring the appropriate quality and quantity of mitochondria by sequestering a mitochondrion within a double membrane and delivering it to degradative organelles. Failed mitophagy in neurons is supposed to result in accumulation of dysfunctional mitochondria and ultimately to neurodegeneration. By screening a collection of several hundred yeast mutants for defective mitochondrial autophagy, the four mutants lacking the ER-mitochondria encounter structure (ERMES), which connects ER and mitochondria, were found to have a decreased rate of mitophagy. Strikingly, artificial tethering of mitochondria and ER by a chimeric protein restores mitophagy in the ERMES mutants, indicating that loss of spatial proximity between the two organelles is the main cause of the mitophagy deficit. Moreover, one of the ERMES subunits interacts with the autophagic membrane expansion factor Atg8, which suggests that ERMES plays a role during growth of this membrane. Consequently, ERMES mutants show aberrant autophagic membrane structures, which can again be rescued by artificial mitochondria-ER tethering. It can thus be hypothesized that ERMES mediates the spatial proximity between mitochondria, the membrane expansion factor Atg8 and the ER, and that ERMES thereby promotes lipid flux from the ER to the autophagic membrane.

In the second part, a genetic screen revealed that mitochondrial dynamics is important for the inheritance of mitochondria into the daughter cell. In yeast, mitochondria are transported along the actin cytoskeleton by the myosin V motor protein Myo2. The mutant *myo2(LQ)* allele carries two amino acid substitutions resulting in impaired mitochondrial motility. By introducing this allele into yeast deletion mutants on a genome-wide scale by synthetic genetic array technology, it was shown that mutants lacking fusion-competent mitochondria heavily depend on a functional transport machinery, since otherwise mitochondria are not transported into the daughter cell. However, if mitochondrial division is blocked in the *myo2(LQ)* mutant, mitochondrial inheritance is restored, indicating that mitochondrial dynamics regulates the amount of mitochondria that is transported into the bud.

In sum, this study provides new insights into how the interplay of mitochondria with different cellular structures orchestrates mitochondrial behavior.

Zusammenfassung

Mitochondrien sind membranumschlossene Organellen, die für zahlreiche zelluläre und physiologische Prozesse wichtig sind. Der Verlust funktioneller Mitochondrien kann zum Zelltod führen und ist mit neurodegenerativen Krankheiten wie Parkinson und amyotropher Lateralsklerose assoziiert. Um ihre Aufgaben zu bewältigen, müssen Mitochondrien mit verschiedenen zellulären Strukturen, wie anderen Organellen oder dem Zytoskelett, kommunizieren und interagieren.

Im ersten Teil dieser Arbeit wird gezeigt, dass Kontakte zwischen dem endoplasmatischen Retikulum und Mitochondrien wichtig für den mitochondrialen Abbau über Autophagie sind, der auch als Mitophagie bezeichnet wird. Mitophagie stellt sicher, dass Mitochondrien in angemessener Anzahl und Qualität vorhanden sind, indem Mitochondrien in einer Doppelmembran eingeschlossen und in abbaubare Organellen transportiert werden. Man geht davon aus, dass der Verlust der Fähigkeit zur Mitophagie in Neuronen dazu führt, dass nicht-funktionelle Mitochondrien akkumulieren, was schließlich in Neurodegeneration resultiert. Indem mehrere hundert Hefemutanten hinsichtlich veränderter Mitophagieraten untersucht wurden, konnten vier Mutanten als Mitophagie-defizient identifiziert werden, denen die *ER-mitochondrion encounter structure* (ERMES) fehlt, welche ER und Mitochondrien verbindet. Erstaunlicherweise konnte dieser Defekt gerettet werden, indem mittels eines chimären Proteins die mitochondrialen ER-Kontakte wieder künstlich hergestellt wurden. Dies deutet darauf hin, dass der Verlust der räumlichen Nähe zwischen den beiden Organellen der Hauptgrund für das Mitophagie-Defizit ist. Zudem interagiert eine der ERMES-Untereinheiten mit dem Autophagie-Membranexpansionsfaktor Atg8, was nahelegt, dass der ERMES-Komplex eine Rolle beim Wachstum von Autophagiemembranen spielt. Dementsprechend zeigen ERMES-Mutanten veränderte Autophagiemembran-Strukturen, die wiederum durch künstliche ER-Mitochondrien-Verbindungen wiederhergestellt werden können. Deshalb kann angenommen werden, dass der ERMES-Komplex die räumliche Nähe zwischen Mitochondrien, dem Membranexpansionsfaktor Atg8 und dem ER herstellt, wodurch der Komplex den Lipidfluss vom ER zur Autophagiemembran unterstützt.

Im zweiten Teil wurde ein genetisches Screening durchgeführt, welches zeigte, dass die mitochondriale Dynamik wichtig für die Vererbung von Mitochondrien an die Tochterzelle ist. In Hefe werden Mitochondrien entlang des Aktin-Zytoskeletts über das Klasse V Myosin-Motorprotein Myo2 transportiert. Das mutante *myo2(LQ)* Allel führt zu reduzierter mitochondrialer Beweglichkeit. Indem dieses Allel genomweit über *synthetic genetic array*-Technologie in Hefedeletionsmutanten eingeführt wurde, konnte gezeigt werden, dass Hefen ohne fusionskompetente Mitochondrien stark von einer funktionellen Transportmaschinerie abhängen, da ansonsten Mitochondrien nicht in die Tochterzelle transportiert werden können. Wenn allerdings die mitochondriale Teilung in der *myo2(LQ)* Mutante unterbunden wird, führt dies zu verbesserter mitochondrialer Vererbung. Dies deutet darauf hin, dass die mitochondriale Dynamik die Menge an Mitochondrien reguliert, die in die Tochterzelle transportiert wird.

Zusammengefasst bietet diese Arbeit neue Einsichten, wie das Zusammenspiel von Mitochondrien mit verschiedenen zellulären Strukturen das Verhalten von Mitochondrien beeinflusst.

Introduction

The mitochondrial life cycle

Mitochondria are semi-autonomous organelles. They derived from an α -proteobacterial ancestor, which was taken up by a phagocytic archaea-like host cell. The prey survived the feast and was integrated into the host cell's physiology (Gray et al., 1999). The prey's genome was reduced and most of its genes were transferred to the host nucleus. Nowadays, mitochondrial DNA (mtDNA) codes only for few RNAs and proteins in most organisms. Accordingly, the majority of mitochondrial proteins has to be imported from the cytosol (Reichert and Neupert, 2004). To this end, mitochondria contain a sophisticated system of import machineries which recognize their substrates and transfer them to their destination within the organelle (Schmidt et al., 2010).

Mitochondria consist of several distinct compartments (Frey and Mannella, 2000). Mitochondria are surrounded by the mitochondrial outer membrane (MOM), which encloses the inter membrane space (IMS) lying between MOM and mitochondrial inner membrane (MIM; Figure 1A). The MIM invaginates into cristae, the lumen of which is continuous to the IMS and which are connected to it by cristae junctions. ATP is generated by oxidative phosphorylation at the cristae membrane since the electron transport chain complexes and the ATP synthase reside there (Vogel et al., 2006; Wurm and Jakobs, 2006). Enclosed by the MIM is the mitochondrial matrix, where the mtDNA is packed into nucleoids, iron-sulfur clusters are synthesized and the citric acid cycle takes place, to name only some of the most prominent features.

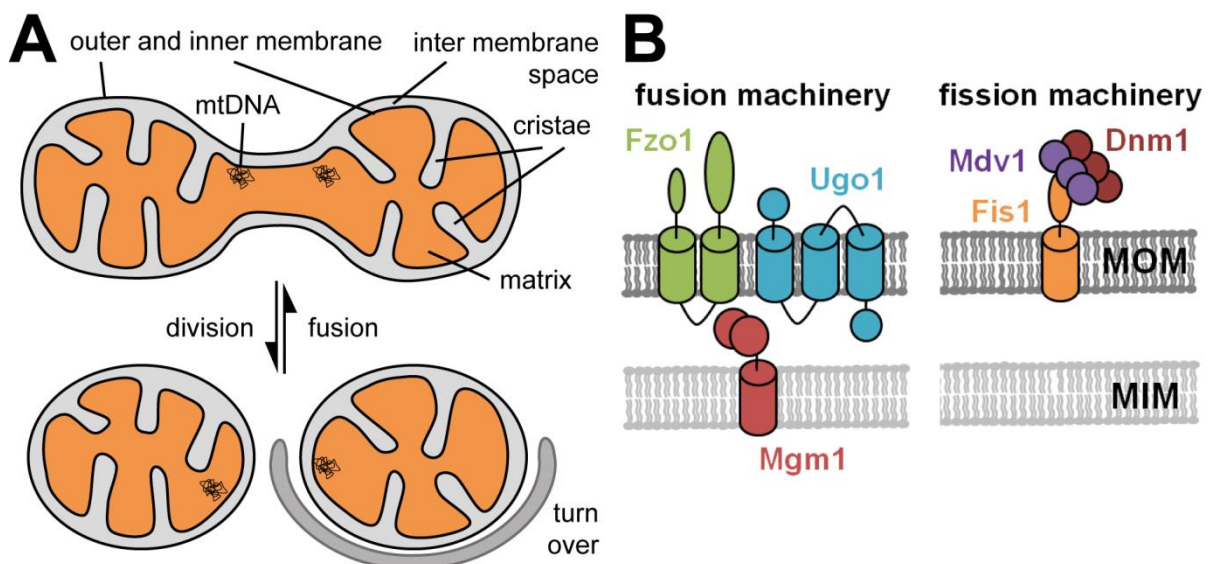


Figure 1. The mitochondrial life cycle. (A) Schematic representation of a mitochondrion, which divides into two daughter units. One unit can then be sequestered by a double-membraned autophagic vesicle and turned over. If this does not happen, the two mitochondria can fuse. **(B)** Schematic representation of the basic components of mitochondrial fusion (left) and division (right) in yeast. MOM, mitochondrial outer membrane; MIM, mitochondrial inner membrane.

Cells benefit from mitochondria in various ways. Efficient energy generation relies on oxidative phosphorylation in the MIM and cells depend on proteins containing iron-sulfur clusters, which are exclusively assembled in mitochondria (Lill and Mühlenhoff, 2005). Furthermore, mitochondria are involved in calcium signaling (Rizzuto et al., 2012), programmed cell death (Tait and Green, 2010), oxidation of fatty acids (Kunau et al., 1995) and cell cycle regulation (McBride et al., 2006).

Another characteristic trait of mitochondria is their dynamic nature. Like many membrane-bounded organelles, mitochondria cannot form *de novo*. This results in the necessity to grow by import of proteins and lipids and to multiply by fission, which is reminiscent of the bacterial ancestry of mitochondria. Whilst bacterial cell division machineries assemble on the inside of the cell, the mitochondrial fission machinery operates from the organelle's exterior (Friedman and Nunnari, 2014). Since the work in this study was solely carried out in yeast, the focus will be on the situation in *Saccharomyces cerevisiae*. In this organism, the transmembrane protein Fis1 recruits the dynamin-related protein Dnm1 via the redundant adaptor proteins Mdv1 or Caf4 (Figure 1B; Bleazard et al., 1999; Mozdy et al., 2000; Tieu and Nunnari, 2000; Tieu et al., 2002; Schauss et al., 2006). Dnm1 then assembles into oligomers on the mitochondrial surface and forms spirals wrapping around mitochondria, which subsequently sever the membranes upon GTP hydrolysis (Ingelman et al., 2005). Interestingly, mitochondria constrict prior to Dnm1 assembly as they are otherwise too big to be surrounded by Dnm1 spirals. It had been a long standing question what mediates this constriction. It became clear that ER tubules enwrap and constrict mitochondria, which are eventually divided by Dnm1 (Friedman et al., 2011).

If the genes coding for the fission components are missing, mitochondria form giant networks that are hyper-connected. The hyper-connected morphology in fission mutants is caused by the ongoing fusion activity, which is not counteracted by mitochondrial division. If both, mitochondrial fusion and division are blocked, a wild type-like mitochondrial network can be maintained (Sesaki and Jensen, 1999). Mitochondrial fusion basically depends on three components (Figure 1B; reviewed in Westermann, 2010). *In trans* interactions of the MOM GTPase Fzo1 tether the mitochondria to be fused and GTP hydrolysis provides the energy for lipid bilayer mixing of the MOMs. Afterwards, the MIMs of the parental mitochondria are fused in a very similar manner by the GTPase Mgm1. In addition, the MOM protein Ugo1 is required for mitochondrial fusion by connecting Fzo1 and Mgm1. If *FZO1*, *MGM1* or *UGO1* are deleted, mitochondria are present as fragmented, unconnected entities since mitochondria are constantly divided but cannot refuse (Hermann et al., 1998; Wong et al., 2000; Sesaki and Jensen, 2004). Mitochondrial fusion is regulated by ubiquitylation and deubiquitylation of Fzo1 and its subsequent degradation or stabilization, respectively (Fritz et al., 2003; Cohen et al., 2008; Anton et al., 2013). The MIM protein Mgm1 is present in two isoforms as it is cleaved by the protease Pcp1 in an ATP level-dependent manner (Herlan et al., 2004). Since both isoforms are necessary for fusion, ATP levels might regulate the fusion competence of single mitochondria.

Mitochondrial dynamics serves several purposes. If fusion is blocked, mitochondria quickly lose their genome (Merz and Westermann, 2009) probably since division often results in some mitochondrial

daughter units devoid of mtDNA. If these units cannot regain mtDNA from fusing with another mitochondrion and are transferred to daughter cells, these cells contain no mtDNA at all. Thus, fusion is important for the inheritance of the mitochondrial genome. Furthermore, if mtDNA is mutated in one mitochondrion, fusing with another mitochondrion with intact mtDNA can complement the defect and therefore preserve respiratory-competent mitochondria (Nakada et al., 2001; Ono et al., 2001).

During the mitochondrial life cycle, mitochondrial fission results in functionally distinct mitochondrial entities with different metabolic capacities. In higher eukaryotes, mitochondria with a low membrane potential are less likely to fuse with the rest of the network and are prone to degradation by autophagy (Figure 1A). Thus, fission contributes to the maintenance of a healthy mitochondrial population (Twig et al., 2008). It remains controversial, whether fission is also necessary for mitochondrial autophagy in yeast (Mendl et al., 2011; Mao et al., 2013). Mitochondrial fission is furthermore required for the release of cytochrome *c* from the IMS into the cytosol, which is an important event during the activation of programmed cell death (Fannjiang et al., 2004; Youle and Karbowski, 2005). In higher eukaryotes, it has been observed that mitochondria fragment during mitosis. Prevention of the fragmentation results in an unequal mitochondrial distribution between daughter cells and metabolically inactive cells (Taguchi et al., 2007; Kashatus et al., 2011), highlighting the importance of mitochondrial dynamics for mitochondrial inheritance.

Mitochondrial contacts with other organelles

In the early years of cell biology, mitochondria were regarded as isolated, bean-shaped compartments – as seen by electron microscopy – which were primarily responsible for energy production by oxidative phosphorylation. However, fluorescence microscopy has shown that mitochondria have diverse morphologies ranging from filamentous, interconnected mitochondria in fibroblasts, which allow energy-transmission within cells (Amchenkova et al., 1988), to highly fragmented mitochondria during yeast meiosis (Gorsich and Shaw, 2004). Moreover, it has become obvious that mitochondria do not just import substrates, metabolize them and export the products, but that they also communicate with other organelles by membrane contact sites. In yeast, mitochondria form physical contacts with the plasma membrane (PM), the vacuole, the ER and possibly peroxisomes.

Mitochondrial ER contacts are the best-characterized contacts of mitochondria with another organelle so far. Close and extended proximity between mitochondria and ER can easily be seen by microscopy in yeast and mammalian cells (Rizzuto et al., 1998; Achleitner et al., 1999). The presence of physical contacts was shown by the isolation of ER membranes associated with mitochondria, the so-called mitochondria associated membranes (MAM; Vance, 1990).

The situation in higher eukaryotes is complex. The proteins proposed to tether ER and mitochondria are the mitofusin Mfn2 (de Brito and Scorrano, 2008), the mitochondrial porin VDAC and the calcium channel IP₃R bridged by grp75 (Szabadkai et al., 2006), the mitochondrial VABP and the ER localized

PTPIP51 (De Vos et al., 2012), or mitochondrial Fis1 and ER resident Bap31 (Iwasawa et al., 2011), to name just a few. Presumably, this diversity reflects the variety of different cell types and tissues in higher eukaryotes. The functions of these contacts range from lipid transfer and calcium exchange to apoptosis (reviewed in Rowland and Voeltz, 2012; Kornmann, 2013).

The situation in yeast appears to be simpler. In order to identify proteins tethering ER and mitochondria, Kornmann et al. (2009) performed a synthetic biology screen. They envisioned that yeast strains carrying mutations in genes coding for the tether(s) would grow poorly and that they could be rescued by expression of an artificial protein called chiMERA (construct helping in mitochondrion–ER association). This protein consists of an N-terminal mitochondrial membrane anchor, GFP, and a C-terminal ER tail anchor and thereby bridges both organelles. Indeed, growth defects of strains with mutations in the genes *MMM1*, *MDM10*, *MDM12* and *MDM34* were rescued by chiMERA (Kornmann et al., 2009). These four components form the ER-mitochondria encounter structure (ERMES; Figure 2A). Mmm1 is a glycosylated protein in the ER membrane, Mdm10 and Mdm34 are MOM proteins, and Mdm12 is a soluble factor. Later, the MOM protein Gem1 was identified as an integral component and regulator of ERMES' number and size (Kornmann et al., 2011; Stroud et al., 2011). ERMES is present in several foci per cell (Figure 2B).

MMM1, *MDM10*, *MDM12* and *MDM34* were initially discovered in screens searching for genes which are important for the maintenance of mitochondrial morphology since the mutants were found to have huge, spherical mitochondria (Burgess et al., 1994; Sogo and Yaffe, 1994; Berger et al., 1997; Dimmer et al., 2002; Youngman et al., 2004). Subsequently, the corresponding proteins were reported to have various functions. Mmm1, Mdm10 and Mdm12 were proposed to work in the import of MOM proteins (Meisinger et al., 2004; Meisinger et al., 2007). It was furthermore suggested that the same proteins form a so-called 'mitochore' complex which links mitochondria to actin cables and promotes mitochondrial movement towards the bud (Boldogh et al., 2003). In addition, several studies found that ERMES mutants have defects in mitochondrial lipid composition and proposed that ERMES transfers lipids between ER and mitochondria (Kornmann et al., 2009; Osman et al., 2009; Tamura et al., 2012; Tan et al., 2013), although a direct involvement of ERMES in this process has recently been questioned (Nguyen et al., 2012).

Originally, Mmm1 was mistakenly assigned to be an integral protein of the MOM (Burgess et al., 1994). Later it was found to be glycosylated at its N-terminus, which – together with microscopy data – demonstrates that Mmm1 is localized in the ER membrane (Kornmann et al., 2009). This, in turn, is hard to reconcile with Mmm1 functioning in mitochondrial outer membrane biogenesis or as a mitochore. However, Mmm1, Mdm12 and Mdm34 have tubular lipid-binding (TULIP)-like domains, which are known to bind lipids (Kopeck et al., 2010). Furthermore, ERMES' localization at the mitochondrial ER interface suggests a role in lipid traffic. It is reasonable to assume that primary defects of ERMES mutants in lipid transfer result in an altered lipid composition and as secondary effects in disturbed MOM biogenesis, mitochondrial morphology and inheritance.

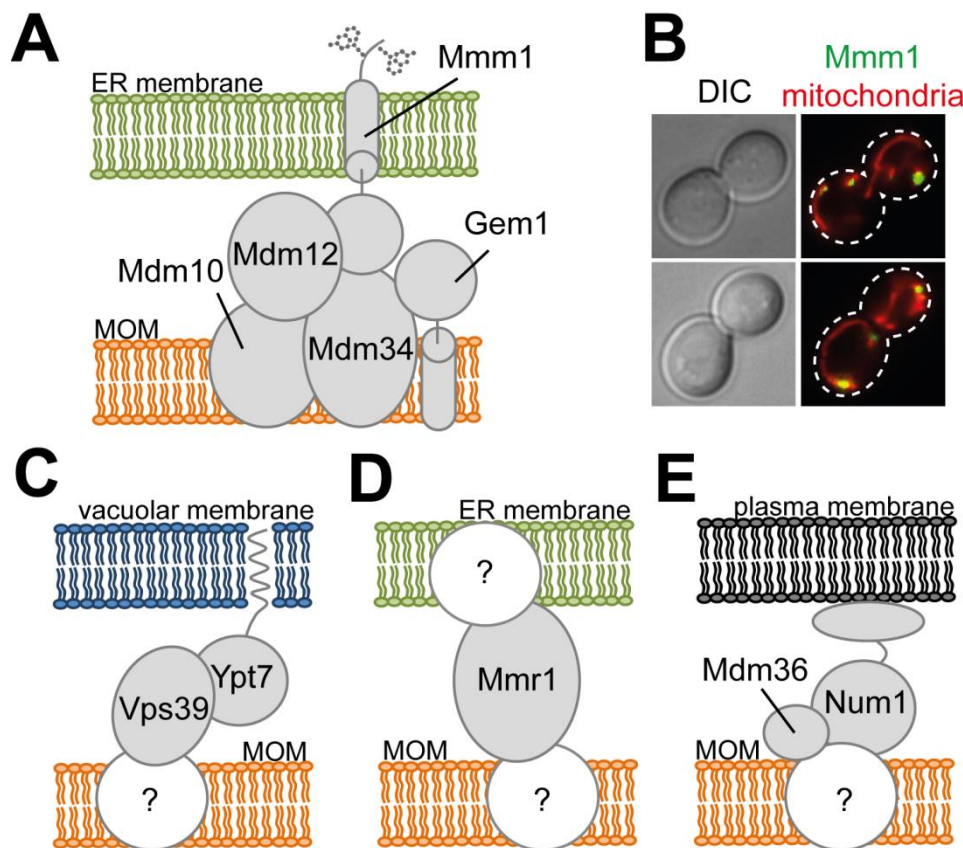


Figure 2. Molecular nature of mitochondrial contact sites. (A) Structure of ERMES. (B) Cells expressing mtGFP and Mmm1-3xmCherry were analyzed during logarithmic growth by epifluorescence microscopy. DIC and merged fluorescence (false colors) images are shown. Cell boundaries are indicated by broken lines. (C) Structure of vCLAMP. The unknown mitochondrial binding partner of Vps39 is indicated with "?". (D) Structure of mitochondrial ER contacts tethered by Mmr1. The factors recruiting Mmr1 to ER or mitochondria, respectively, are indicated with "?". (E) Structure of contacts between mitochondria and plasma membrane. The factor recruiting Mdm36 to the MOM is indicated with "?".

Evidence in favor of the lipid transfer hypothesis came from an unanticipated direction. ERMES mutants are viable even if they are presumably not able to import lipids from the ER. Since mitochondria do not receive lipids from vesicles, mitochondria must have at least one more lipid import pathway apart from ERMES. Elbaz-Alon et al. (2014) assumed that, if this alternative pathway was missing, there should be more lipid traffic from the ER and accordingly more ERMES dots per cell to sustain mitochondrial lipid composition. Hence, they screened yeast mutants for the appearance of excess ERMES foci and found the $\Delta vps39$ mutant. Vps39, a protein responsible for vacuolar fusion, is enriched at sites of close proximity between mitochondria and vacuoles. Furthermore they observed that mitochondria of ERMES mutants form extended vacuolar contacts. Strikingly, $\Delta vps39$ and ERMES double mutants are inviable indicating that they function in redundant pathways which are essential for cell viability. Characterization of conditional double mutants revealed that the mutants suffer from severe defects in lipid composition, suggesting that ERMES and Vps39 transfer lipids to mitochondria from the ER and the vacuole, respectively. Overexpression of Vps39 results in increased association of mitochondria with vacuoles and this depends on another vacuolar fusion protein, Ypt7, which is a known binding partner of Vps39 (Honscher et al., 2014). This led to the

model of vCLAMP (vacuole and mitochondria patch). Ypt7, which is prenylated and anchored in the vacuolar membrane, interacts with Vps39 acting as a molecular hinge between vacuole and mitochondria (Figure 2C). The mitochondrial binding partner of Vps39 remains unknown. In sum, this suggests that mitochondrial biogenesis relies on lipid supply from ER and vacuoles.

Recently, another potential mediator of lipid transfer from the ER to mitochondria has been proposed (Lahiri et al., 2014). The ER membrane protein complex (EMC) consists of six proteins (Emc1-6), which all interact with the translocase of the outer membrane (TOM) complex in the MOM, thus connecting ER and mitochondria. Loss of this complex renders ERMES essential, which can be rescued by chiMERA, suggesting that both complexes execute redundant functions and tether ER and mitochondria. Disturbance of the EMC results in fewer contacts between the ER and mitochondria and in reduced lipid transfer from the ER to mitochondria. Interestingly, contacts between TOM and EMC colocalize with ERMES, raising the question why two different tethering complexes are required at the same site.

Mmr1 has been proposed as a mitochondrial ER tether which is unrelated to lipid transfer. Mmr1 is a peripheral mitochondrial protein, which has been implicated in mitochondrial inheritance (Itoh et al., 2004). Swayne et al. (2011) gathered evidence that Mmr1 is not only present on mitochondria but also associated with the ER and that it localizes to sites of mitochondrial ER contacts in the bud tip (Figure 2D). The function of this tether is to anchor mitochondria in the bud to prevent retrograde movement back into the mother cell and will be discussed more thoroughly in the next chapter.

Contacts between mitochondria and the PM are thought to fulfill the antagonistic function of retaining some mitochondria in the mother cell (Klecker et al., 2013; Lackner et al., 2013). Num1 is a 313 kDa cortical protein containing a pleckstrin homology (PH) domain, which allows association of Num1 with the PM by binding to phosphoinositide $\text{PtdIns}(4,5)\text{P}_2$. By interaction with the peripheral mitochondrial protein Mdm36 and an unknown mitochondrial binding partner it mediates the contacts between mitochondria and the PM (Figure 2E), the function of which will be discussed in more detail below. Interestingly, Lackner et al. (2013) found the ER to be in close proximity to the mitochondrial PM interface, suggesting an anchor comprising components of mitochondria, PM, and ER, which is called mitochondria–ER–cortex anchor (MECA). However, electron microscopic studies found no involvement of the ER at mitochondrial retention sites (Klecker et al., 2013). Mitochondrial contacts with the PM in mammalian cells are less frequent because of interjacent ER stacks (Csordas et al., 2010) and little is known about the molecular identity of the tethers, although recently it has been proposed that mitochondria are attached to domains of the PM which are enriched in the gap junction component Cx32 (Fowler et al., 2013).

In addition, peroxisomes appear to be linked to mitochondria in the ‘peroxisome–mitochondrion connection’ (Schrader et al., 2013). Not only do mitochondria and peroxisomes both function in metabolic pathways like detoxification of ROS or oxidation of fatty acids and share their division machinery (Schrader et al., 2012), but the movement of both organelles is coupled in *Schizosaccharomyces pombe* (Jourdain et al., 2008). They are found in close proximity in *S. cerevisiae* (Rosenberger et al., 2009) and can be copurified from rat liver (Islinger et al., 2006). Cohen et al.

(2014) found that a subpopulation of yeast peroxisomes is located near mitochondria at sites of ERMES complex and acetyl-CoA synthesis. Moreover, ERMES mutants show peroxisomes with morphological aberrations, suggesting that peroxisomal localization at the ER-mitochondrion interface has a functional significance in the biogenesis of peroxisomes. The molecular nature of these contacts, however, remains elusive.

Another way of mitochondria to connect to other organelles are the recently discovered mitochondrion-derived vesicles (MDV). These vesicles bud off from mitochondria and fuse with peroxisomes or endosomes in mammalian cells (Neuspiel et al., 2008; Soubannier et al., 2012). The subpopulation targeted to peroxisomes might be involved in peroxisomal biogenesis (Mohanty and McBride, 2013), whereas the endosome-targeted MDVs provide a way for mitochondria to degrade superfluous proteins (Sugiura et al., 2014).

In sum, these findings convincingly demonstrate that mitochondria are not at all isolated organelles within a cell, but that contacts to other organelles shape both mitochondria themselves and the cell's physiology as a whole.

Mitochondrial transport and partitioning

Mitochondria are membrane-bounded organelles, which cannot form de novo and accordingly have to be inherited (Warren and Wickner, 1996). In contrast to metazoa or fungi like *S. pombe* and *Neurospora crassa*, whose mitochondria rely on microtubules for transport (Steinberg and Schliwa, 1993; Yaffe et al., 1996; Lawrence and Mandato, 2013), mitochondrial transport in *S. cerevisiae* exclusively depends on the actin network (Drubin et al., 1993). Since budding yeast exhibits an asymmetrical cell division, mitochondria have to be actively segregated into the new bud. For the process of budding, a bud site is selected and the assembly of actin cables from this position establishes an axis of polarity (Pruyne et al., 2004).

Yeast has two formins, Bni1 and Bnr1, which nucleate actin polymerization into filaments (Goode and Eck, 2007). Bnr1 assembles actin filaments at the bud neck (Kikyo et al., 1999), whilst Bni1 localizes to the bud tip in early cell cycle stages and is later found at the bud neck (Ozaki-Kuroda et al., 2001). Cells can cope with deletion of either gene but deletion of both genes results in synthetic lethality, indicating that the formins have redundant roles and can complement each other's loss (Ozaki-Kuroda et al., 2001). Actin formation by formins results in the flow of actin cables from the bud into the mother cell, since actin is incorporated into the filament at the positions of formins. This retrograde flow has to be overcome by mitochondria and thereby provides a potential quality control mechanism, as it has been hypothesized that only fitter mitochondria master this challenge (Vevea et al., 2014). Genetical enforcement of the actin flow did indeed lead to the inheritance of mitochondria with a more reducing milieu and to an increase in replicative life span (Higuchi et al., 2013), which corroborates the idea of retrograde flow as a quality filter.

There are conflicting models on how mitochondria are transported along actin cables. In a motor-protein independent scenario developed by the group of Liza Pon, the proteins Jsn1 and Puf3 recruit

another initiator of actin polymerization, the Arp2/3 complex, to mitochondria (Fehrenbacher et al., 2005; Garcia-Rodriguez et al., 2007). The actin polymerization on the mitochondrial surface is then supposed to push mitochondria into the bud, resembling the way how the intracellular pathogen *Listeria monocytogenes* exploits the Arp2/3-dependent actin polymerization to move inside of infected cells. This process, however, provides no directionality which is essential for mitochondrial inheritance. The above mentioned mitochore complex consisting of Mmm1, Mdm12 and Mdm34 is thought to offer a mechanism of directed movement by tethering mitochondrial membranes and DNA to the actin network reminiscent of the kinetochore connecting chromosomes and microtubules (Boldogh et al., 2003). As it has already been noted above, the localization of Mmm1 in the ER is barely compatible with its proposed mitochore function. Moreover, it is hard to imagine how retrograde actin flow might serve as a quality control mechanism, if mitochondria are just passively moving along actin flow but do not have to work against it.

An alternative model suggests that mitochondrial movement along cytoskeletal tracks is mediated by the class V myosin Myo2 (summarized in Westermann, 2014). Class V myosins are processive motors, which transport cargos against the actin cable flow (Reck-Peterson et al., 2000). There are two class V myosins in *S. cerevisiae*, Myo2 and Myo4. Myo4 transports ER tubules into the bud (Estrada et al., 2003). Yet, deletion of the corresponding gene has no impact on mitochondrial inheritance (Simon et al., 1995), not only demonstrating that Myo4 does not transport mitochondria but also that mitochondrial inheritance is not coupled to the ER. *MYO2* is an essential gene and the protein it codes for was shown to transport peroxisomes, vacuoles, secretory vesicles, Golgi cisternae, microtubule plus ends and lipid droplets (reviewed in Pruyne et al., 2004; Knoblach and Rachubinski, 2015). Early actin gliding assays showed that there is ATP-dependent motor activity on isolated mitochondria (Simon et al., 1995). Binding of isolated mitochondria to actin filaments in vitro depends on Myo2 and its essential light chain Mlc1 and can be prevented by addition of antibodies raised against the cargo binding domain (CBD) of Myo2 (Altmann et al., 2008). Depletion of Myo2 or Mlc1 by a titratable promoter results in abnormal mitochondrial morphology and mutations of the CBD lead to buds devoid of mitochondria (Altmann et al., 2008; Förtsch et al., 2011), which demonstrates that Myo2 has an important role in mitochondrial inheritance.

It has been considered that Myo2 is only required for the transport of one or more mitochondrial retention factors into the bud in order to prevent retrograde movement (Boldogh et al., 2004) instead of actively pulling mitochondria into the bud. Using a mitochondria-specific Myo2 variant called Myo2-Fis1, Förtsch et al. (2011) were able to discriminate between the two possibilities. This chimeric protein consists of Myo2, the CBD of which was replaced by the transmembrane segment of the MOM protein Fis1. Hence, Myo2-Fis1 is a MOM anchored motor protein which can only drive the transport of mitochondria but not of putative retention factors. Strikingly, expression of Myo2-Fis1 restores mitochondrial inheritance in *myo2* mutants and even leads to an accumulation of mitochondria in the bud, which is inconsistent with the idea of Myo2 as a transporter of retention factors. Together with the finding that Myo2 can be detected on the surface of highly purified mitochondria by immuno-electron microscopy this demonstrated that Myo2 is responsible for the motor-dependent transport of mitochondria into the bud (Figure 3; Förtsch et al., 2011).

Myo2-dependent transport usually relies on adaptor molecules between the motor protein and its cargo. These adaptors include Inp2 for peroxisomes, Vac17 and Vac8 for vacuoles, Sec4 for secretory vesicles, and Kar9 for microtubule plus ends (Yin et al., 2000; Wagner et al., 2002; Ishikawa et al., 2003; Fagarasanu et al., 2006). Two proteins, Mmr1 and Ypt11, have been discussed as linkers between mitochondria and Myo2. Mmr1 (Mitochondrial Myo2p Receptor-related) is a high-dose suppressor of mitochondrial *myo2* defects, constitutes a peripheral mitochondrial protein, interacts with Myo2 and localizes to mitochondria in the bud (Itoh et al., 2004). Deletion of *MMR1* results in delayed entrance of mitochondria into the bud in a substantial fraction of cells, whereas overexpression leads to an accumulation of mitochondria in the bud similar to *myo2-fis1*, which are characteristics of a myosin receptor.

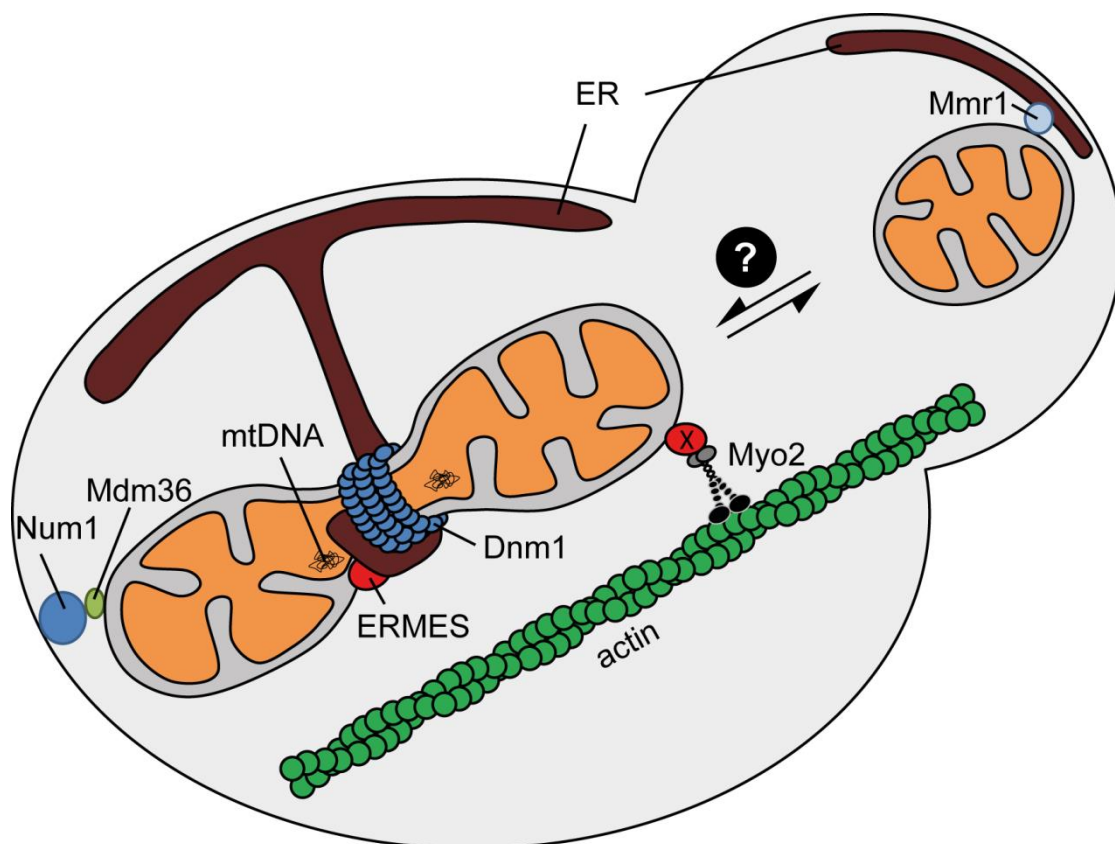


Figure 3. Mitochondrial transport in *S. cerevisiae*. Components involved in mitochondrial transport and partitioning are shown. The arrows indicate a balanced movement between mother and daughter cell. The “?” indicates that factors contributing to the backwards movement are currently unknown. The “X” symbolizes a yet unknown potential MOM protein recruiting Myo2 to mitochondria. See text for details.

Ypt11 is a small Rab-GTPase, which interacts with the CBD of Myo2. Its deletion leads to late arrival of mitochondria in the bud and its overexpression results in mitochondrial accumulation in the bud, which is reminiscent of Mmr1 (Itoh et al., 2002). Ypt11 function was shown to be not mitochondria-specific for it is also involved in the inheritance of cortical ER (cER) and Golgi (Buvelot Frei et al., 2006; Arai et al., 2008; Frederick et al., 2008). Interestingly, Ypt11 was proposed to be involved only in the transport of retention factors to the bud to avoid mitochondrial retrograde movement (Boldogh et al., 2004; Pon, 2008) as it has been suggested for Myo2 (see above). This scenario was

also excluded by a mitochondria-anchored variant of Ypt11 which was only able to drive Myo2-dependent mitochondrial transport but not transport of retention factors and indeed restored mitochondrial inheritance in a *ypt11* mutant (Lewandowska et al., 2013). Therefore, Ypt11 might connect mitochondria and Myo2 like the Rab-GTPase 27a does in the case of a class V myosin and melanosomes, lysosome-related organelles of higher eukaryotes (Wu et al., 2002). Double mutants with deletions of *YPT11* and *MMR1* are inviable due to a complete lack of mitochondrial inheritance and can be rescued by expression of Myo2-Fis1, which demonstrates that the inheritance of mitochondria is essential for cell survival and suggests that both proteins work in parallel and redundant transport pathways (Itoh et al., 2004; Chernyakov et al., 2013). Interestingly, both proteins bind to the CBD of Myo2 at non-overlapping regions (Eves et al., 2012), which is consistent with the idea of Mmr1 and Ypt11 as independent Myo2 receptors.

There are, however, problems with the assumption that these two proteins are solely responsible for mitochondrial inheritance. First of all, mutations in the CBD of Myo2 which result in its inability to either bind Mmr1 or Ypt11 lead to aberrations in mitochondrial morphology and severe inheritance defects (Altmann et al., 2008; Förtsch et al., 2011; Eves et al., 2012). This is not the case for *mmr1* or *ypt11* deletion mutants having only mild defects (Itoh et al., 2002; Itoh et al., 2004). Moreover, neither Mmr1 nor Ypt11 are integral MOM proteins; actually, Ypt11 has never been detected on the mitochondrial surface. Even if the two proteins are able to recruit Myo2, something else must recruit them to mitochondria as in the case of the vacuolar Myo2 receptor. Here, the cytosolic Myo2 receptor Vac17 is linked to vacuoles by the membrane-anchored Vac8 (Ishikawa et al., 2003). Since mitochondrial inheritance is an essential process, potential Myo2 receptor candidates are expected to be essential proteins inserted in the MOM.

The inheritance of diverse cargos by Myo2 provides a mechanism for the regulation of organellar mass which is transferred to the daughter cell. Eves et al. (2012) found that the binding sites for vacuoles and mitochondria on the CBD of Myo2 overlap and that the two organelles compete for Myo2. Overexpression of the vacuolar receptor Vac17 for example results in increased vacuolar volume and decreased mitochondrial mass in the bud. The opposite is true when Mmr1 is overexpressed. Therefore, it is plausible that the binding affinities of Myo2 receptors determine how many motor proteins contribute to the inheritance of either cargo and hence how much organellar mass reaches the daughter cell.

Myo2-driven mitochondrial transport is not the only process contributing to the partitioning of mitochondria. The 313 kDa protein Num1 has been shown to anchor mitochondria in the mother cell opposite to the bud by tethering mitochondria to the PM (Figure 3; Klecker et al., 2013; Lackner et al., 2013). Mutants lacking Num1 have a hyper-connected mitochondrial network, which is reminiscent of mitochondrial division mutants (Cervený et al., 2007). The peripheral MOM protein Mdm36 interacts with Num1 (Lackner et al., 2013) and its loss has been shown to result in a mitochondrial phenotype similar to *num1* mutants (Hammermeister et al., 2010). Strikingly, expression of an artificial mitochondria-PM tether restored mitochondrial morphology and division activity in *num1* and *mdm36* mutants (Klecker et al., 2013). These results support a model in which

Num1 and Mdm36 connect mitochondria and PM. Moreover, the data are consistent with the idea that anchorage of mitochondria at the PM together with Myo2-driven movement provides tension on mitochondrial tubules, which is required for Dnm1-dependent division (Figure 3; Westermann, 2014). Interestingly, ERMES also plays a role in mitochondrial division. ER tubules wrap around mitochondria and constrict them so that Dnm1 can sever the mitochondrial membranes (Figure 3; Friedman et al., 2011). Components of the ERMES complex have been shown to be in very close proximity to mtDNA (Boldogh et al., 2003; Meeusen and Nunnari, 2003) and Murley et al. (2013) demonstrated that ERMES ensures that both mitochondrial daughter units receive mtDNA after the division.

Instead of being the mitochondrial Myo2 receptor, Mmr1 has also been proposed to anchor mitochondria in the bud (Figure 3; Swayne et al., 2011). In this scenario, Mmr1 associates with the MOM and the ER and thereby tethers the two organelles. These Mmr1-mediated contacts are only found at the bud tip. Interestingly, mitochondrial distribution in *mmr1* mutants is shifted towards the mother, whilst it is moved towards the daughter in *num1* mutants, since the anchor in the mother is missing. In the *mmr1 num1* double mutant, however, the normal mitochondrial distribution is reestablished, suggesting that Mmr1 acts antagonistically to Num1, anchors mitochondria in the daughter cell and that both proteins, Mmr1 and Num1, regulate mitochondrial distribution (Klecker et al., 2013).

Only little is known about mitochondrial transport away from the bud tip back to the mother called retrograde movement. Mitochondria frequently move in this direction (Fehrenbacher et al., 2004) presumably by accompanying the retrograde flow of actin filaments (Peraza-Reyes et al., 2010). The mitochore complex was proposed to connect mitochondria and the actin filaments during this process, but the role of this complex is highly controversial as has been outlined above. It is currently unclear which particular proteins are involved in the retrograde movement of mitochondria.

Autophagy

Autophagy is the most important degradative pathway in cells besides the proteasome system. During autophagy, proteins, aggregates, pathogens or organelles are sequestered from the cytosol and transferred to the lysosome or the lysosome-like yeast vacuole for degradation (Inoue and Klionsky, 2010; Yang and Klionsky, 2010). Autophagy plays important roles in developmental processes, life span, immunity, neurodegeneration and survival of tumor cells. During autophagy in yeast, cargos are sequestered from the cytosol by a double-membraned structure called isolation membrane or phagophore arising from the phagophore assembly site (PAS) near the vacuole (Figure 4). When the phagophore seals around the cargo, it forms a mature autophagosome, which subsequently fuses with the vacuole and upon hydrolysis of lipids and coat proteins releases its cargo into the vacuolar lumen. After processing the cargo, its building blocks can be recycled.

Many proteins which are essential for autophagy have been initially identified by genetic screens in yeast (Tsukada and Ohsumi, 1993). These screens and subsequent efforts led to the discovery of

more than thirty autophagy-related (Atg) proteins. Autophagy is commonly induced by nitrogen starvation resulting in the inhibition of the TOR (target of rapamycin) complex, a master regulator of cell growth, which in its active form hyperphosphorylates Atg13 (Loewith and Hall, 2011). Upon TOR inhibition, Atg13 is dephosphorylated, the Atg1 kinase complex becomes active and allows formation of the PAS. There, components of the core autophagic machinery coalesce and cooperate in the initiation, elongation and maturation of the autophagosomal membrane (Suzuki et al., 2001; Kim et al., 2002; Suzuki et al., 2007). The amount of the small 13 kDa protein Atg8 determines the size of the autophagosome. Atg8 is a component of the mature autophagosome and is involved in the fusion of the autophagosome with the vacuole (Kirisako et al., 1999; Nakatogawa et al., 2007). It has an ubiquitin-like fold and is covalently coupled to phosphatidylethanolamine (PE) by an ubiquitin-like conjugation system, which enables the insertion of Atg8 into the autophagosomal membrane (Ichimura et al., 2000; Kirisako et al., 2000). A second ubiquitin-like conjugation system comprising the proteins Atg5/7/10/12/16 is also required for Atg8 lipidation and many more proteins at the PAS for maturation of the phagophore (reviewed in Nakatogawa et al., 2009; Mizushima et al., 2011). Upon completion of the autophagosome, the Atg proteins have to dissociate from the autophagosome, which involves the PtdIns3P phosphatase Ymr1, whose loss leads to accumulation of autophagosomes with Atg proteins still attached to them (Cebollero et al., 2012b). Fusion of the outer autophagosomal membrane with the vacuole is subsequently mediated by the Rab GTPase Ypt7 and the t-SNARE Vam3 (Darsow et al., 1997; Kirisako et al., 1999). The remaining autophagic body is then disintegrated by the lipase Atg15, the cargo is broken down and exported out of the vacuole to fuel metabolism (Epple et al., 2001; Reggiori and Klionsky, 2013).

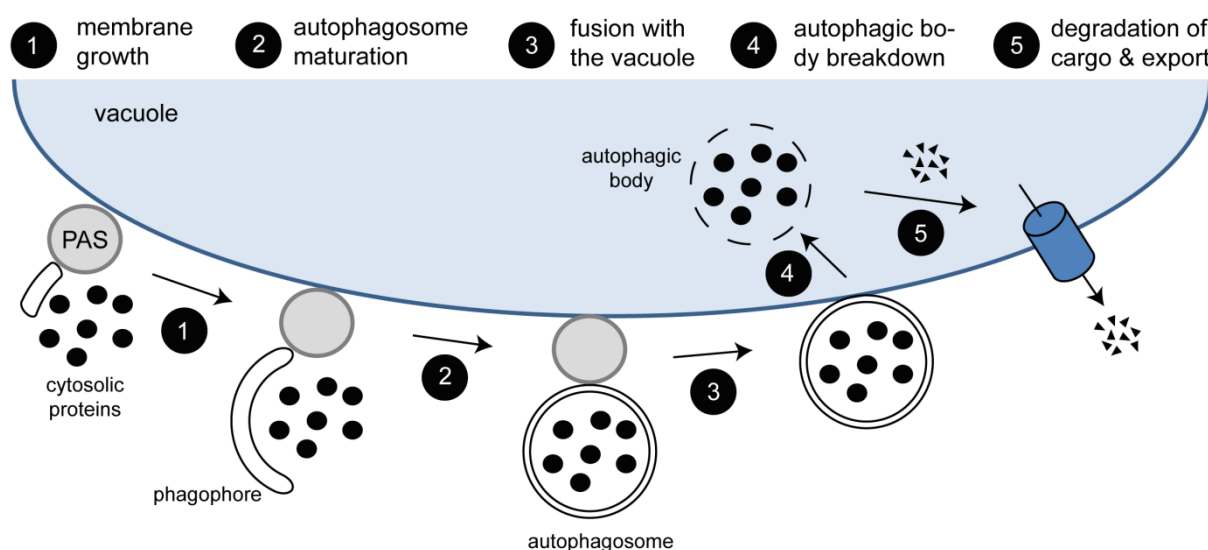


Figure 4. Autophagic degradation of cytosolic proteins by autophagy. (1) Phagophore growth is initiated at the phagophore assembly site (PAS) in close proximity to the vacuole in order to sequester cytosolic proteins. (2) The phagophore matures and seals to form an autophagosome. (3) The outer membrane of the autophagic vesicle fuses with the vacuole and releases an autophagic body with one remaining membrane. (4) The autophagic body is disintegrated and (5) the cargo is degraded and exported.

The origin of the autophagosomal membrane has been a matter of debate for decades (Tooze and Yoshimori, 2010). Plasma membrane, Golgi apparatus and endosomes were proposed to contribute

to autophagosome formation (Tooze, 2013) but mounting evidence points to an important role of ER and mitochondria in this process. Hailey et al. (2010) found that mitochondrial and autophagosomal membranes are transiently continuous and autophagosomes contain mitochondrial membrane markers in mammalian cells. In contrast, other studies showed that autophagosomal precursors arise from dynamic ER domains, which due to their shape were named omegasomes (Axe et al., 2008; Hayashi-Nishino et al., 2009). These conflicting results could be reconciled when Hamasaki et al. (2013) had a closer look and demonstrated that autophagosome formation happens at and relies on mitochondrial ER contacts. Furthermore, yeast mutants defective in the secretory pathway are autophagy-deficient (Ishihara et al., 2001; Reggiori et al., 2004; Lynch-Day et al., 2010) and ER exit sites (ERES), where vesicles leave the ER, are functional components of the core autophagic machinery and are necessary for phagophore growth (Graef et al., 2013; Suzuki et al., 2013), which suggests that the ER contributes membrane material to autophagosomes.

The selective degradation of mitochondria by mitophagy

Besides bulk autophagy, which degrades cytosolic components independent of substrate identity, there are selective forms of autophagy specific for particular cargos. Selective autophagy exists for the degradation of ribosomes (ribophagy), protein aggregates (aggrephagy), ER (ER-phagy or reticulophagy), peroxisomes (pexophagy), nuclei (nucleophagy), mitochondria (mitophagy), and pathogens (xenophagy) (Kraft et al., 2008; Manjithaya et al., 2010; Youle and Narendra, 2011; Cebollero et al., 2012a; Lamark and Johansen, 2012; Mijaljica et al., 2012; Gomes and Dikic, 2014; Schuck et al., 2014). These processes are responsible for the degradation of superfluous or harmful components. In contrast, the yeast cytoplasm-to-vacuole-targeting (Cvt) pathway ensures the transport of a folded cargo across the vacuolar membrane (Teter and Klionsky, 1999). The precursors of two peptidases, Ams1 and Ape1, are transported into the vacuole in autophagic vesicles, auto-inhibitory peptides are cleaved off and the mature proteins are active at their destination.

Mitochondrial autophagy attracted a lot of interest since blockage of this pathway is associated with Parkinson's disease (PD), presumably because mitochondrial quality control cannot prevent the accumulation of dysfunctional mitochondria in neurons. In healthy mammalian cells the kinase PINK1 is imported from the cytosol into the MIM in a membrane potential-dependent manner and rapidly degraded. In dysfunctional mitochondria with a low membrane potential, however, PINK1 cannot be imported into the MIM, but accumulates on the MOM and recruits the E3 ubiquitin ligase parkin (Narendra et al., 2010), which results in ubiquitination of mitochondrial substrates (Figure 5A; Matsuda et al., 2010). Afterwards, the ubiquitin-binding adaptor p62 accumulates on these mitochondria and interacts with LC3, the mammalian Atg8 homolog, in order to promote autophagic sequestration of the mitochondrion (Pankiv et al., 2007; Geisler et al., 2010). It has been found that PD patients carry mutations in the genes coding for PINK1 and parkin which lead to compromised mitophagy in cell culture systems (Narendra et al., 2010), suggesting that mitophagy maintains a healthy mitochondrial population especially needed in vulnerable cells like neurons. If this pathway fails, it might have detrimental effects on brain function. Mouse models confirming this assumption

are, however, not available yet. Remarkably, a recent study connected mitophagy with amyotrophic lateral sclerosis (ALS), an abundant neurodegenerative disorder. Mutations in optineurin, which cause ALS, lead to reduced mitophagy (Wong and Holzbaur, 2014). Optineurin can bind to ubiquitinated mitochondrial substrates and recruit LC3 in a similar way p62 does.

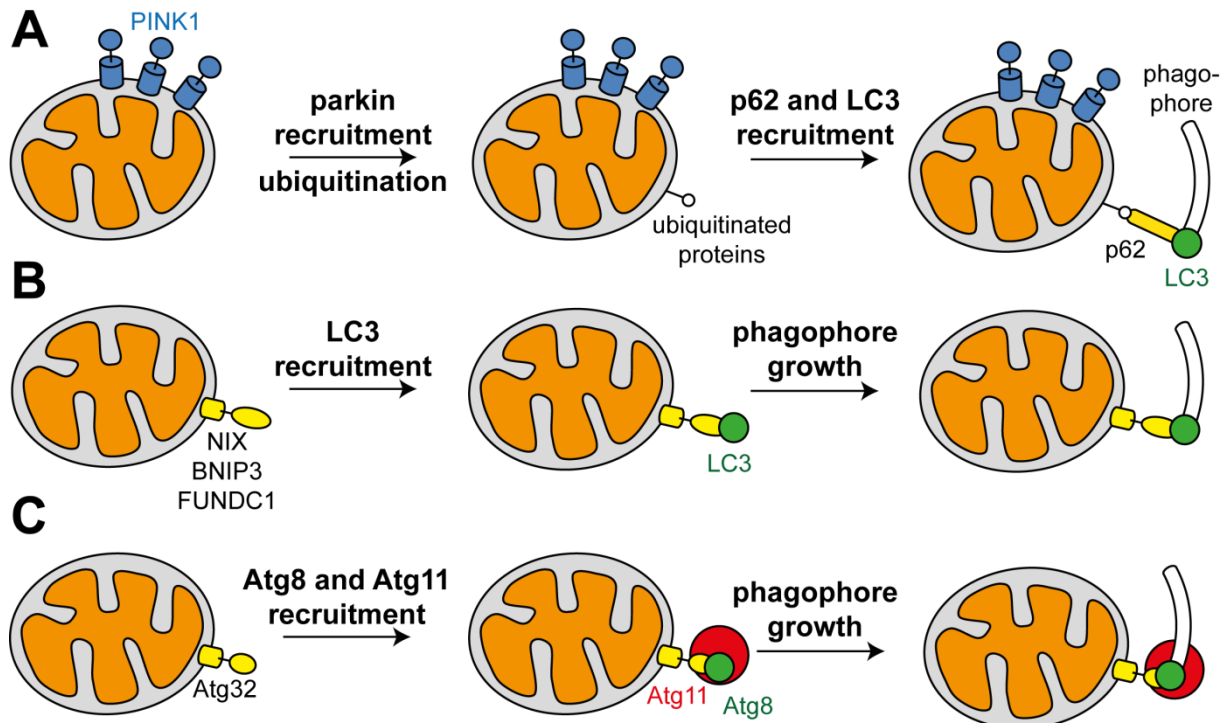


Figure 5. Different molecular mechanisms of mitophagy. See text for details. (A) PINK1/parkin-mediated mitophagy in mammalian cells. **(B)** Receptor-mediated mitophagy in mammalian cells. **(C)** Receptor-mediated mitophagy in yeast. Atg8 is the yeast ortholog of mammalian LC3.

Apart from the PINK1/parkin-mediated mitophagy depending on ubiquitination, there exists another type called receptor-mediated mitophagy. Red blood cells are completely devoid of mitochondria since they are degraded by mitophagy already during the maturation of reticulocytes, precursors of erythrocytes (Kundu et al., 2008). The MOM protein NIX contains an LC3-interacting region (LIR) which interacts with LC3 as well as the LC3 paralog GABA receptor-associated protein (GABARAP) and functions as a mitophagy receptor (Figure 5B). Consistently, loss of NIX results in red blood cells still retaining mitochondria and the development of anemia in mice (Sandoval et al., 2008). Additionally, the proteins BNIP3 and FUNDC1 also have LIRs and are thought to function as mitophagy receptors in a similar manner (reviewed in Liu et al., 2014).

This is reminiscent of how mitophagy works in yeast. Here, the MOM protein Atg32 has an Atg8-family interacting motif (AIM, corresponding to LIR in mammals) and acts as a mitophagy receptor. Atg32 has been discovered by two independent screens for mutants with defective mitochondrial autophagy (Kanki et al., 2009a; Kanki et al., 2009b; Okamoto et al., 2009). Atg32 is essential for mitophagy, but dispensable for all other kinds of autophagy, demonstrating its specificity. Atg32 is massively induced upon respiratory growth and is thought to mediate the recruitment of the autophagic machinery to mitochondria when cells enter the stationary phase and surplus

mitochondria are degraded (Okamoto et al., 2009). Atg32 activity is regulated by post-translational modifications at least by two different mechanisms: the domain facing the IMS is processed by the protease Yme1, which is important for mitophagy (Wang et al., 2013), and Atg32 is activated by casein kinase 2 (CK2) mediated phosphorylation (Aoki et al., 2011; Kanki et al., 2013). Atg32 acts as an autophagic degron and appears to be rate-limiting, since its overexpression results in mitophagy under non-mitophagy inducing conditions (Okamoto et al., 2009) and its relocalization to peroxisomes is sufficient to trigger pexophagy (Kondo-Okamoto et al., 2012). Atg32 interacts with Atg8 and Atg11, a scaffold protein necessary for selective types of autophagy (Figure 5C; Kanki et al., 2009b; Okamoto et al., 2009). Atg11, in turn, recruits the mitochondrial fission machinery in order to isolate mitochondrial pieces destined for degradation (Mao et al., 2013). The requirement of mitochondrial division for mitophagy in yeast is controversial since fission mutants exhibited mitophagy defects in some studies (Kanki et al., 2009a; Abeliovich et al., 2013; Mao et al., 2013), whilst others (Okamoto et al., 2009; Mendl et al., 2011) found no effect. A recent study showed that mitochondrial matrix proteins are degraded by mitophagy to different extents (Abeliovich et al., 2013). The aconitase Aco1, for example, is evenly distributed within the mitochondrial network and efficiently degraded together with mitochondria, whereas the mitochondrial chaperone Hsp78 changes its even distribution upon mitophagy induction and concentrates in several foci which are spared from mitophagy. Strikingly, this depends on mitochondrial dynamics and demonstrates the importance of this process during mitophagy. In mammalian cells, mitochondrial division constantly produces daughter units with a low membrane potential. These mitochondria are less likely to fuse with the network and are prone to degradation; here, mitochondrial division is necessary for mitophagy (Twig et al., 2008).

It is largely unknown how mitophagy in yeast is exactly regulated and which proteins contribute to the pathway. Mitophagy relies on the components of the core autophagic machinery which are mandatory for induction of autophagy and mitophagosome (an autophagosome sequestering mitochondria) formation (summarized in Kanki and Klionsky, 2010). Two MAPK signaling pathways are required upstream of Atg32 for induction of mitophagy (Mao et al., 2011) and the redox potential of cells determines the level of mitophagic degradation (Deffieu et al., 2009). The stress sensor Whi2 also appears to be involved in mitophagy (Mendl et al., 2011), although this has recently been questioned (Mao et al., 2013). It remains elusive how and if the signaling pathways are connected.

Although not much is known about the regulation of mitophagy, the characterization of mitophagy-deficient mutants demonstrated that it has a pivotal role in cell physiology. *atg32* mutants frequently lose their mitochondrial genome under starvation conditions, presumably due to excess ROS produced by superfluous mitochondria (Kurihara et al., 2012). Furthermore, under conditions of caloric restriction, compromised mitophagy results in reduced membrane potential and respiration, increased ROS levels and ultimately in a decreased life span (Richard et al., 2013). Mitophagy is also induced in yeast when mitochondria are damaged, as has been shown for disturbance of F_1F_0 -ATPase biogenesis or genetically induced osmotic swelling of mitochondria (Priault et al., 2005; Nowikovsky et al., 2007). Moreover, loss of the mitochondrial quality control factor Vms1, which mediates the proteasomal degradation of mitochondrial proteins, results in increased mitophagy (Heo et al.,

2010). In sum, this suggests that mitophagy ensures that mitochondrial quality and quantity meet the cellular needs.

Functional genetics in yeast

Yeast has proven an invaluable tool to assign functions to genes, which is a central challenge of the post-genomic era. It was the first domesticated microorganism and was used for baking bread and brewing beer. Besides, it was the first eukaryote whose genome was completely sequenced (Goffeau et al., 1996). The genome contains 12 megabases of information on 16 linear chromosomes and stores about 6000 genes. More than 40% of the yeast proteins have human homologs, thus providing a potential model for human diseases (Lander et al., 2001).

A great step towards an understanding of the yeast genome was the construction of the first deletion collection (also known as yeast knock-out [YKO] collection) containing mutants in which each open reading frame (ORF) is replaced by a cassette conferring resistance to an antibiotic (Winzeler et al., 1999; Giaever et al., 2002). This collection exists in different variations, which contain haploid mutants with different mating type or hetero- and homozygous diploids (Giaever and Nislow, 2014). Later, additional libraries were produced covering essential genes with a titratable promoter or genes whose mRNA stability is disturbed (Mnaimneh et al., 2004; Breslow et al., 2008). More than 1000 genome-wide screens were performed and led to an expanding annotation of the genome (Giaever and Nislow, 2014). Several of these screens addressed genes required for mitochondrial activity and morphology and expanded our knowledge about mitochondrial biogenesis (Dimmer et al., 2002; Altmann and Westermann, 2005; Luban et al., 2005; Merz and Westermann, 2009).

Comprehensive, functional information was not only derived from deletion mutant analysis but also from a strain collection containing all ORFs fused to a GFP coding sequence allowing the microscopic localization of proteins under different conditions (Huh et al., 2003; Breker et al., 2013). Protein-protein interactions were assessed by the yeast tandem affinity purification collection (Krogan et al., 2006), genome-scale two-hybrid studies (Ito et al., 2001) and protein-fragment complementation assay (PCA) collections (Tarassov et al., 2008).

Nonetheless, many genes remain functionally unclassified. Only about 20% of the yeast genes are essential, suggesting a great amount of redundancy among the genes (Winzeler et al., 1999; Giaever et al., 2002). The identification of genetic interactions is one way to take advantage of this redundancy in order to uncover gene functions. Genetic interactions occur when two mutations of different genes are combined and produce an unexpected phenotype; e. g., when deletions of two genes, which individually are not harmful to the cell, result in synthetic lethality of the double mutant (summarized in Dixon et al., 2009). This concept is based on the assumption that a combination of mutations, which individually result in a growth defect, has a multiplicative effect. If mutant *a* has a fitness of 0.7 compared to wild type and mutant *b* has a fitness of 0.4, one expects a fitness of $0.7 \times 0.4 = 0.28$ for the double mutant *ab* (Figure 6A). There are two classes of genetic interactions:

negative and positive ones. If *ab* has fitness below 0.28, it is a negative interaction, if the fitness exceeds 0.28, it is a positive one.

The concept intuitively becomes clear in the case of symmetric positive interactions. If the products of two genes *C* and *D* are components of a complex and if disintegration of the complex by deletion of either gene results in a growth defect of 0.6, the combination of the two deletions will not result in a double mutant *cd* with a fitness of $0.6 \times 0.6 = 0.36$ but 0.6, since the complex is dysfunctional to the same extent in the single mutants and the double mutant and hence they have the same fitness (Figure 6B). This fitness is better than expected and demonstrates that gene products physically interacting with each other have the tendency to show positive genetic interactions (Collins et al., 2007). Another possible cause for positive interactions is that the genes function in antagonistic pathways and the double mutants have a more wild type-like situation like in the case of $\Delta num1 \Delta mmr1$ double mutants. Loss of *NUM1* results in a mitochondrial distribution shifted towards the bud, while *Mmr1* depletion leads to a shift towards the mother. Double mutants, however, show a rather wild type-like distribution (Klecker et al., 2013). Alternatively, the genes work in the same pathway and blocking the pathway flux results in a comparable outcome in both single and double mutants. Negative interactions can occur when genes work in parallel or redundant pathways contributing to the same biological process. Cells can cope with deletion of either gene but have a severe fitness defect when the deletions are combined with the extreme case of being inviable (synthetic lethality) as in the case of the two formin coding genes *BNI1* and *BNR1*.

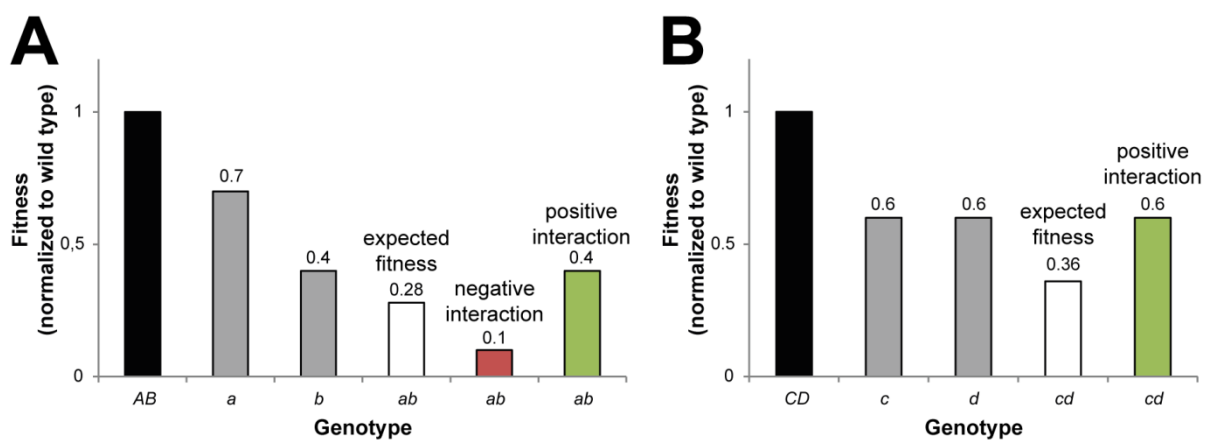


Figure 6. Genetic interactions. (A) Two hypothetical single mutants *a* and *b* have a reduced fitness compared to wild type *AB*. The actual fitness of the double mutant *ab* can equal the expected fitness of the combined single mutants' fitness (no interaction), be lower (negative interaction) or higher (positive interaction) than the expected fitness. **(B)** A special case of a hypothetical symmetric positive interaction, where the single mutants *c* and *d* have the same fitness as the double mutant *cd*.

Genetic interaction networks have turned out to be powerful tools and contributed to the identification of genes working in chromosome biology, lipid quality control and many other processes (Collins et al., 2007; Dixon et al., 2009; Surma et al., 2013). In order to identify genetic interactions on a genome-wide scale, the synthetic genetic array (SGA) technology was developed. In SGA technology, a query strain carrying a mutation is crossed to an array of mutants. Selectable markers allow the subsequent isolation of double mutants, whose fitness can be quantified and

genetic interactions can be uncovered (Tong et al., 2001). Automated replica-plating enabled the high-throughput screening of more than a thousand query mutations, resulting in the first “*genetic landscape of a cell*” (Tong et al., 2004; Costanzo et al., 2010). Applying this method with a focus on mitochondria gave rise to the MITO-MAP and led to the discovery of six genes involved in the biogenesis of cristae (Hoppins et al., 2011). Exactly the same genes were found at the same time by two independent groups using different methods (Harner et al., 2011; von der Malsburg et al., 2011), which demonstrates that genetic interactions are a powerful tool in order to assign functions to genes.

The technology is now broadly applied by geneticists and the automation of the process will lead to a highly anticipated map, where all digenic interaction data from deletion mutants are integrated. However, the genetic interactomes of essential genes remain largely unknown since deletion mutants are not available. Hypomorphic alleles with reduced expression of the query gene have been screened but may not yield a comprehensive picture of the interactomes (Breslow et al., 2008; Costanzo et al., 2010). Yet, determination of the interactomes of specific point mutants of essential genes with a defined spectrum of phenotypes are an attractive alternative to hypomorphic alleles and will expand our knowledge about biological processes, which are essential in yeast.

Aim of this thesis

One major goal of this study was the identification of yet unknown regulators of mitochondrial autophagy. Two genome-wide screens for mutants with defective mitophagy have already improved our knowledge about mitophagy by identifying the mitochondrial outer membrane receptor Atg32, which recruits the core autophagic machinery to mitochondria (Kanki et al., 2009a; Kanki et al., 2009b; Okamoto et al., 2009). However, these screens missed all strains that were not able to respire due to the used growth conditions. These strains are of particular interest because of their potential involvement in mitochondrial function. In order to test whether respiratory-deficient yeast mutants exhibit altered mitophagy, a deletion library comprising about 380 strains with compromised growth on respiratory medium (Merz and Westermann, 2009) was assayed for mitophagy by using a fluorescent biosensor and a novel culturing protocol. The four mutants lacking the genes coding for ERMES complex proteins had an impaired mitochondrial autophagy and their role during mitophagy was further characterized.

The second major objective was to gain new insights into the process of mitochondrial inheritance. To this end, genetic interactions of the mutant myosin motor allele *myo2(LQ)*, which results in a mitochondrial inheritance defect (Förtsch et al., 2011), were mapped on a genome-wide scale using SGA methodology. This method enables the identification of genes with similar functions by assaying the growth of double mutants (Dixon et al., 2009). Genetic interactors of *myo2(LQ)* and thus potential players in mitochondrial transport and inheritance were characterized.

Results

Mitochondrial ER contacts are the sites of mitophagosome biogenesis

Respiratory activity is not necessary for mitophagy

Two genome-wide screens for mutants with defects in mitophagy identified the mitochondrial outer membrane receptor Atg32 (Kanki et al., 2009a; Kanki et al., 2009b; Okamoto et al., 2009). In these studies, cells were cultured on non-fermentable carbon sources, which leads to substantial proliferation of mitochondria which are degraded during starvation. Yet, these studies missed respiratory-deficient mutants, since these were not able to proliferate in the used growth media.

In order to work with respiratory-deficient mutants another protocol had to be established that allows cells to grow on fermentable carbon sources. A fluorescent biosensor called mtRosella was used for the detection of mitophagy (Nowikovsky et al., 2007; Rosado et al., 2008). mtRosella consists of a pH-stable, fast maturing DsRed (Bevis and Glick, 2002) fused to a pH-sensitive GFP variant called pHluorin (Miesenböck et al., 1998). This fusion protein carries an N-terminal mitochondrial targeting sequence (MTS; Figure 7A), which ensures its localization in the mitochondrial matrix (pH 7.0).

During growth, the green and red fluorescence signals overlap in the mitochondrial network but do not appear in the vacuolar lumen, where the autophagic degradation is taking place (Figure 7B). After starvation, however, mtRosella is transported to the vacuole together with mitochondria, and the green fluorescence signal is lost due to the acidic pH of the vacuole (pH 6.2), while the red signal persists. This assay is specific for mitochondrial autophagy, since the red vacuolar fluorescence is missing in the mitophagy-deficient strain $\Delta atg32$ (Figure 7B).

For induction of mitophagy, the cells were cultured using a synthetic medium containing the fermentable carbon sources galactose (2%) and raffinose (2%) called SGalRD. Since glucose is able to repress mitochondrial function and proliferation (Gancedo, 1998), its amount was reduced to a minimum (0.1%) that still enables substantial cell growth. After logarithmic growth in SGalRD and nitrogen starvation for one day, the fraction of cells exhibiting red vacuolar fluorescence was determined. Over 60% percent of the cells were mitophagy positive, indicating that the induction was robust and reliable, although it was not as strong as the induction after growth on the non-fermentable carbon source glycerol (Figure 7C).

To test whether respiratory deficiency per se might have an effect on mitochondrial autophagy, ρ^0 cells were used as a model for respiratory-deficient strains. ρ^0 cells lack mtDNA and therefore several parts of the respiratory chain complexes, which results in their inability to respire. Since it was shown that these cells were unable to perform bulk autophagy under some conditions (Graef and Nunnari, 2011), it appeared reasonable to assume that mitophagy might also be affected. On the other hand,

mitophagy is perceived as a quality control mechanism that may sense the reduced mitochondrial membrane potential as an indicator of mitochondrial dysfunction and thus mitophagy might even be enhanced in this strain. After growing ρ^0 cells in SGalRD and starving them for one day, it became apparent that these cells did not display any mitophagy defect compared to ρ^+ cells (Figure 7D and E) and that neither the presence of mtDNA nor respiratory activity are necessary for mitophagy.

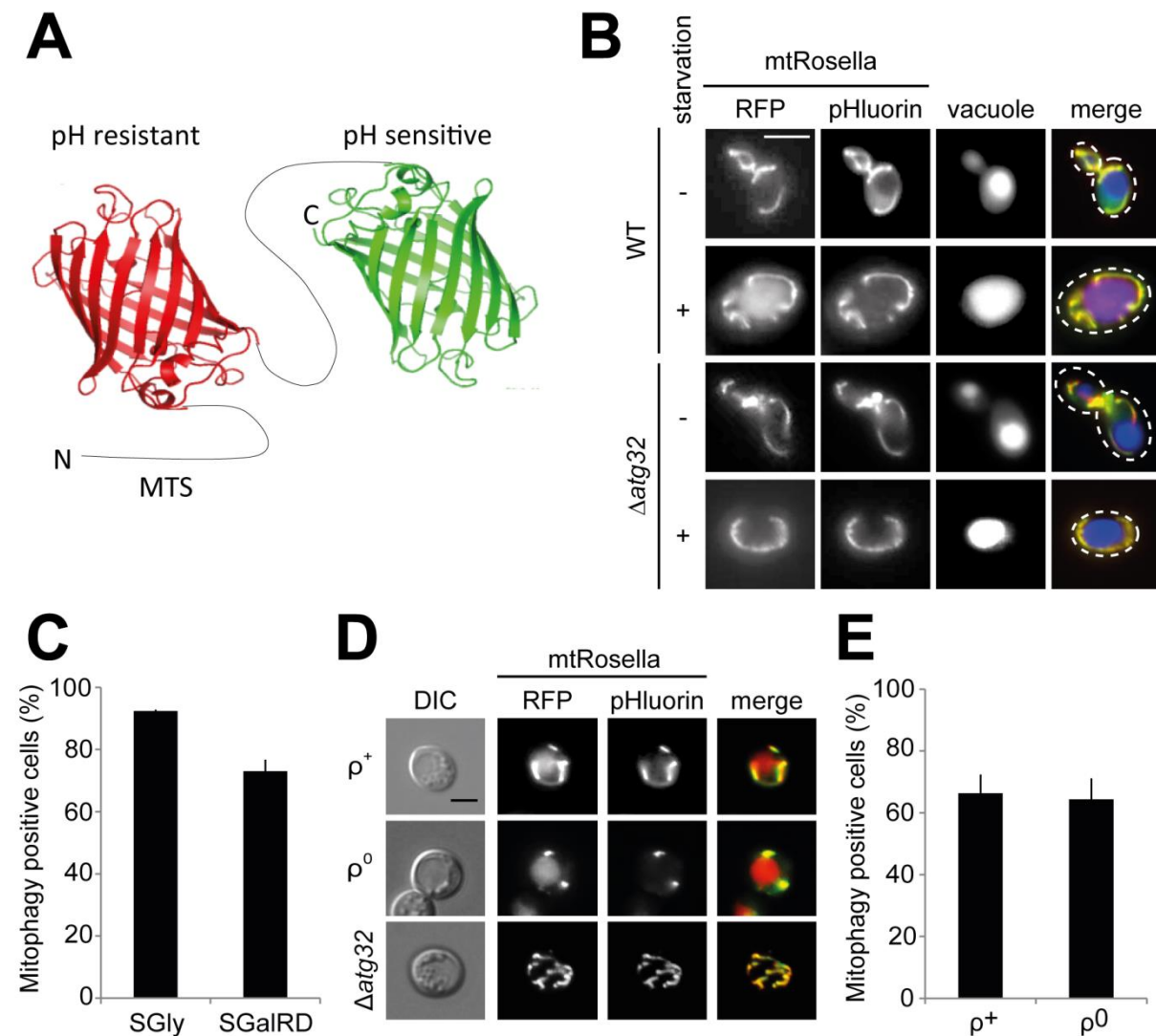


Figure 7. Monitoring mitophagy by using the biosensor mtRosella in respiratory-deficient mutants. (A) Schematic representation of mtRosella. See text for details. N, N-terminus; C, C-terminus; MTS, mitochondria targeting sequence. (B) Cells expressing mtRosella were grown in synthetic medium with glucose to logarithmic growth (- starvation) and starved for two days in sporulation medium (+ starvation). The vacuole was stained using CellTracker Blue CMAC. Cell boundaries are indicated by broken lines. Bar, 5 μ m. (C) Cells expressing mtRosella were either cultured to logarithmic growth in synthetic medium with glycerol and glucose (3% and 0.1%, respectively; SGly) or galactose, raffinose and glucose (2%, 2%, and 0.1%, respectively; SGalRD) and starved for one day in SD-N. At least 100 cells were scored for red vacuolar fluorescence. Values represent the mean of triplicate experiments + SD. (D) Cells expressing mtRosella were grown to logarithmic growth in SGalRD and starved in SD-N. Bar, 5 μ m. (E) Quantification of ρ^+ and ρ^0 cells cultured as in (D) and starved for one day in SD-N. Values represent the mean of triplicate experiments + SD.

These results show that the novel protocol for mitophagy induction upon growth on SGalRD and subsequent nitrogen starvation leads to detectable levels of mitophagy and that this also works in non-respiring yeast mutants, revealing for the first time that these mutants are capable of mitophagy at a wild type-rate despite their defects like a decreased membrane potential. It is therefore promising to test respiratory-deficient mutants for defective mitophagy by applying this protocol.

Screening of respiratory-deficient mutants for altered mitophagy

Strains with compromised respiratory capacity are of great interest because of their putative defects in mitochondrial functions, but these strains have been neglected in recent mitophagy screens (Kanki et al., 2009a; Okamoto et al., 2009). The *pet* library is a collection of such strains derived from a genome-wide screen for yeast mutants which are unable to grow on non-fermentable carbon sources (Merz and Westermann, 2009). It contains over 380 strains, each harboring an ORF locus where a gene of interest is replaced by a cassette conferring resistance to geneticin. These strains are listed in Table 6 (Appendix).

To identify mutants with defective mitophagy the collection was transformed with a plasmid coding for mtRosella, cultured in SGalRD in deep-well microtiter plates, starved for two days and the fraction of cells showing red vacuolar fluorescence was determined. Wild type cultures had about 50% mitophagy positive cells, whereas 39 strains had reduced mitophagy rates (< 20%) and 54 strains had increased rates (> 80%; Figure 8A and B). These strains are listed in Table 1. The mitophagy rates of all strains are recorded in Table S1 (Appendix).

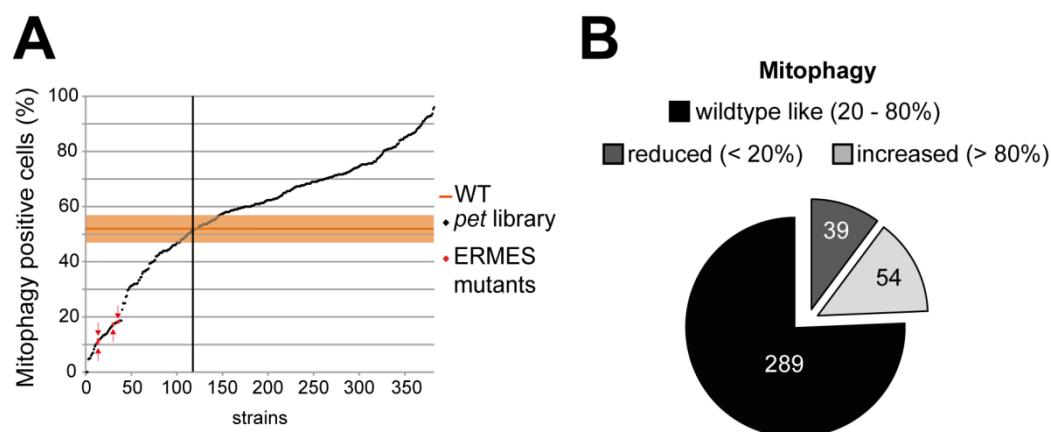


Figure 8. Screening of respiratory-deficient mutants for altered mitophagy. (A) 382 respiratory-deficient mutants from the *pet* library were cultured in SGalRD in deep-well microtiter plates and starved for two days. At least 100 cells were scored for red vacuolar fluorescence. Values represent the mean of at least two independent experiments. ERMES mutants are highlighted with red arrows. The mean value of WT (orange line) and the SD of WT (light orange) are indicated. (B) Analysis of the screening results reveals that about one quarter of the tested strains show either reduced or increased mitophagy rates.

Remarkably, almost two thirds of the strains showed mitophagy rates higher than the WT (52%) and the median of all strains was 61%. This might reflect the biased nature of the screen, which only


includes non-respiring mutants and points to the possibility that these mutants harbor mitochondrial defects resulting in increased mitochondrial degradation.


The mitophagy-defective mutants $\Delta pep12$, $\Delta vps16$ and $\Delta kgd2$ were all found in at least one of the earlier screens (Kanki et al., 2009a; Okamoto et al., 2009), confirming the reliability of the screening assay. Strikingly, all of the four mutants lacking the mitochondrial ER tether ERMES had defects in mitochondrial autophagy and will be described in depth in the following chapters.

Table 1. Strains with defective mitophagy. Strains with less than 20% or more than 80% mitophagy positive cells are highlighted in red and green, respectively. Strains appear in alphabetical order with regard to their systematic names.

Sytematic name	Standard name	Systematic name	Standard name	Systematic name	Standard name
YAL010C	MDM10	YAL013W	DEP1	YLR144C	ACF2
YBL019W	APN2	YAL016W	TPD3	YLR369W	SSQ1
YBL021C	HAP3	YBL053W		YLR403W	SFP1
YBL031W	SHE1	YBR026C	ETR1	YML061C	PIF1
YBL036C		YBR081C	SPT7	YMR070W	MOT3
YBL062W		YBR146W	MRPS9	YNL052W	COX5A
YBL080C	PET112	YBR251W	MRPS5	YNL071W	LAT1
YBR282W	MRPL27	YBR283C	SSH1	YNR025C	
YCR024C	SLM5	YCL001W-A		YNR037C	RSM19
YDL107W	MSS2	YCR028C-A	RIM1	YNR041C	COQ2
YDL192W	ARF1	YCR046C	IMG1	YOL051W	GAL11
YDR010C		YDL012C		YOL095C	HMI1
YDR065W	RRG1	YDL039C	PRM7	YOL148C	SPT20
YDR148C	KGD2	YDL091C	UBX3	YPL031C	PHO85
YDR296W	MHR1	YDL099W	BUG1	YPL148C	PPT2
YDR337W	MRPS28	YDR115W		YPL254W	HFI1
YGL218W		YDR448W	ADA2		
YGR220C	MRPL9	YEL027W	CUP5		
YHR006W	STP2	YEL061C	CIN8		
YHR009C	TDA3	YER014C-A	BUD25		
YHR038W	RRF1	YER155C	BEM2		
YHR168W	MTG2	YGL071W	AFT1		
YHR194W	MDM31	YGL135W	RPL1B		
YJL180C	ATP12	YGL215W	CLG1		
YKR006C	MRPL13	YGR155W	CYS4		
YLL006W	MMM1	YGR174C	CBP4		
YLL042C	ATG10	YIL125W	KGD1		
YLR226W	BUR2	YIL153W	RRD1		
YMR035W	IMP2	YIL157C	FMP35		
YMR064W	AEP1	YJL096W	MRPL49		
YMR188C	MRPS17	YJL101C	GSH1		
YNL185C	MRPL19	YJL121C	RPE1		
YOL009C	MDM12	YJL184W	GON7		
YOR036W	PEP12	YKL054C	DEF1		
YOR135C	IRC14	YKL087C	CYT2		
YOR150W	MRPL23	YKL119C	VPH2		
YPL013C	MRPS16	YKL155C	RSM22		
YPL045W	VPS16	YKR001C	VPS1		
YPR099C		YLR055C	SPT8		
YPR116W	RRG8	YLR139C	SLS1		

Mitophagy rate

 < 20%

 > 80%

Notably, $\Delta pho85$, $\Delta clg1$ and five deletions associated with the SAGA complex ($\Delta spt7$, $\Delta spt8$, $\Delta spt20$, $\Delta ada2$, $\Delta hfi1$) showed increased mitophagy rates. Pho85 is a cyclin-dependent kinase, which interacts with Clg1 and whose absence is known to result in increased bulk autophagy (Yang et al., 2010). The SAGA complex is a global regulator of transcription and especially involved in *PHO85*-related gene transcription (Lee et al., 2000). Presumably, the increased mitophagy defect of $\Delta pho85$ and of the associated deletion mutants is an indirect consequence of their augmented bulk autophagy, indicating that mitophagy is regulated alongside with bulk autophagy.

Upregulated mitophagy is a phenomenon which has been rarely observed until now. Deffieu et al. (2009) showed that the deletion of *GSH2*, the gene product of which catalyzes the second step of glutathione synthesis, results in increased mitophagy. However, they were unable to show that $\Delta gsh1$ lacking the first step of glutathione synthesis behaves in a similar way, since this mutant is respiratory-deficient and was not compatible with their techniques. $\Delta gsh1$ is here shown to also have enhanced mitophagy rates like $\Delta gsh2$, confirming that glutathione regulates mitophagy. Together with the result from $\Delta pho85$, this highlights the fact that the screening assay reveals candidates which are likely to show increased mitophagy, in turn indicating that the screen is reliable.

The deletions of *RIM1*, *HMI1*, *IMG1* and *PIF1*, which are involved in the maintenance and repair of the mitochondrial genome, resulted in amplified mitophagy, too, pointing to the possibility that mtDNA absence does not interfere with mitophagy (Figure 7D and E), while presence of non-functional mtDNA has an effect on mitophagy. Loss of three proteins working in mitochondrial metabolism (Coq2, Lat1, and Kgd1) as well as proteins associated with the respiratory chain (Fmp35, Cox5a, Cbp4, and Cyt2) increased the level of mitophagy. Interestingly, deletion of a mitochondrial Hsp70-type molecular chaperone, Ssq1, also rendered mitochondria more prone to mitophagy, which indicates that when quality control acting at the molecular level is absent, mitophagy might take over and act at the organellar level.

Apart from the components of the ERMES complex, none of the genes identified in the screen has been further characterized with regard to its role in mitophagy. Some of them point to interesting hypotheses and may deserve further investigation.

Mutants lacking the ER-mitochondria tether ERMES have a mitophagy defect

The mitophagy screen revealed that the four mutants $\Delta mmm1$, $\Delta mdm10$, $\Delta mdm12$ and $\Delta mdm34$ show defective mitophagy (Figure 8A). All of them lack a gene coding for a subunit of the mitochondrial ER tether ERMES connecting mitochondria with the ER (Kornmann et al., 2009). ERMES consists of the ER membrane protein Mmm1, two mitochondrial outer membrane proteins, Mdm10 and Mdm34, and the soluble factor Mdm12 (Figure 2A). If one component is missing, the mutants display several defects like aberrantly swollen mitochondria, mtDNA loss and defective mitochondrial lipid composition (Hobbs et al., 2001; Kornmann et al., 2009; Osman et al., 2009; Tan et al., 2013).

To check the mitophagy defect, mutants with a confirmed genotype were transformed with a plasmid coding for mtRosella and grown in SGalRD. The increase in the proportion of mitophagy positive cells was observed over four days of starvation by fluorescence microscopy. All four ERMES mutants had strong defects in mitophagy after one day of starvation compared to WT (Figure 9A and B). With increasing time, almost all cells of a culture managed to degrade part of their mitochondria in $\Delta mmm1$, $\Delta mdm10$ and $\Delta mdm34$, but not in $\Delta mdm12$, which had less than 50% mitophagy positive cells after four days of starvation. The defect is, however, not as strong as in $\Delta atg32$ cells, where mitophagy was never observed (data not shown).

The mitophagy defect was also checked by assaying free GFP on a Western blot. Rosella is processed between DsRed and GFP in the vacuole and the amount of free GFP, which is itself protease resistant, compared to Rosella full-length protein is proportional to autophagic degradation (Mijaljica et al., 2012). While the WT efficiently processed mtRosella after one day of starvation and processing was completely absent in $\Delta atg32$, all four ERMES mutants showed an intermediate phenotype (Figure 9C). In sum, these results demonstrate that ERMES is important for mitophagy, albeit not essential, and that loss of ERMES leads to delayed degradation of mitochondria by autophagy.

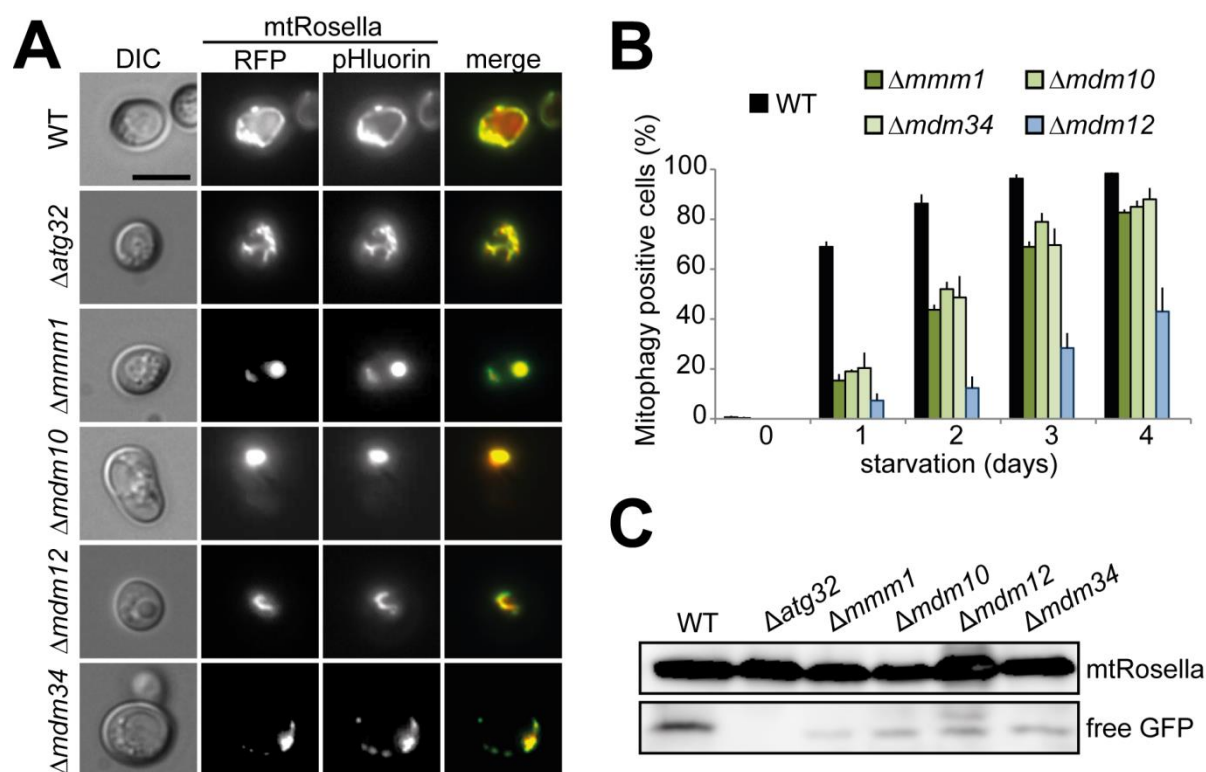


Figure 9. ERMES mutants degrade mitochondria slower than wild type cells. (A) Cells expressing mtRosella were grown to logarithmic growth and starved for one day in SD-N. Representative images are shown. Bar, 5 μ m. **(B)** Cells expressing mtRosella were cultured as in (A) and starved for the indicated time points. At least 100 cells per strain were scored for red vacuolar fluorescence at the different time points. Values represent the mean of triplicate experiments + SD. **(C)** Cells were cultured in SGalRD and starved for one day. Cell extracts were subjected to SDS-PAGE and Western blotting. mtRosella and processed free GFP were detected with an anti-GFP antibody.

ERMES mutants show no defect in bulk autophagy and the Cvt pathway

The origin of autophagosomal membranes has been discussed for a long time (Tooze and Yoshimori, 2010; Mizushima et al., 2011). It has been proposed that lipid transport from the ER to mitochondria at contact sites and from mitochondria to autophagosomes is necessary for autophagy (Hailey et al., 2010) and that autophagosomes form at mitochondria-ER contacts in mammalian cells (Hamasaki et al., 2013). If this was also true in yeast, all autophagy pathways could be expected to be compromised in ERMES mutants, since mitochondrial ER contacts are missing and lipid transport from ER to mitochondria and vice versa are hampered.

To this end, the localization of GFP-Atg8 was determined under growth and starvation conditions. GFP-Atg8 is localized in the cytosol under growing conditions and recruited to the phagophore assembly site after induction of starvation. As a permanent component of autophagosomes it is transported into vacuoles, a process which depends on bulk autophagy. The localization of Atg8 is therefore indicative of the pathway's functionality (Abeliovich et al., 2003; Klionsky et al., 2012). WT, $\Delta atg1$ and ERMES mutants expressing GFP-Atg8 were grown to logarithmic phase, starved for five hours and the localization of GFP-Atg8 was determined by fluorescence microscopy. Atg1 is a kinase essential for autophagy (Matsuura et al., 1997) and its deletion mutant served as a negative control. Under growing conditions, GFP-Atg8 was present in the cytosol in all strains as expected (Figure 10A). After starvation GFP-Atg8 persisted in the cytosol in the negative control $\Delta atg1$, while it was localized in the vacuole in WT and ERMES mutants, suggesting that bulk autophagy still works in the absence of ERMES-mediated ER-mitochondria contacts. In order to see whether the effect on bulk autophagy might be quantitative, autophagic flux was analyzed by using the GFP-Atg8 processing assay. Analogous to mtRosella, the Atg8 moiety of GFP-Atg8 is degraded in the vacuole, while GFP is protease-resistant and the amount of free GFP compared to full-length protein is proportional to autophagic activity (Shintani and Klionsky, 2004; Klionsky et al., 2012). This assay revealed that the ERMES mutants processed GFP-Atg8 in a wild type-like manner (Figure 10B). To confirm these results, a Rosella protein localized in the cytosol (cytRosella) was expressed in WT, $\Delta atg1$ and ERMES mutants and processing of this construct was analyzed after one day of starvation. This test showed that processing of cytRosella was not reduced in ERMES mutants while it was absent in $\Delta atg1$ (Figure 10C), which confirms that this process depends on autophagy. In two of the mutants, $\Delta mmm1$ and $\Delta mdm10$, processing rather appeared increased which together with the GFP-Atg8 experiments demonstrates that decreased mitophagy does not correlate with decreased bulk autophagy in ERMES mutants.

Considering the possibility that ERMES might not be required for bulk autophagy but for selective forms of autophagy, the cytoplasm-to-vacuole-targeting (Cvt) pathway was analyzed in ERMES mutants. During the Cvt pathway, a precursor form of Aminopeptidase 1 (prApe1) is constitutively sequestered by autophagic vesicles in the cytosol and transported into the vacuole in an autophagy-dependent manner, where an auto-inhibitory peptide is cleaved off and the enzyme matures into its active form, mApe1 (Lynch-Day and Klionsky, 2010). prApe1 and mApe1 can be separated by SDS-PAGE and detected by Western blotting (Klionsky et al., 1992). WT, $\Delta atg1$ and ERMES mutants were

grown to early stationary phase and cell extracts were analyzed in regard to Ape1 processing. While the $\Delta atg1$ mutant was defective in Ape1 maturation, ERMES mutants processed Ape1 to the same extent as the WT (Figure 10D), which rules out an important role for ERMES in this type of selective autophagy.

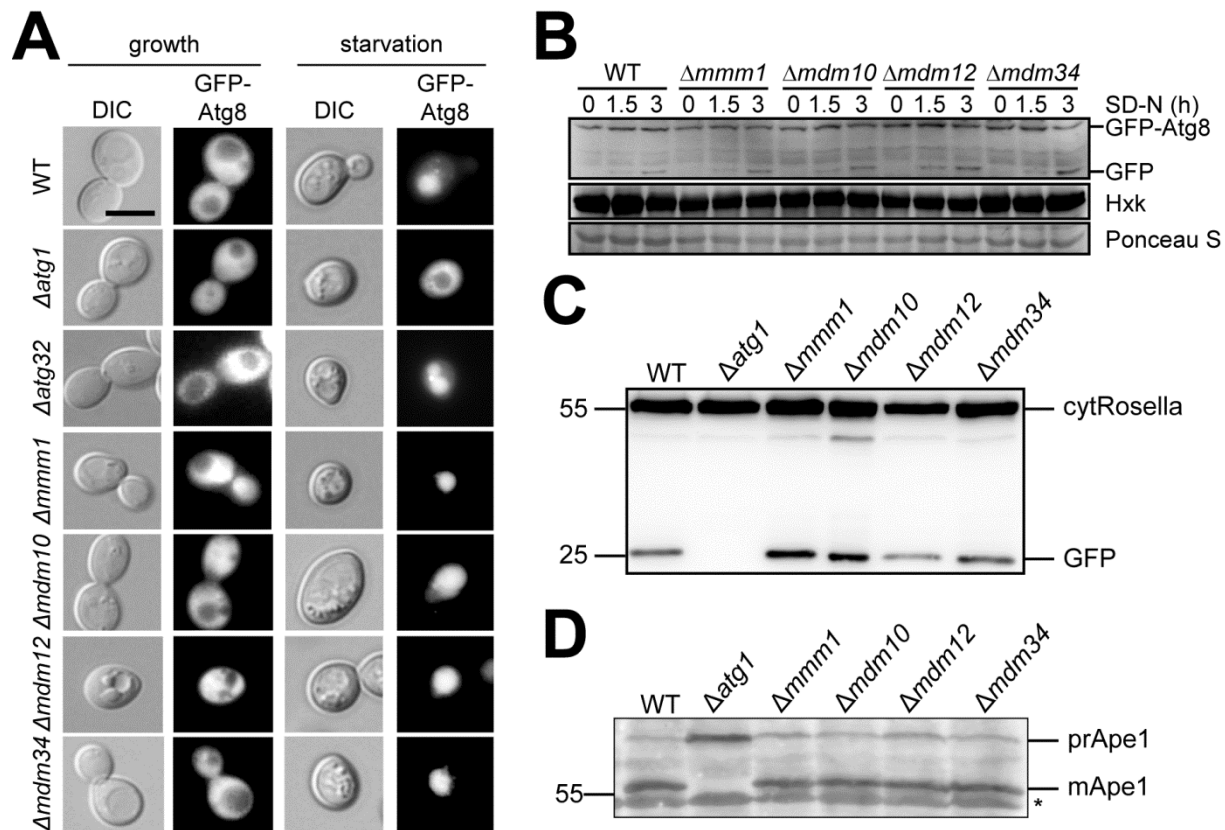


Figure 10. ERMES mutants show normal bulk autophagy and Ape1 processing. (A) Cells expressing GFP-Atg8 from its endogenous promoter were cultured to logarithmic growth in SGalRD (growth) and starved for 5 h (starvation). The localization of GFP-Atg8 was analyzed by fluorescence microscopy. Bar, 5 μ m. (B) Cells expressing GFP-Atg8 from its endogenous promoter were starved for the indicated time points. Cell lysates were subjected to SDS-PAGE and Western blotting. Processing of GFP-Atg8 was assayed using an anti-GFP antibody; Hexokinase (Hxk) and Ponceau S staining served as loading controls. (C) Cells expressing cytosolic Rosella (cytRosella) were cultured in synthetic medium and starved for one day. Cell lysates were subjected to SDS-PAGE and Western blotting using anti-GFP antibodies. The experiment was carried out together with the student Markus Spindler. (D) Cells were cultured to early stationary phase in glucose-containing rich medium, cell lysates were obtained and subjected to SDS-PAGE and Western blotting using anti-Ape1 antibodies. The asterisk marks a cross-reaction of the antibody. prApe1, premature Ape1; mApe1, mature Ape1.

Taken together, these results demonstrate that ERMES-mediated contacts and lipid transport are not necessary for efficient bulk autophagy or the Cvt pathway. This suggests that the mitophagy defect in ERMES mutants is a specific defect of mitochondrial autophagy and not an indirect consequence of other compromised pathways that might be necessary for autophagic degradation of mitochondria.

Altered mitochondrial mass or membrane biogenesis are not the cause of aberrant mitophagy in ERMES mutants

ERMES mutants have a variety of defects. They have a tendency to lose their mitochondrial genome (Merz and Westermann, 2009), form giant, swollen mitochondria (Burgess et al., 1994; Sogo and Yaffe, 1994; Berger et al., 1997; Dimmer et al., 2002) and have problems in outer membrane biogenesis (Meisinger et al., 2004; Meisinger et al., 2007). Presumably, most of these deficits are secondary effects deriving from the altered mitochondrial lipid composition as proposed in Klecker et al. (2014). Thus, it appeared reasonable to consider the possibility that the mitophagy defect in ERMES mutants might also be an indirect effect caused by some of these phenotypes. It is unlikely that the enhanced mtDNA loss is the cause of the mitophagy defect since ρ^0 mutants show no such effect (Figure 7D and E).

Maybe ERMES mutants have an altered mitochondrial mass due to their altered lipid composition and mitochondrial morphology. If they have less mitochondrial mass in the first place, they could degrade the same fraction but less mitochondrial mass than the WT, which could appear as a mitophagy defect. To see whether this was true and whether this was a possible explanation for the mitophagy defect, steady-state levels of marker proteins of mitochondrial sub-compartments were determined in whole cell extracts. Levels of proteins residing in the outer membrane, Tom40, the inner membrane, Ndi1, and in the matrix, Ilv5, were comparable to WT (Figure 11A). It is therefore unlikely that the overall mitochondrial mass is changed in ERMES mutants and that the mitophagy defect is an artefact.

In order to see whether disturbed outer membrane biogenesis or aberrant mitochondrial morphology per se result in mitophagy deficiency, $\Delta mdm33$ and $\Delta sam37$ mutants were assayed for mitophagy. $\Delta mdm33$ cells have mitochondria which form large, hollow spheres (Messerschmitt et al., 2003), whereas $\Delta sam37$ mutants have defects in the assembly of β -barrel proteins in the outer membrane and in the maintenance of mitochondrial morphology, resembling the defects in ERMES mutants (Meisinger et al., 2004). $\Delta mdm33$ and $\Delta sam37$ mutants expressing mtRosella were starved for one day and the fraction of mitophagy positive cells was determined. Mitophagy was effectively taking place in both mutants in a qualitative and quantitative manner (Figure 11B and C). This demonstrates that disturbance of mitochondrial morphology or outer membrane biogenesis does not interfere with mitophagy in general and that these processes are not likely causes of mitophagy defects.

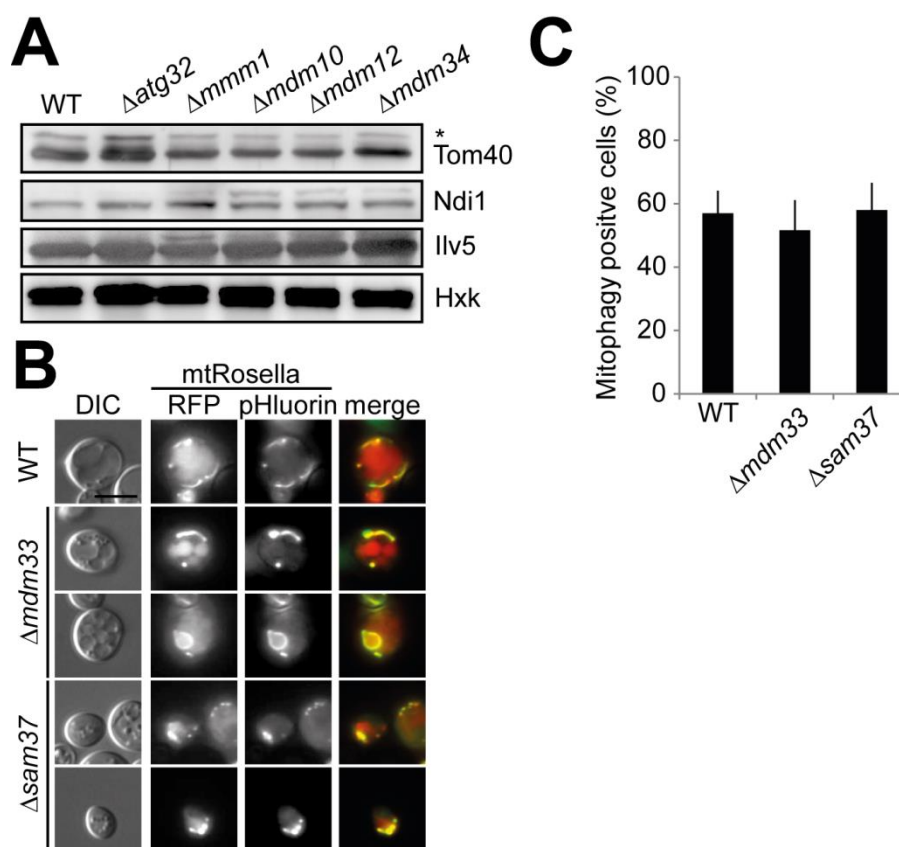


Figure 11. Altered mitochondrial mass, membrane biogenesis or morphology do not explain the mitophagy defect in ERMES mutants. (A) The strains were cultured to logarithmic growth in SGalRD and cell lysates were subjected to SDS-PAGE and Western blotting. Tom40 is a subunit of the preprotein translocase of the mitochondrial outer membrane, Ndi1 is localized in the mitochondrial inner membrane and involved in electron transfer within the respiratory chain, Ilv5 is a mtDNA binding protein and resides in the mitochondrial matrix and Hxk is a cytosolic protein serving as a loading control. The asterisk marks a cross-reaction of the anti-Tom40 antibody. **(B)** Cells expressing mtRosella were cultured to logarithmic growth in SGalRD, starved for one day and analyzed by fluorescence microscopy. Representative images are shown. Bar, 5 μ m. **(C)** 100 cells per strain from (B) were scored for red vacuolar fluorescence. Data are mean percentages + SD from triplicate experiments.

Mitophagy in ERMES mutants is not compromised due to misshapen mitochondria

Since ERMES mutants have such huge mitochondria, it was conceivable that mitophagophores were not able to sequester these mutant mitochondria, even if altered mitochondrial morphology does not result in a mitophagy deficiency per se (Figure 11B and C). To address this question more directly, normal mitochondrial morphology was restored in ERMES mutants and a possible rescue of mitophagy was determined. Defects of ERMES mutants concerning stability of respiratory chain complexes, mitochondrial lipid composition and morphology can be rescued by overexpression of either *MCP1* or *MCP2* (Tan et al., 2013). These genes code for mitochondrial proteins of poorly characterized function, were identified in a screen for overexpression suppressors of $\Delta mdm10$ and were proposed to work in mitochondrial lipid homeostasis (Tan et al., 2013).

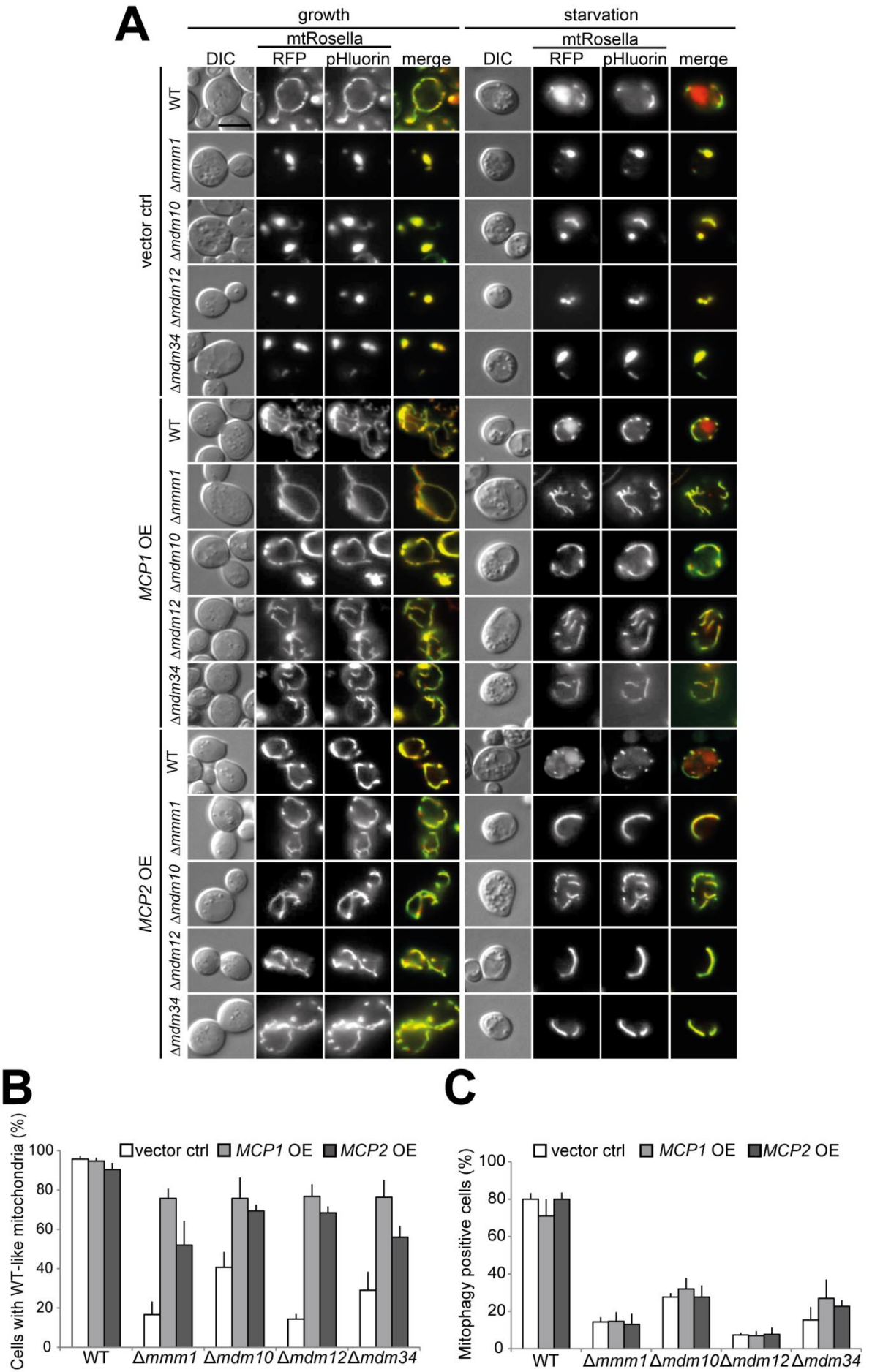


Figure 12. Restoring mitochondrial morphology in ERMES mutants does not rescue mitophagy. (A) Cells expressing mtRosella and carrying *MCP1*, *MCP2* overexpression (OE) plasmids or a vector control were cultured to logarithmic growth, starved for one day and analyzed by fluorescence microscopy before (growth) and after starvation. Representative images are shown. Bar, 5 μ m. **(B)** At least 100 cells per strain from (A) were scored for presence of WT-like mitochondria before starvation. Data represent the mean percentages of triplicate experiments + SD. **(C)** At least 100 cells per strain from (A) were scored for red vacuolar fluorescence after starvation. Data represent the mean percentages of triplicate experiments + SD.

ERMES mutants overexpressing either *MCP1* or *MCP2* showed restoration of mitochondrial morphology under growing conditions as expected (Figure 12A and B) with the tendency of *MCP1* to have stronger effects. The essential question was now, whether the rescued ERMES mutants would still have problems degrading their mitochondria. ERMES mutants overexpressing *MCP1* or *MCP2* were starved for one day and the fraction of mitophagy positive cells was determined by mtRosella. Strikingly, mitophagy was not restored in ERMES mutants with wild type-like mitochondrial morphology (Figure 12A and C). It can thus be excluded that the abnormal mitochondrial morphology is the reason for the mitophagy defect in ERMES mutants. Since *MCP1* and *MCP2* overexpression are thought to also restore mitochondrial lipid composition and stability of respiratory chain complexes (Tan et al., 2013), which has not been confirmed here, these defects are also unlikely to be the origin of the mitophagy defect.

Deletion of *DNM1* in an ERMES mutant background has no additional influence on mitophagy

In recent years it has become evident that mitochondrial ER contacts play an important role during mitochondrial fission in yeast and mammalian cells in a process called ER-assisted mitochondrial division (ERMD; Friedman and Nunnari, 2014). ER tubules wrap around mitochondria and constrict them prior to recruitment of Dnm1 (or the human homolog Drp1), which ultimately divides mitochondrial tubules (Friedman et al., 2011). It has been shown in yeast that ERMD happens at ERMES-mediated contacts and is important for segregation of mtDNA during fission (Murley et al., 2013). Interestingly, Mao et al. (2013) found that the mitophagy adaptor protein Atg11 recruits the mitochondrial division machinery to mitochondria in order to isolate small pieces of mitochondria suitable for mitophagy. They propose that this mitophagy-specific fission process occurs at sites marked by ERMES.

If defective mitochondrial division was the cause for reduced mitophagy in ERMES mutants, the effect should be amplified, when *DNM1* is deleted in an ERMES mutant background, since mitochondrial division would be completely absent then. To this end, double mutants lacking Dnm1 and one of the ERMES subunits (in the following called $\Delta dnm1 \Delta ermes$) were constructed by tetrad dissection, and mitochondrial morphology as well as mitophagy were analyzed (with the notable exception of $\Delta dnm1 \Delta mmm1$ because the two loci reside on the same chromosome and meiotic recombination was too rare and thus no double mutants were obtained). $\Delta dnm1$ showed net-like mitochondria and ERMES mutants had big, globular mitochondria as expected (Figure 13A and B).

The mitochondrial morphology of ERMES mutants is epistatic to the *DNM1* deletion, as $\Delta dnm1$ $\Delta ermes$ double mutants had the same morphology as the ERMES single mutants, but did not show any net-like structures.

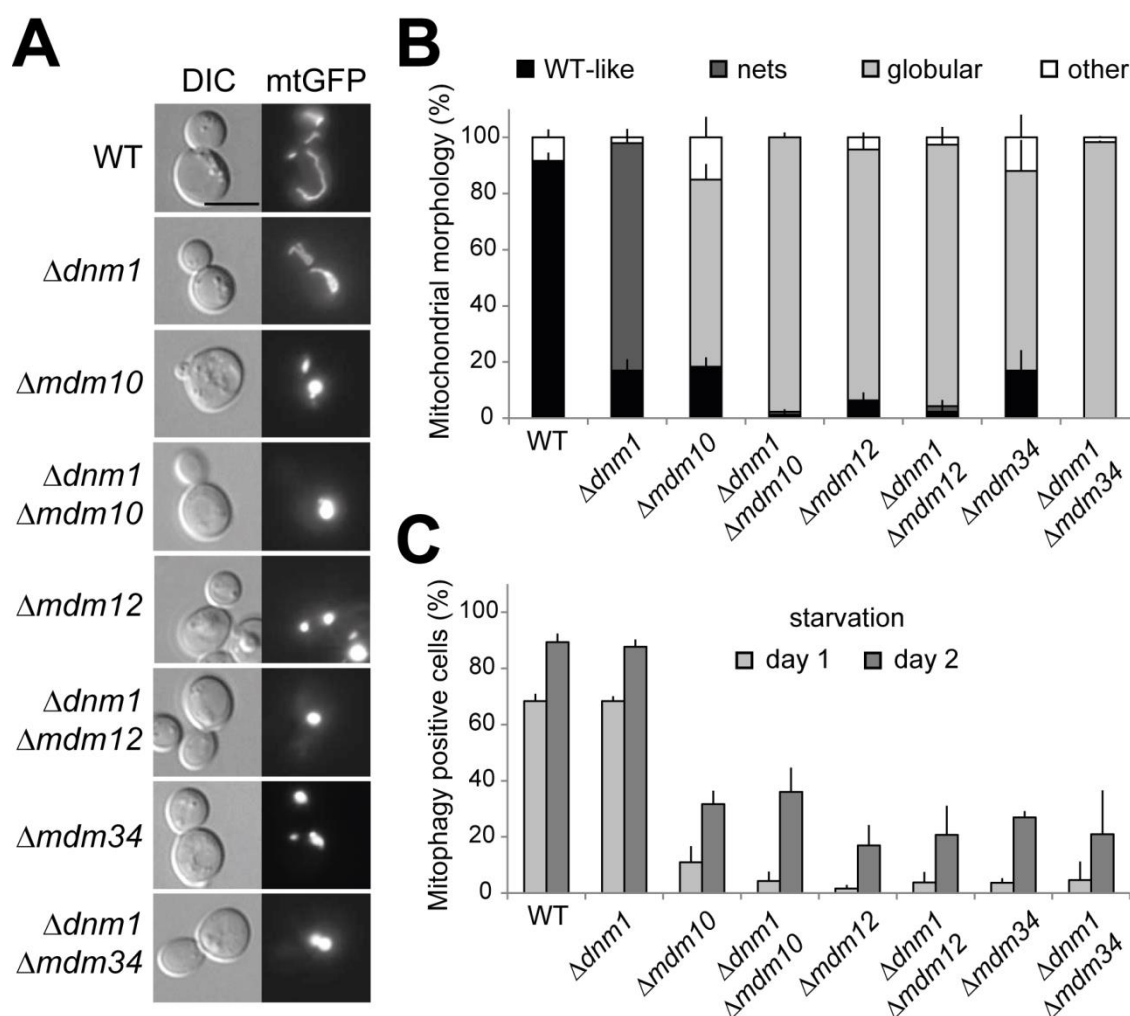


Figure 13. Analysis of $\Delta dnm1$ $\Delta ermes$ double mutants with regard to mitochondrial morphology and mitophagy. (A) Cells expressing mtGFP were cultured to logarithmic growth in glucose-containing synthetic medium and analyzed by fluorescence microscopy. Representative images are shown. Bar, 5 μ m. (B) Cells were prepared as in (A) and at least 100 cells per strain were scored for mitochondrial morphology. Data represent the mean percentages of triplicate experiments + SD. (C) Cells expressing mtRosella were cultured to logarithmic growth in SGalRD, starved for the indicated time points and analyzed by fluorescence microscopy. At least 100 cells were scored for red vacuolar fluorescence at the indicated time points. Data represent the mean percentages of triplicate experiments + SD.

In terms of mitophagy, the $\Delta dnm1$ mutants behaved like the WT (Figure 13C). ERMES single mutants showed almost no mitophagy after one day of starvation, but detectable levels after two days. These levels were very similar to the ones of the corresponding double mutants, suggesting that *DNM1* deletion in an ERMES mutant background does not augment the mitophagy defect. Thus, hampered mitochondrial division is not a likely cause of the defect in ERMES mutants.

The observation that the ERMES mutants had only very few mitophagy positive cells after one day of starvation in this experiment in comparison to earlier experiments (for example Figure 9B) can be explained in terms of strain construction. In former experiments, the strains were obtained from a deletion library and these strains carried the deletions for many generations and had the opportunity to adapt by epigenetic modifications or age-associated changes. In this experiment, however, strains were derived from tetrad dissection after sporulation. It is known that yeast cells are cured from age-associated damages during gametogenesis and life-span is reset (Unal et al., 2011). This may explain the different outcome of these experiments.

Artificial mitochondrial ER tethering promotes mitophagy in the absence of ERMES

The ERMES complex has initially been identified in a synthetic biology screen (Kornmann et al., 2009). It had been considered that if tethering of mitochondria to the ER is important, mutation of potential tethering proteins would be harmful to the cell and might be complemented by expression of an artificial tether named chiMERA. chiMERA consists of the transmembrane domain derived from the MOM protein Tom70 at the N-terminus and of the ER tail anchor of Ubc6, which are connected by a GFP moiety allowing microscopic visualization of the protein (Figure 14A). Using this construct, Kornmann et al. (2009) were able to show that Mmm1, Mdm10, Mdm12 and Mdm34 connect ER and mitochondria.

If the mitophagy defect in ERMES mutants was directly caused by loss of proximity between the ER and mitochondria, it could be predicted that expression of chiMERA restores mitophagy in the mutants by connecting mitochondria and ER. ERMES mutants expressing chiMERA under control of two different promoters were starved and the percentage of mitophagy positive cells was determined by using mtRosella. chiMERA slightly reduced mitophagy in WT, whereas strikingly the process was largely restored in $\Delta mmm1$, $\Delta mdm10$ and $\Delta mdm34$, but not in $\Delta mdm12$ (Figure 14B). This indicates that loss of contacts between mitochondria and the ER per se is the major cause of the mitophagy defect in ERMES mutants.

Epifluorescence (Figure 14C) and confocal (Figure 14D) microscopy confirmed that chiMERA exhibits a preferentially ER-like staining pattern, which partially overlaps with mitochondria as has already been described (Kornmann et al., 2009). This was also true for $\Delta mdm12$, indicating that chiMERA is properly localized in this mutant. Steady-state levels of chiMERA showed that only low levels were present in $\Delta mdm12$ (Figure 14E). They were, however, comparable to $\Delta mdm34$ for the P_{ADH} construct and to $\Delta mdm10$ for the P_{TEF} construct, in which the rescue worked. This might suggest that Mdm12 has an additional role in mitophagy apart from mitochondrial ER tethering.

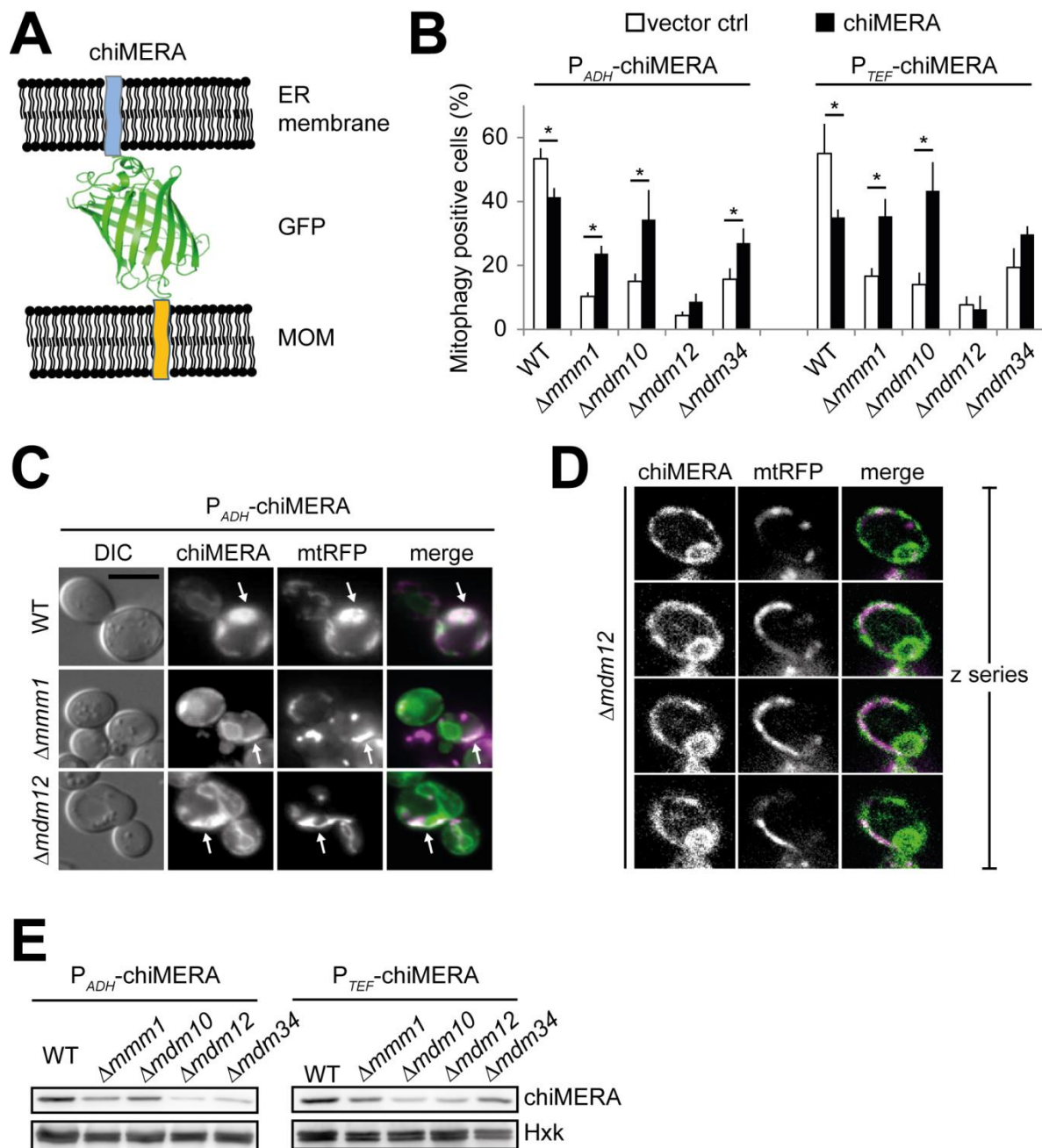


Figure 14. Expression of chiMERA rescues the mitophagy defect in ERMES mutants. (A) Schematic representation of chiMERA, which consists of an ER and a mitochondrial transmembrane anchor at either terminus which are linked by GFP. **(B)** Cells expressing mtRosella and chiMERA either from *ADH* or *TEF* promoter or carrying a vector control were cultured to logarithmic growth and starved for two days. At least 100 cells were scored for red vacuolar fluorescence. Values represent the mean of at least two independent experiments. Asterisks indicate statistical significance (* $p < 5\%$; two-tailed Student's t-test). **(C)** Cells expressing chiMERA from the *ADH* promoter and mtRFP were cultured in SGaIRD and chiMERA localization was analyzed by fluorescence microscopy. Arrows indicate colocalization of chiMERA and mitochondria. Bar, 5 μ m. **(D)** $\Delta mdm12$ cells prepared as in (C) were analyzed by confocal microscopy. Images are from a z-series with a distance of 0.6 μ m between the planes. **(E)** Lysates from cells expressing chiMERA either from *ADH* or *TEF* promoter were subjected to SDS-PAGE and Western Blotting. chiMERA was detected using anti-GFP antibodies. Hexokinase (Hxk) served as a loading control.

Mitophagosomes form at ER-mitochondria contact sites

Since loss of direct contacts between ER and mitochondria is the main cause of mitophagy deficiency in ERMES mutants (Figure 14), it was considered that mitophagosomes might form at ERMES-mediated contacts in yeast. To test this, autophagosomes were labeled with GFP-Atg8, ERMES was visualized by Mmm1-ERFP and cells were starved for one hour to induce formation of autophagosomes. Mmm1 signals in close vicinity to or even overlapping with GFP-Atg8 could be observed in the case of small Atg8 patches, nascent isolation membranes and mature autophagosomes (Figure 15A). Quantification revealed that ERMES is associated with Atg8 patches in over 40% of the cells and that this is increased to over 75% when isolation membranes and mature autophagosomes were analyzed (Figure 15B). Additional staining of the vacuole demonstrated that ERMES is present at the isolation membrane edge distal to the vacuole, which presumably is its growing end (Figure 15C). Since ERMES mutants have a mitophagy-specific defect (Figure 10), these structures likely represent mitophagosomes, and the association between them and ERMES indicates that ERMES has a direct role in their biogenesis.

To confirm that mitophagosomes form at these contact sites, the localization of GFP-Atg32 and Mmm1-ERFP was analyzed. GFP-Atg32 stains the mitochondrial network under growing conditions, but concentrates during starvation into few distinct foci (Kanki et al., 2009b) likely marking mitophagosomes. These GFP-Atg32 foci overlap with ERMES marked by Mmm1-ERFP (Figure 15D), strengthening the idea that mitophagosomes form at mitochondrial ER-contacts.

If mitophagosomes form at mitochondrial ER contacts, the Atg32-marked mitophagosomes should colocalize not only with ERMES but also with the ER in general. To test this idea, the ER was stained with GFP targeted to the ER lumen by a signal sequence and fused to the retention signal HDEL. Mitophagosomes were stained with ERFP-Atg32. After a two hour starvation, colocalization of ER and mitophagosomes could be seen (Figure 15E).

In sum, these results demonstrate that mitophagosomes form at ERMES-mediated mitochondrial ER contacts and that ERMES localizes to the growing end of the mitophagophore, which suggests that the contacts contribute to the progression of mitophagosome development.

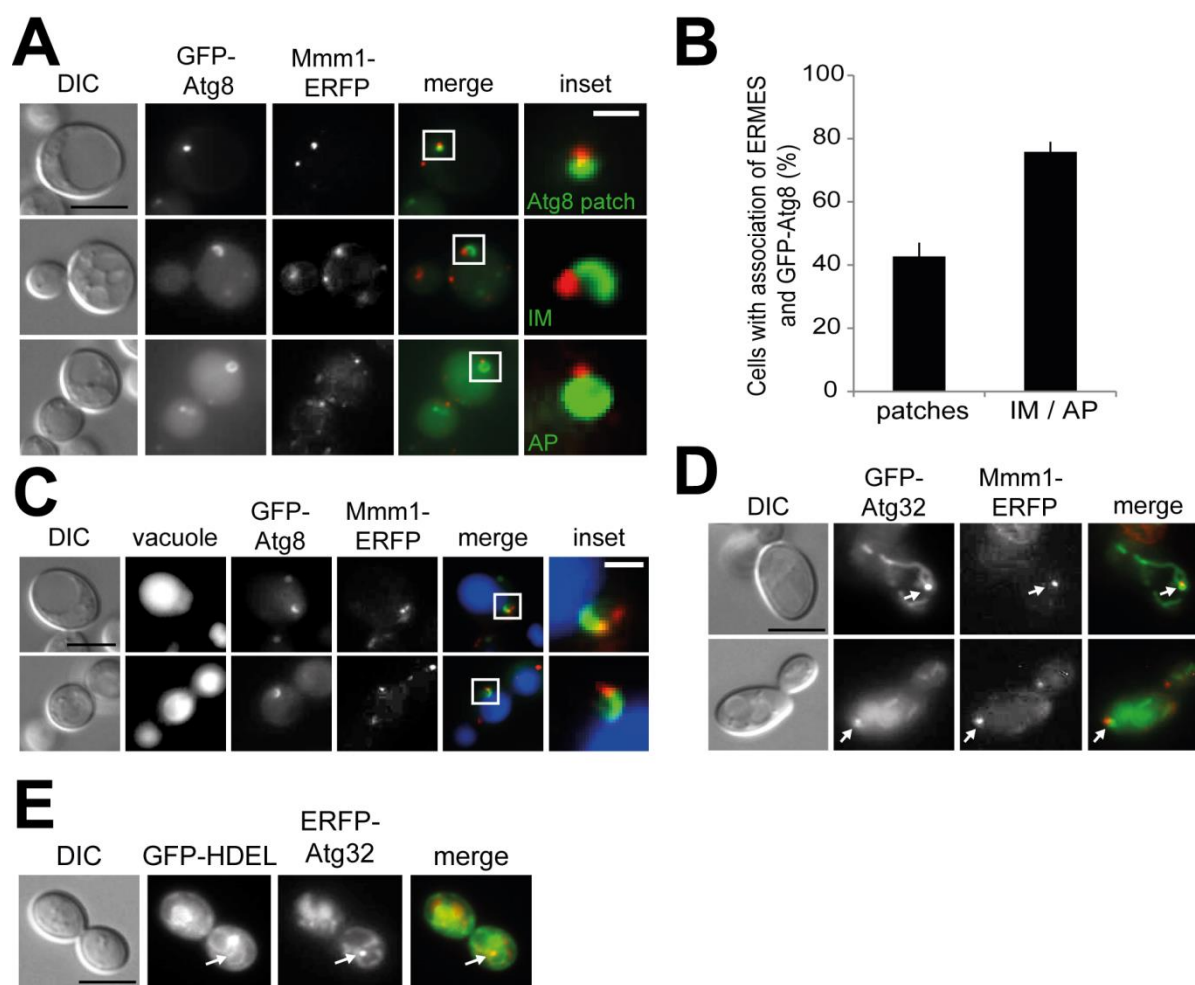


Figure 15. Mitochondrial ER contacts are sites of mitophagosome biogenesis. (A) $\Delta mmm1$ cells expressing plasmid-borne GFP-Atg8 and Mmm1-ERFP from their endogenous promoters were cultured to logarithmic growth in SGalRD, starved for 1 h and analyzed by fluorescence microscopy. IM, isolation membrane; AP, mature autophagosome. Bars, 5 μ m (main images); 1 μ m (insets). (B) Cells from (A) were quantified for association of GFP-Atg8 patches or IMs and APs with Mmm1-ERFP. Values represent the mean of triplicate experiments + SD (n = 194 cells). (C) $\Delta mmm1$ cells were prepared as in (A) and the vacuole was stained using CellTracker Blue CMAC. Bars, 5 μ m (main images); 1 μ m (insets). (D) Cells expressing GFP-Atg32 from the *MET25* promoter and Mmm1-ERFP were cultured in SGalRD with 10 μ g/ml methionine to logarithmic growth, starved for 2 h and analyzed by fluorescence microscopy. Arrows indicate the sites of overlapping signals. Bar, 5 μ m. (E) $\Delta atg32$ cells expressing GFP targeted to the ER (GFP-HDEL) and ERFP-Atg32 from the *MET25* promoter were prepared and analyzed as in (D). Arrows mark sites of overlapping signals. Bar, 5 μ m.

Mmm1 interacts with Atg8 in vivo independent of Atg8 lipidation

Since ERMES and Atg8 associate during mitophagy, it was tested whether Mmm1 and Atg8 directly interact. To this end, GFP-tagged Atg8 was isolated from cell extracts of starved cells with beads coated with anti-GFP single chain antibodies. Eventually, co-immunoprecipitation of Protein A-tagged Mmm1 was tested. GFP-Atg8 was efficiently purified by IP together with free GFP (Figure 16A), which presumably was released during autophagy-dependent processing of GFP-Atg8. However, Mmm1

was not detectable in the eluate fraction, indicating that ERMES and Atg8 either do not interact or the interaction is unstable or transient and the interacting proteins cannot be co-purified from cell extracts. Alternatively, the ProteinA and the GFP tags of Mmm1 or Atg8 might hinder the interaction.

In order to detect an interaction of Mmm1 and Atg8 *in vivo*, a bimolecular fluorescence complementation (BiFC) approach was used. In this assay, two proteins of interest are each fused to two different fragments of a fluorescent protein (Kerppola, 2008a, b). The fragments do not give fluorescence signals when expressed within one cell unless they are brought into close proximity by tagging them with two interacting proteins (Hu et al., 2002). Thus, interactions of proteins can be detected in living cells. Accordingly, the C-terminus of Mmm1, which is exposed to the cytosol (Burgess et al., 1994), was fused to the C-terminal fragment of an enhanced YFP (Nagai et al., 2002), called Y_C. Atg8 was tagged with the N-terminal fragment of YFP, Y_N, at its N-terminus because at its C-terminus an arginine is cleaved off during starvation (Ichimura et al., 2000; Kirisako et al., 2000) and the C-terminus is therefore unsuitable for tagging. The fusion proteins were expressed from multicopy plasmids and were under control of the *ADH* promoter in a BiFC expression system adopted to yeast (Skarp et al., 2008). Initially, a $\Delta atg1$ strain was used since Atg proteins are recruited to PAS in this strain, but turnover of the autophagosomes is blocked (Suzuki et al., 2007) and it was thus expected that interactions of proteins involved in mitophagosome biogenesis are more stable.

After starvation, fluorescence complementation was observed between Mmm1-Y_C and Y_N-Atg8 but not between the appropriate controls (Figure 16B), demonstrating an interaction between the two proteins *in vivo*. As expected, this interaction occurred on the mitochondrial surface (Figure 16C). In order to test, whether the interaction depends on the post-translational modification and localization of Atg8, BiFC was analyzed in $\Delta atg3$, where Atg8 cannot be coupled to PE (Ichimura et al., 2000). Moreover, Atg8 cannot be targeted to the PAS when its lipidation is obstructed as can be seen in $\Delta atg3$ after starvation (Figure 16D). WT, $\Delta atg1$ and $\Delta atg3$ cells showed fluorescence complementation, which demonstrates that Atg8 lipidation and PAS localization are not necessary for the Mmm1-Atg8 interaction (Figure 16E).

In sum, these results show that Mmm1 and Atg8 interact in the course of mitophagy on the mitochondrial surface independent of Atg8 lipidation, suggesting that ERMES plays a direct role in mitophagosome biogenesis prior to lipidation of Atg8 with PE.

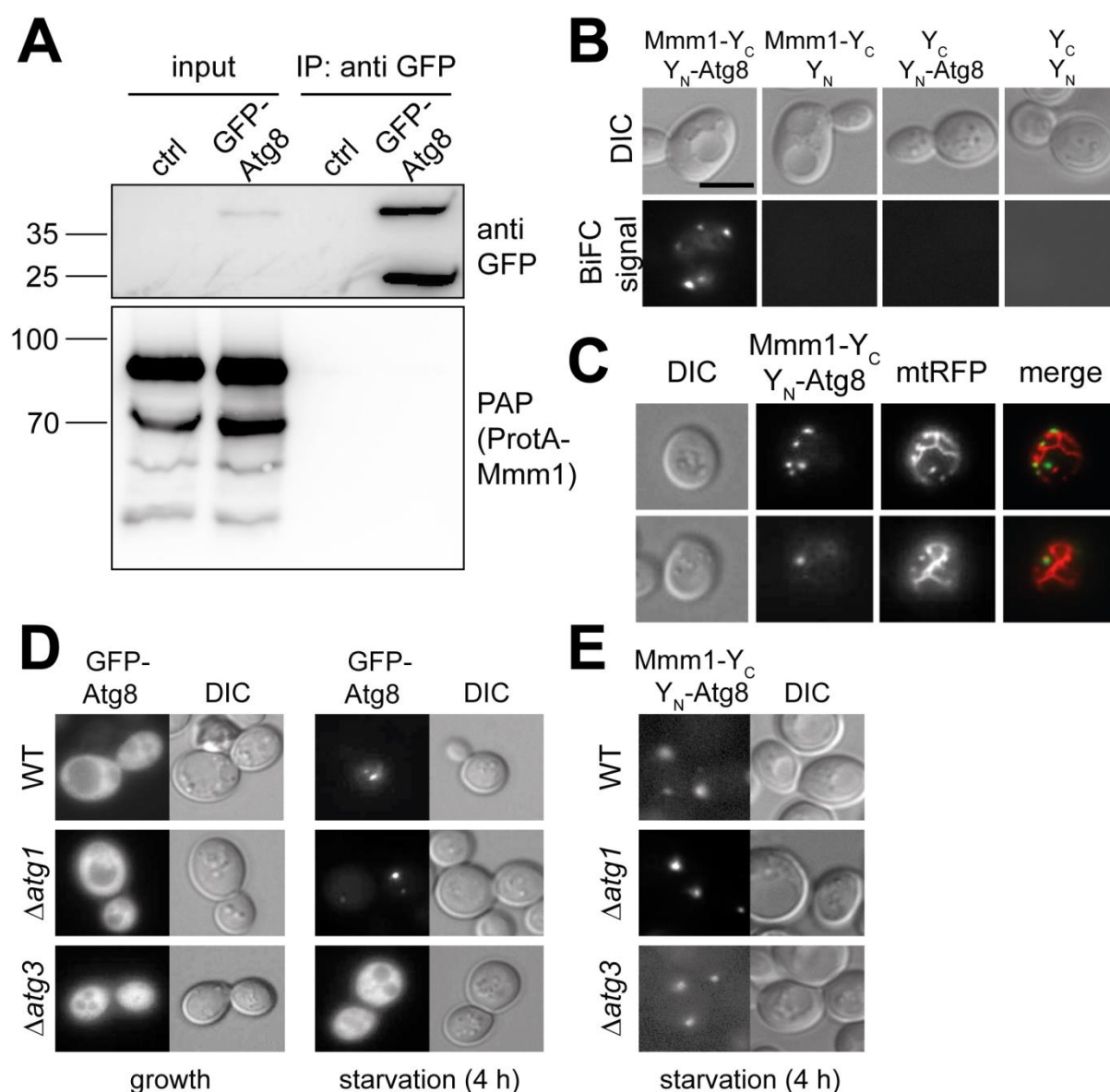


Figure 16. Analysis of Mmm1 and Atg8 interaction. (A) Strains expressing ProtA-Mmm1 and carrying either an empty vector (ctrl) or a vector coding for GFP-Atg8 were cultured in synthetic medium with glycerol (3%) and small amounts of glucose (0.1%) to logarithmic growth, starved for 1 h and harvested. After shock-freezing, cryo-grinding and solubilisation, co-immunoprecipitation was performed using GFP binding protein coupled beads and subsequently input (0.5%) and IP (10%) fractions were subjected to SDS-PAGE and Western blotting using anti-GFP and PAP antibodies. (B) $\Delta atg1$ cells expressing the indicated split-YFP fusions or control proteins were cultured to logarithmic growth in SGalRD, starved for 3 - 4 h and analyzed by fluorescence microscopy. Y_C, C-terminal fragment of YFP; Y_N, N-terminal fragment of YFP. Bar, 5 μ m. (C) $\Delta atg1$ cells expressing Mmm1-Y_C, Y_N-Atg8 and mtRFP were prepared and analyzed as in (B). (D) Cells expressing GFP-Atg8 from its endogenous promoter were prepared as in (B) and analyzed before (growth) and after 4 h of starvation. (E) Cells expressing Mmm1-Y_C and Y_N-Atg8 were prepared and analyzed as in (B).

ERMES is dispensable for mitochondrial localization of Atg8

Atg32 interacts with both Atg8 and Atg11 in the course of mitophagy (Kanki et al., 2009b; Okamoto et al., 2009) and is necessary for the recruitment of Atg8 to mitochondria (Okamoto et al., 2009). Since ERMES colocalizes and interacts with Atg8 during mitophagosome biogenesis, it appeared reasonable to assume that ERMES might also be important for the recruitment of Atg8 to mitochondria or for the interaction of Atg8 with Atg32.

Mitochondrial localization of GFP-Atg8 was therefore tested in $\Delta atg32$, ERMES single and $\Delta atg32 \Delta ermes$ double mutants by fluorescence microscopy after starvation. Surprisingly, Atg8 was efficiently targeted to mitochondria independent of all deletions tested (Figure 17A), which suggests that neither Atg32 nor ERMES is necessary for Atg8 recruitment to mitochondria. This is in contrast to observations made by Okamoto et al. (2009) who showed that Atg8 cannot target to mitochondria in the absence of Atg32. In these experiments mitophagy was induced by culturing the cells on non-fermentable carbon sources to stationary phase and this difference might be the reason for the conflicting results, which means that ERMES and Atg32 are dispensable for Atg8 recruitment to mitochondria under the conditions used here. Another possible explanation is that determining mitochondrial recruitment of Atg8 by fluorescence microscopy is not sensitive enough and mitochondrial Atg8 localization occurred by chance in $\Delta atg32$ and ERMES mutants. However, no evidence was found in favor of the hypothesis that ERMES recruits Atg8 to mitochondria.

Still, ERMES could be important for the interaction of Atg8 and Atg32, which occurs on the mitochondrial surface and marks mitochondria for degradation (Mao et al., 2013). Colocalization of GFP-Atg8 and ERFP-Atg32 was tested as an indicator of protein-protein-interaction in WT and ERMES mutants after starvation. Fluorescence microscopy showed that colocalization of the two proteins could be observed in all strains (Figure 17B), indicating that the interaction of both proteins was not hampered, that this step of mitophagy is not disturbed and that mitophagy is blocked at a later stage.

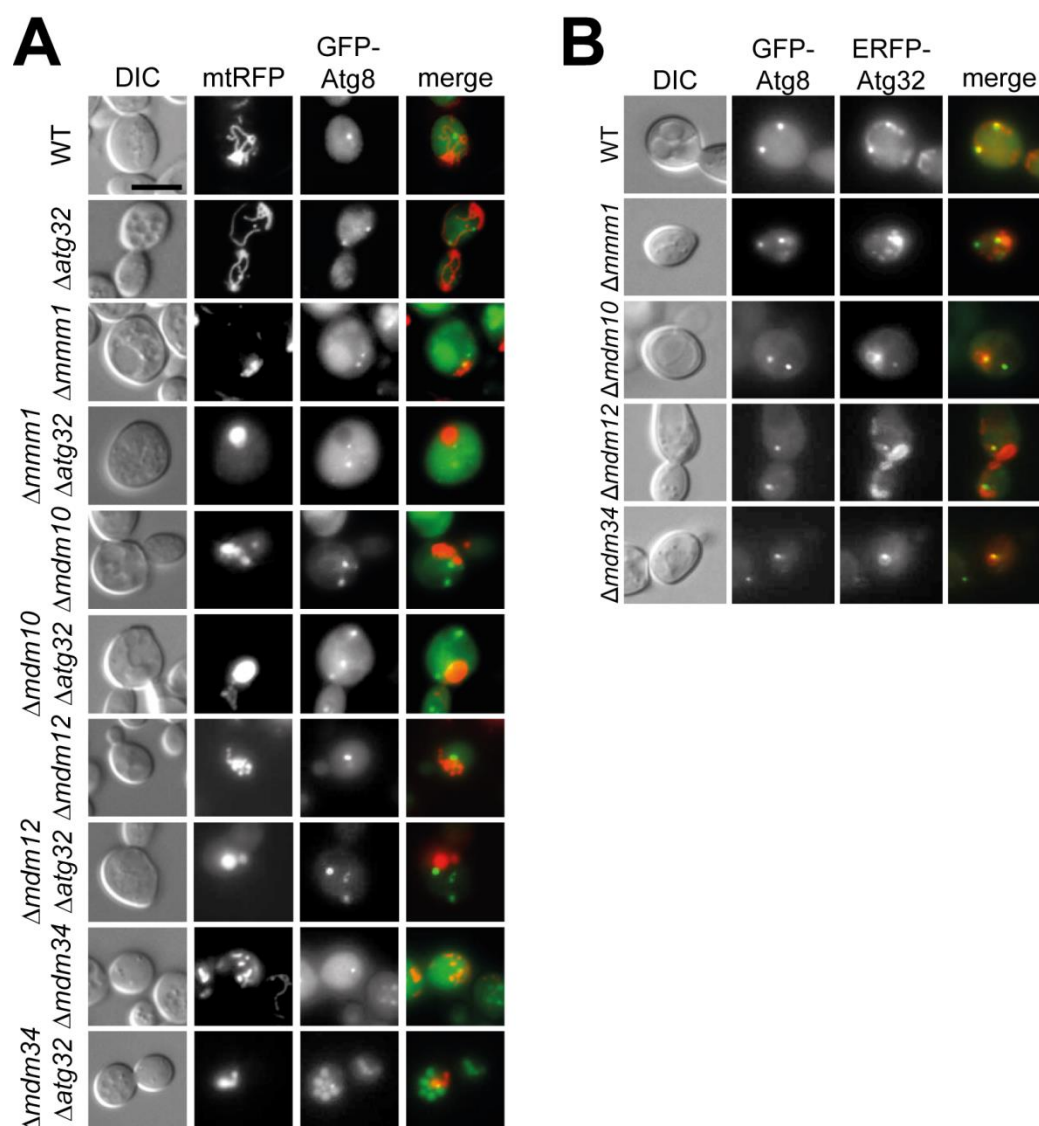


Figure 17. ERMES is not necessary for Atg8 recruitment to mitochondria. (A) Cells expressing mtRFP and GFP-Atg8 from its endogenous promoter were cultured to logarithmic growth in SGalRD, starved for 4 h and analyzed by fluorescence microscopy. Bar, 5 μm . **(B)** Cells expressing GFP-Atg8 from its endogenous promoter and ERFP-Atg32 from the *MET25* promoter were cultured to logarithmic growth in SGalRD with 10 $\mu g/ml$ methionine, starved for 1 - 2 h and analyzed by fluorescence microscopy.

Mitochondrial ER contacts are important for the formation of the mitophagophore

During bulk and selective autophagy, Atg proteins coalesce at the PAS (Suzuki et al., 2001). From this dot-like structure, an isolation membrane or phagophore (mitophagophore in the case of mitophagy) grows and matures into an autophagosome (mitophagosome in the case of mitophagy). It has been shown in a recent study that Atg proteins are differentially distributed along the phagophore and mark different steps of phagophore biogenesis (Suzuki et al., 2013).

In order to determine whether mitophagy is blocked at a particular step, two different Atg proteins were chosen as markers and their localization was analyzed in WT and $\Delta mmm1$ after starvation. Atg14-GFP is a component of the phosphatidylinositol 3-kinase (PI3K) complex (Kihara et al., 2001; Obara et al., 2006) and marks an early step of membrane growth, as it is present at the junction between vacuole and phagophore termed vacuole-isolation membrane contact site (VICS; Suzuki et al., 2013). Atg5-GFP is in a complex with Atg12 and Atg16 and contributes to lipidation of Atg8 (reviewed in Mizushima et al., 2011; Ohsumi, 2001). The complex is not a constituent of mature autophagosomes (Suzuki et al., 2001), but labels growing phagophores (Suzuki et al., 2013).

As expected Atg14-GFP and Atg5-GFP both colocalize with ERMES after starvation (Figure 18A), which further demonstrates the presence of ERMES at the site of mitophagosome biogenesis. Atg14-GFP shows a punctate pattern on mitochondria in WT as well as in $\Delta mmm1$ (Figure 18B), indicating that formation of the VICS is not affected in ERMES mutants, which is consistent with the finding that Atg8-Atg32 colocalization was not affected (Figure 17B). Atg5-GFP also exhibits this staining pattern but only in WT cells (Figure 18C, upper panels). In absence of ERMES, Atg5-GFP was present in multiple dots on mutant mitochondria (Figure 18C, middle panels). Quantification of Atg5-GFP dots showed that they are significantly enriched in $\Delta mmm1$ (Figure 18D).

As has already been noted, a recent study proposed that ERMES is present at sites of mitophagy-specific fission because it is involved in ERMD (Mao et al., 2013). If compromised mitochondrial fission was the reason for the Atg5-GFP phenotype, it should also be visible in the $\Delta dnm1$ mutant, where mitochondrial fission is absent. Analysis of Atg5-GFP in $\Delta dnm1$ after starvation revealed that only one to two Atg5-GFP structures marking autophagosomal membrane growth are present at the giant mitochondrial networks (Figure 18C and D) and that fission defects are not the cause of aberrant mitophagosome biogenesis in ERMES mutants. This is in good agreement with the experiments that exclude compromised ERMD as origin of the mitophagy defect in ERMES mutants (Figure 13).

Taken together, these results strongly suggest that mitophagy is blocked in ERMES mutants at the step after induction of mitophagosome biogenesis at mitochondria, where the mitophagophore grows. Excess mitophagophores likely arise in $\Delta mmm1$ because limited lipid transport from the ER to the growing mitophagophore prevents maturation of phagophores and mitophagosome biogenesis is induced at a different site of the mitochondrion. In the wild type situation on the other hand, ERMES promotes mitophagy by ensuring spatial proximity between mitochondria, ER, and the phagophore expansion factor Atg8 and thus likely facilitates lipid flux from the ER to the growing phagophore.

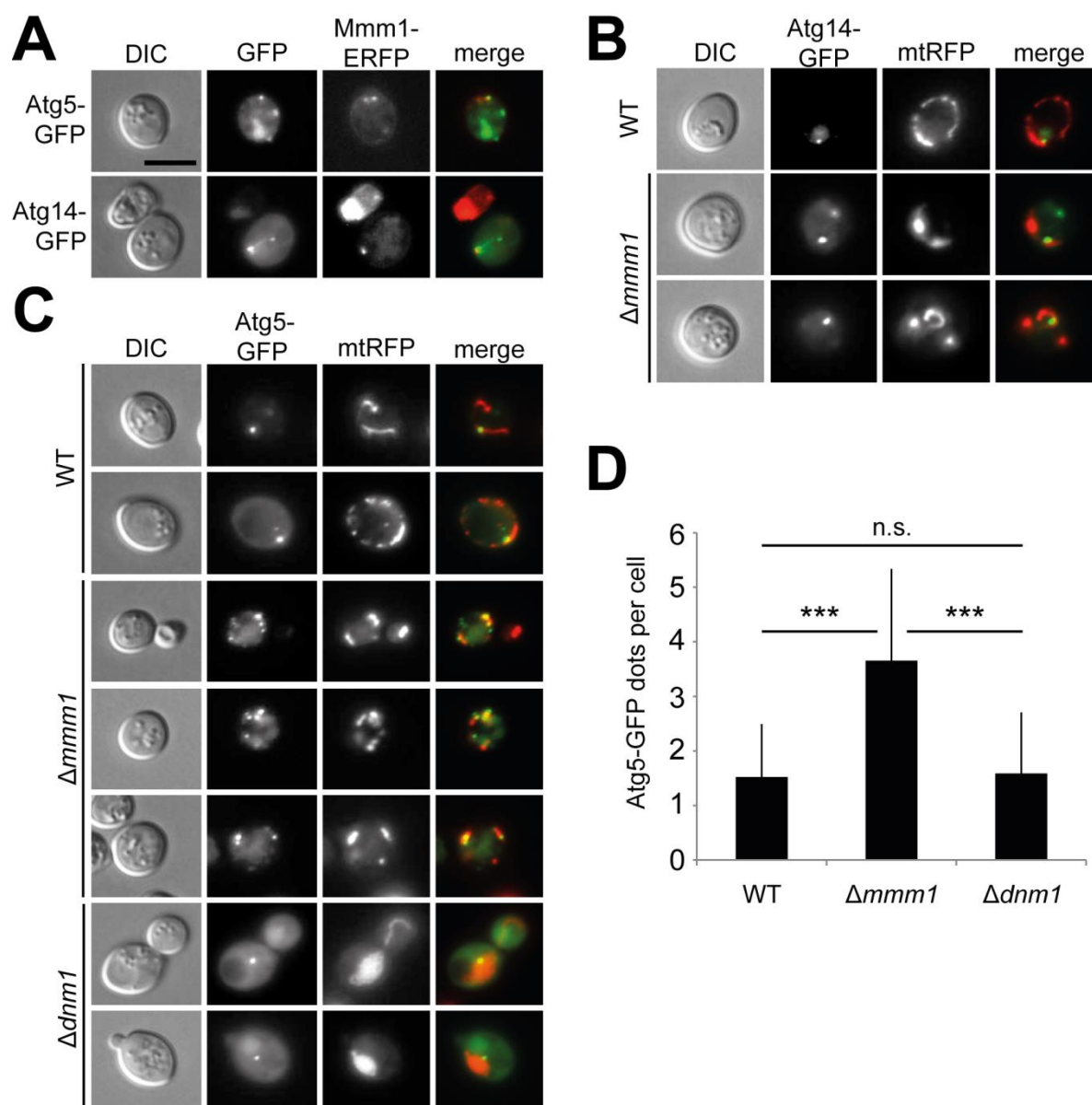


Figure 18. $\Delta mmm1$ cells show an altered staining pattern of the phagophore marker Atg5. (A) $\Delta mmm1$ cells expressing either Atg5-GFP (upper panel) or Atg14-GFP (lower panel) from the *GPD* promoter and Mmm1-ERFP from its endogenous promoter were cultured to logarithmic growth in SGaRD, starved for 1.5 h and analyzed by fluorescence microscopy. Bar, 5 μ m. (B, C) Cells expressing Atg14-GFP or Atg5-GFP from the *GPD* promoter and mtRFP were prepared and analyzed as in (A). (D) Cells were prepared as in (C) and scored for Atg5-GFP dots in cells with at least one dot. Data represent the mean of at least 150 cells per strain + SD. Asterisks indicate statistically significant differences (*** $p < 0.05\%$; n. s., not significant; two-tailed Student's t-test).

Mitophagophore biogenesis is rescued by artificial ER-mitochondria tethering but not by restoring normal mitochondrial morphology

Artificial mitochondrial ER tethering by ERMES restores mitophagy in ERMES mutants (Figure 14). If the surplus Atg5-GFP structures (Figure 18) represent the major defect responsible for the mitophagy deficit, this phenotype should also be rescued by expression of chiMERA.

Indeed, chiMERA had no influence on the quantity of Atg5-GFP dots in WT cells, but strikingly reduced the amount to a wild type-like level in $\Delta mmm1$ (Figure 19A and B). This result demonstrates that loss of mitochondrial ER contacts is the reason for the Atg5-GFP phenotype and that restoring these contacts leads to physiological mitophagophore biogenesis and in consequence to reestablished mitophagy.

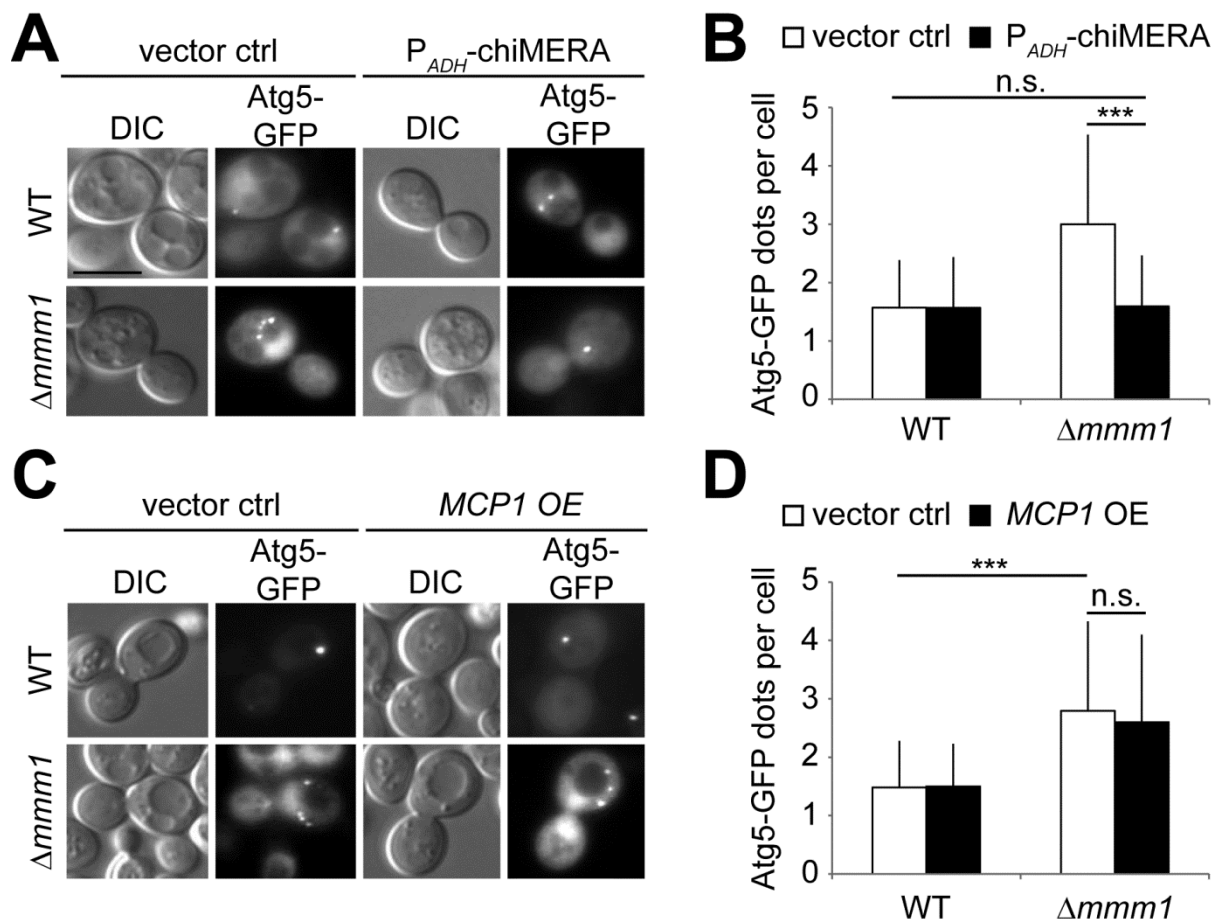


Figure 19. Expression of chiMERA but not *MCP1* overexpression rescues the Atg5-GFP phenotype of $\Delta mmm1$ cells. (A) Cells expressing Atg5-GFP from the *GPD* promoter and chiMERA from the *ADH* promoter or carrying a vector control were cultured to logarithmic growth in SGaIRD, starved for 1.5 h and analyzed by fluorescence microscopy. (B) Cells from (A) were scored for Atg5-GFP dots per cell in cells with at least one dot. Data represent the mean of at least 75 cells per strain + SD. (C) Cells expressing Atg5-GFP from the *GPD* promoter and overexpressing *MCP1* from the *TPI* promoter or carrying a vector control were prepared and analyzed as in (A). (D) Cells from (C) were analyzed as in (B). Asterisks indicate statistical significance (***) $p < 0.05$; n. s., not significant; two-tailed Student's t-test).

In order to test whether this was a specific effect of chiMERA, mitochondrial morphology and lipid composition was restored in $\Delta mmm1$ by overexpression of *MCP1*, which did not rescue mitophagy (Figure 12). *MCP1* overexpression did not have an effect on the quantity of Atg5-GFP dots, neither in WT nor in $\Delta mmm1$ (Figure 19C and D), showing that mutant mitochondrial morphology is not the reason for the Atg5 phenotype.

Taken together, these results are in good agreement with the findings that only the reestablishment of mitochondrial ER contacts, but not of mitochondrial morphology, rescues the mitophagy defect in ERMES mutants. Furthermore, they demonstrate that ER-mitochondria contacts are important for regular maturation of mitophagophores.

ERMES is important for the localization of Atg9 to mitochondria

Atg9 is outstanding among the Atg proteins because it is the only Atg protein with transmembrane domains (Noda et al., 2000). Atg9-positive vesicles do not only localize to the PAS but also to dot-like structures on or near mitochondria already under nutrient-rich conditions and are thought to provide membrane material to the phagophore (Mari et al., 2010). Atg9-GFP labels the edges of the phagophore (Suzuki et al., 2013), where membrane growth likely occurs. If ERMES is important for growth of the phagophore and if this growth is compromised in $\Delta mmm1$, Atg9-GFP staining patterns should be altered in ERMES mutants.

It was first tested whether Atg9-GFP colocalizes with ERMES, which was indeed the case (Figure 20A). Interestingly, this association could already be seen under nutrient-rich conditions and independently of mitophagy induction. Atg9-GFP dots localized to mitochondria under nutrient-rich and under starvation conditions in WT cells (Figure 20B, upper panels). In nutrient-rich medium, the staining pattern of Atg9-GFP changed in some cells of $\Delta mmm1$, but it was still present on mitochondria (Figure 20B, lower panels). If mitophagy was induced by starvation, the appearance of the Atg9-GFP staining was completely altered in cells lacking ERMES. While Atg9-GFP was present as a distinct dot on a single mitochondrion in wild type cells, these discrete structures were rare in $\Delta mmm1$ and Atg9 positive structures wrapped around a mitochondrion (Figure 20B).

In sum, ERMES is important for correct localization of Atg9 after induction of mitophagy. Since Atg9 is important for the growth of the phagophore, this further strengthens the idea that ERMES is a vital hub for mitophagophore biogenesis.

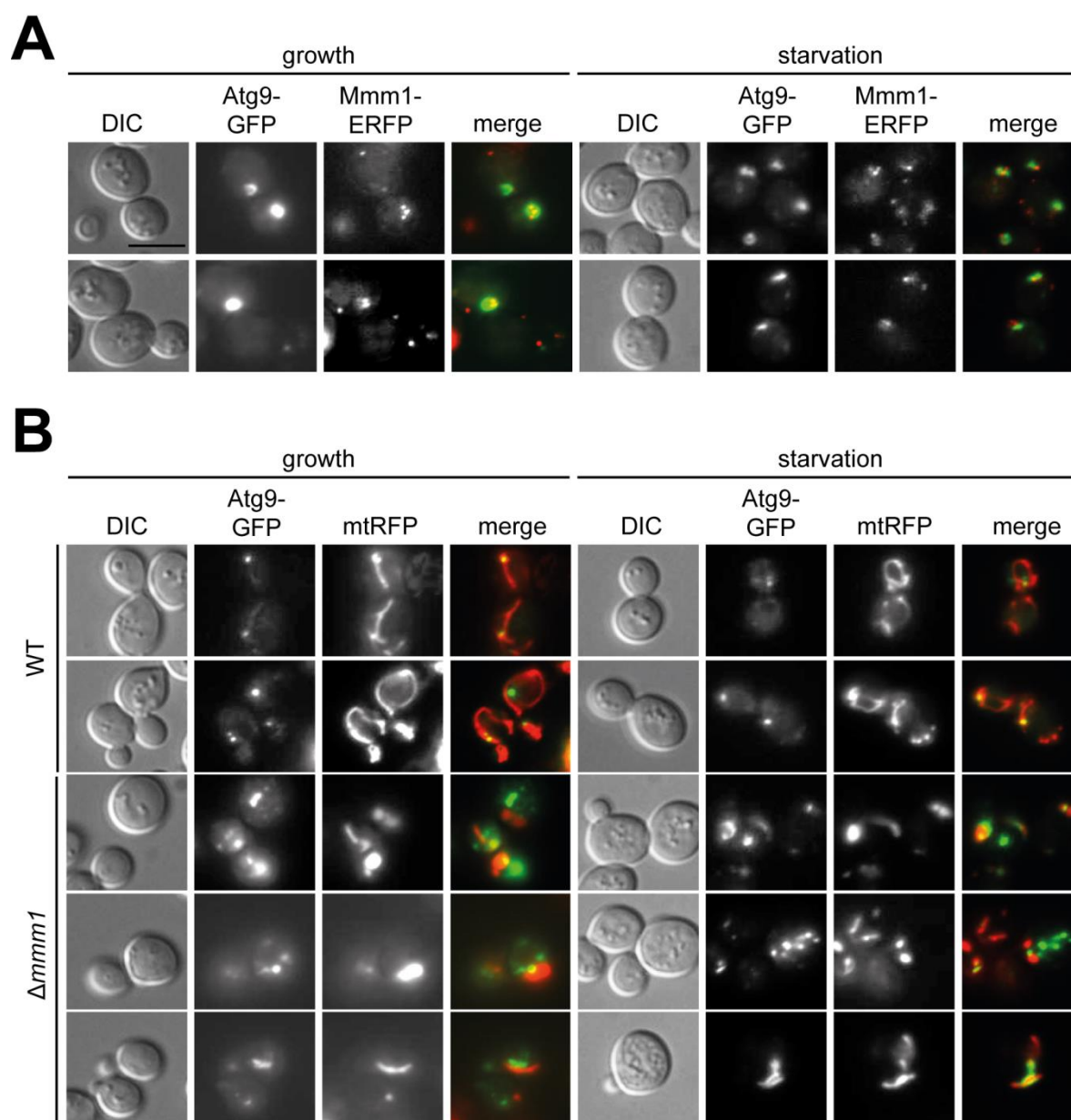


Figure 20. Atg9 associates with ERMES and is mislocalized when ERMES is absent. (A) $\Delta mmm1$ cells expressing Atg9-GFP from the *GPD* promoter and Mmm1-ERFP from its endogenous promoter were cultured to logarithmic growth in SGalRD, starved and analyzed by fluorescence microscopy before (growth) and after 1.5 h starvation. Bar, 5 μ m. **(B)** Cells expressing Atg9-GFP from the *GPD* promoter and mtRFP were prepared and analyzed as in (A).

Artificial mitochondrial localization of a peroxisome-specific autophagy receptor complements the mitophagy defect in ERMES mutants

Apart from mitophagy, the autophagic degradation of peroxisomes, called pexophagy, is among the best studied selective autophagy pathways so far. During pexophagy, the peroxisomal membrane protein Pex3 recruits the specificity factor Atg36, which in turn interacts with Atg8 and Atg11. Subsequently, the peroxisome gets sequestered by a phagophore (Motley et al., 2012). Interestingly,

Pex3 that is artificially targeted to mitochondria by fusion to the MOM protein Om45 (Om45-Pex3) is able to rescue the mitophagy defect in $\Delta atg32$ (Figure 21A, Motley et al., 2012). Moreover, Pex3 is also involved in tethering peroxisomes to the ER (Knoblach et al., 2013). A subpopulation of Pex3 resides in the ER and interacts with Inp1, which builds a molecular bridge to peroxisomal Pex3. Because of these characteristics of Pex3 it was asked, whether Om45-Pex3 can restore mitophagy in ERMES mutants (see schematic Figure 21A).

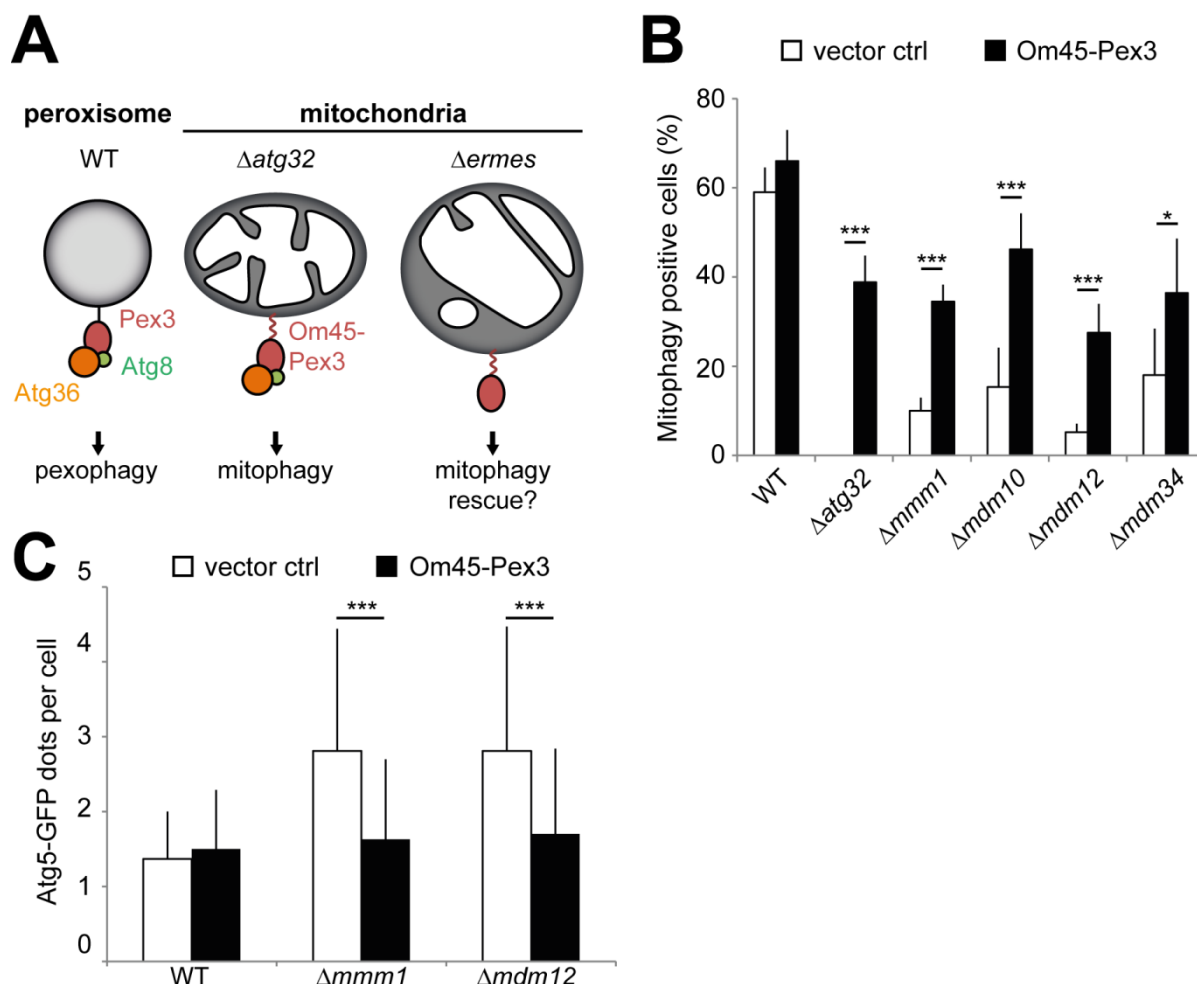


Figure 21. Om45-Pex3 rescues the mitophagy defect in ERMES mutants and the Atg5 phenotype in $\Delta mmm1$ and $\Delta mdm12$ cells. (A) Schematic representation of the experiment's rationale. See text for details. (B) Cells expressing mtRosella and Om45-Pex3 or carrying a vector control were cultured in SGalRD to logarithmic growth, starved for 1 day and analyzed by fluorescence microscopy. At least 100 cells were scored for red vacuolar fluorescence. Values represent the mean of at least five quantifications per strain + SD. Asterisks indicate statistical significance (* $p > 5\%$; *** $p > 0,05\%$; two-tailed Student's t-test). (C) Cells expressing Atg5-GFP from the *GPD* promoter and Om45-Pex3 or carrying a vector control were cultured as in (B), starved for 1.5 h and analyzed by fluorescence microscopy. Cells were scored for Atg5-GFP dots per cell in cells with at least one dot. Data represent the mean of at least 100 cells per strain + SD.

To this end, Om45-Pex3 was expressed in $\Delta atg32$ as well as in ERMES mutants, and mitophagy was quantified after one day of starvation by using mtRosella. As expected, Om45-Pex3 efficiently restored mitophagy in $\Delta atg32$. Interestingly, Om45-Pex3 also enhanced mitophagy in all ERMES

mutants (Figure 21B), even in $\Delta mdm12$, which has not been rescued by chiMERA expression. Expression of Om45-Pex3 also reestablished the regular formation of the phagophore, which was tested by quantification of Atg5-GFP dots in $\Delta mmm1$ and $\Delta mdm12$ (Figure 21C).

How exactly Om45-Pex3 restores the mitophagic pathway in ERMES mutants is unclear. Is the rescue caused by the ability of Om45-Pex3 to recruit the autophagic machinery to mitochondria or by its capacity to reestablish the contacts with the ER by interaction with Inp1, the hinge between peroxisomes and ER? Since recruitment of Atg8 to mitochondria and its interaction with Atg32 still work in ERMES mutants anyway (Figure 17), the former is not a likely explanation. Since the mitophagy defect in ERMES mutants is caused by loss of ER-mitochondria contacts, the latter is a plausible alternative. However, this remains to be shown by construction of $\Delta ermes \Delta inp1$ double mutants, where artificial tethering by Om45-Pex3 is supposedly absent and Om45-Pex3 expression should not result in a mitophagy rescue.

Mapping the genetic interactome of the mitochondrial inheritance mutant *myo2(LQ)*

Genomic integration of the *myo2(LQ)* mutations leads to reduced growth, diminished mitochondrial inheritance and synthetic lethality with $\Delta ypt11$

In yeast, mitochondria are transported along the actin cytoskeleton via the myosin V motor protein Myo2 (reviewed in Westermann, 2014). Mutations in the proximal half of Myo2's cargo binding domain (CBD) can result in mitochondrial inheritance defects (Altmann et al., 2008). A very severe impairment of mitochondrial morphology and inheritance results from the combination of the two amino acid substitutions L1301P and Q1233R, termed *myo2(LQ)* (Figure 22A, Förtsch et al., 2011).

myo2(LQ) appears as a suitable tool to screen for novel regulators of mitochondrial transport and distribution by application of a genetic interaction approach. Mapping of genetic interactions on a genome-wide scale can reveal genes working in the same or antagonistic pathways and thereby uncover unanticipated functions of known or previously uncharacterized genes.

To this end, a query strain with a mutation of interest like *myo2(LQ)* is crossed to an ordered array of viable yeast deletion mutants, double mutants are isolated using synthetic genetic array (SGA) technology and their growth is quantified to identify genetic interactions (Baryshnikova et al., 2010). Therefore, the *myo2(LQ)* mutation has to be introduced into the genome of a starter strain suitable for SGA and it has to be ensured that this mutation leads to the expected phenotypes. It has to be noted that effects of *myo2(LQ)* have been previously analyzed in strains lacking genomic *MYO2* ($\Delta myo2$) but harboring a plasmid coding for *myo2(LQ)* under control of its endogenous promoter (Förtsch et al., 2011).

A DNA fragment comprising part of the *MYO2* locus and coding for the *LQ* substitutions was fused to a cassette that confers uracil prototrophy to the starter strain (Figure 22B). This DNA fragment was introduced into the starter strain, thereby replacing the wild type *MYO2*, and recombinants were selected on medium lacking uracil. Sequencing the *MYO2* locus revealed that the *myo2(LQ)* mutations were successfully introduced into the starter strain producing the *myo2(LQ)* query strain (data not shown). As a control, a *MYO2* query strain was constructed with a DNA fragment coding for *MYO2* instead of *myo2(LQ)* in front of the *URA3* cassette.

A drop dilution assay showed that the introduction of the *myo2(LQ)* allele resulted in a mild growth defect, which was enforced when cells were cultured at elevated temperatures (Figure 22C). This is in good agreement with published results (Förtsch et al., 2011). In order to confirm the mitochondrial inheritance defect, the *MYO2* and *myo2(LQ)* query strains were stained with the mitochondria-specific dye rhodamine-B-hexylester during logarithmic growth. The *myo2(LQ)* mutation led to buds that were frequently devoid of mitochondria, which was only very rarely observed in *MYO2* cells (Figure 22D). This demonstrates that the *myo2(LQ)* query strain exhibits the expected mitochondrial inheritance defect.

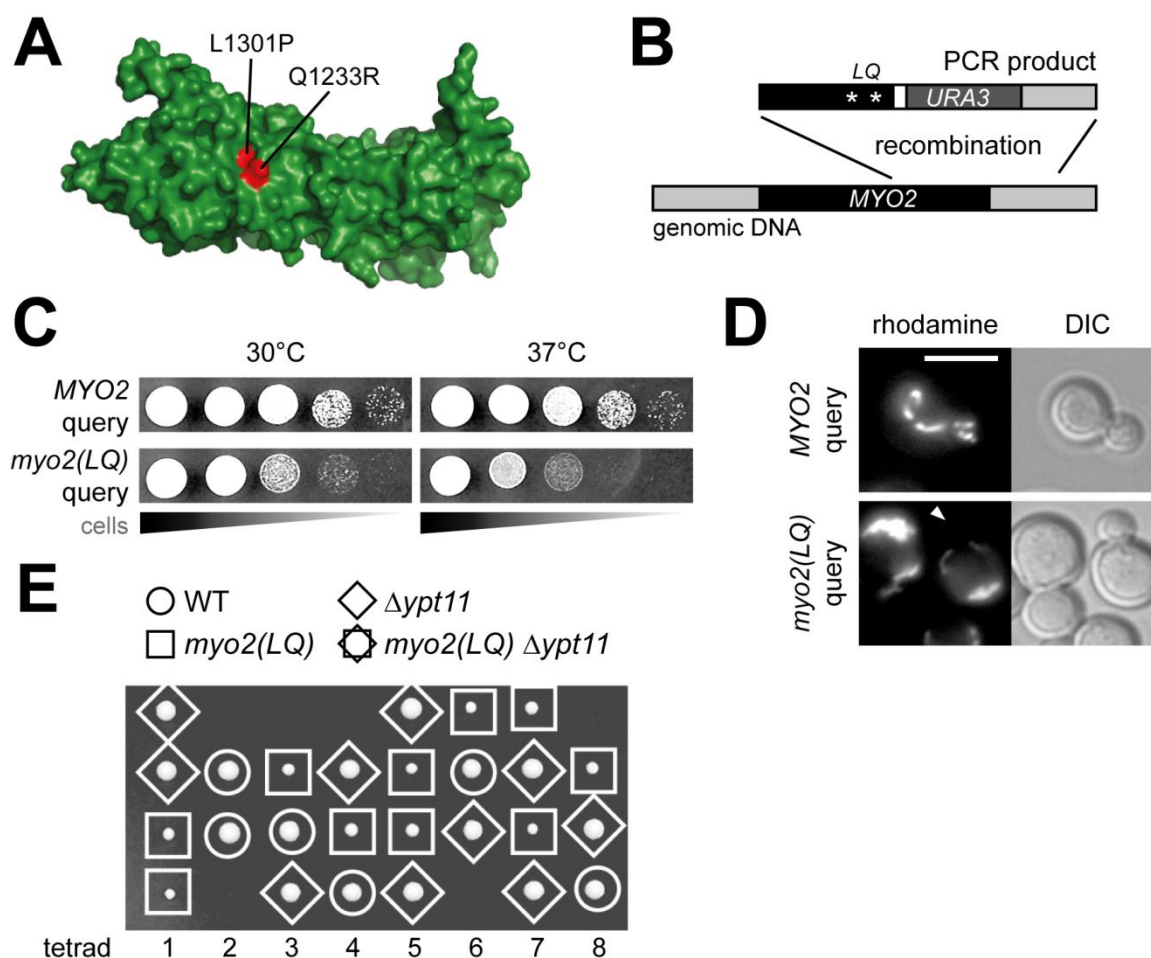


Figure 22. Phenotypes of *myo2(LQ)*. (A) Space-filling diagram of the CBD of Myo2 (PDB 2F6H; Pashkova et al., 2006) generated by using PyMOL software (PyMOL Molecular Graphics System, version 1.3; Schrödinger). The mutated residues of the *myo2(LQ)* allele are highlighted in red. (B) Schematic representation of *myo2(LQ)* strain construction. A PCR construct carrying part of the *myo2* coding region (with mutations leading to amino acid substitutions Q1233R and L1301P) as well as an *URA3* cassette, which confers uracil prototrophy, was inserted into the *MYO2* locus. The two query strains were constructed by Johannes König, Zellbiologie, Bayreuth. (C) The *MYO2* (upper panel) and *myo2(LQ)* (lower panel) query strains were adjusted to the same optical density, diluted in serial 1:10 steps and spotted on glucose-containing rich medium. Plates were incubated at 30°C and 37°C. (D) Cells were cultured to logarithmic growth in glucose-containing rich medium, mitochondria were stained with rhodamine-B-hexylester and cells were analyzed by fluorescence microscopy. The arrowhead indicates a bud devoid of mitochondria. Bar, 5 μ m. (E) The *myo2(LQ)* query and a $\Delta ypt11$ strain were crossed, sporulated and tetrads were dissected on glucose-containing rich medium. After 3 days of incubation, the genotypes were determined by plating the cells on medium lacking uracil and on medium containing geneticin.

Another phenotype of *myo2(LQ)*, which is particularly important for its application in an SGA screen, is its synthetic lethality with $\Delta ypt11$. Ypt11 is a Rab GTPase, which interacts with both Myo2 (Itoh et al., 2002) and Mmr1 (Lewandowska et al., 2013) and whose deletion has mild effects on mitochondrial inheritance (Itoh et al., 2002; Boldogh et al., 2004). However, if *YPT11* is deleted in addition to the *myo2(LQ)* mutation, cells die due to a lack of mitochondrial transport into the bud (Förtsch et al., 2011). To confirm this synthetic lethality, the *myo2(LQ)* query strain was crossed with $\Delta ypt11$ and after sporulation, tetrads were dissected by micromanipulation on rich medium. As

expected, determination of the spores' genotype revealed that not a single double mutant could be obtained (Figure 22E), demonstrating that combining the *myo2(LQ)* and $\Delta ypt11$ mutations in a single cell is lethal.

Taken together, integration of *myo2(LQ)* into the genome of an SGA starter strain results in a mild growth defect, compromised mitochondrial inheritance and synthetic lethality with $\Delta ypt11$. Thereby, the strain proves applicable in an SGA analysis.

Synthetic genetic array analysis with *myo2(LQ)*

In order to identify novel players in the transport and inheritance of mitochondria, a *myo2(LQ)* and a *MYO2* query strain were crossed to an ordered array of more than 4000 yeast deletion mutants (Figure 23A). The mutants of the deletion library carried a cassette conferring resistance to geneticin (*kanMX4*) and replacing a particular ORF, while the query strains carried a *URA3* cassette behind the *MYO2* locus conferring uracil prototrophy (Figure 23B). Diploid cells were consequently selected by growth on plates containing geneticin and lacking uracil. After sporulation, haploid cells were selected by growth on medium containing the antibiotics canavanine and thialysine, for which the query strains carried a recessive resistance and which accordingly kill diploid cells. Haploid double mutants were subsequently isolated by growth on plates containing geneticin and lacking uracil. Images of the plates were acquired. Determination and normalization of colony sizes as well as identification of genetic interactions was performed using the web browser based SGAtools (<http://sgatools.cabr.utoronto.ca/>) as described previously (Wagih et al., 2013). The tool corrects and normalizes the colony sizes, which means it rescales colonies growing close to the edges of the plates since they have usually more access to nutrients and therefore are bigger. Then the program scores every strain by subtracting the estimated fitness from the actually measured fitness. Four replicates of each strain were present on the plates and the mean genetic interaction score was calculated from these.

The genetic interaction scores from replicate 1 are shown in Figure 23C. Most of the screened strains showed no genetic interaction with *myo2(LQ)* as most of the scores are about 0. However, several hundred of them were below the recommended threshold of -0.3 for negative interactions and above 0.3 for positive interactions (Figure 23D, Wagih et al., 2013). Since this number is too high to characterize all of the candidates, the screen was performed once more (Figure 23C). As can be seen from the mean score standard deviation of the two replicates, the first replicate was more reproducible; moreover, it had fewer hits, fewer strains were lost (Figure 23D) and it appears as if the first replicate was of better quality for unknown reasons. However, the overlap of both replicates contained about 100 strains of negative and positive interactors, respectively (Figure 23D), which appears as a reasonable number of interactors for a gene with as many functions like *MYO2*. The genes appearing in both replicates were considered as bona fide interactors (Table 7, Appendix). The genetic interactions scores of all strains from the two replicates are listed in Table S2 (Appendix).

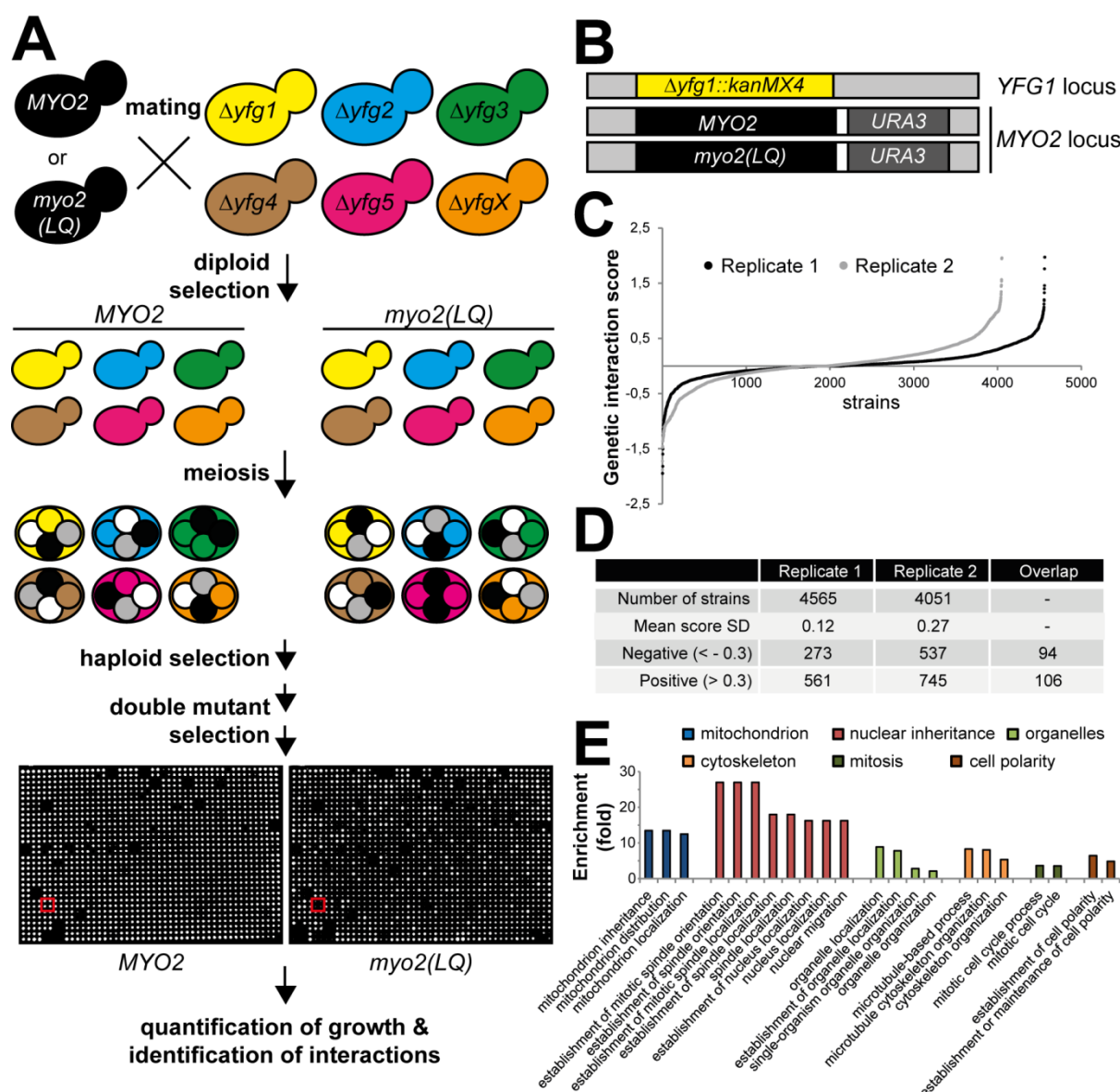


Figure 23. Synthetic genetic array analysis with *myo2(LQ)* as a query mutation. (A) Schematic representation of the *myo2(LQ)* SGA. *MYO2* and *myo2(LQ)* query strains are crossed to the *MATa* yeast deletion library and heterozygous diploid cells are selected. After sporulation (meiosis), haploid and subsequently double mutants are selected. Plates are imaged and colony size is quantified, normalized, and genetic interactions are scored. The red square indicates the position of the $\Delta ypt11$ strains. **(B)** Schematic representation of the chromosomal loci of the used strains. The deletion library contains strains lacking non-essential genes, which were replaced by the *kanMX4* cassette conferring resistance to geneticin (upper panel). The query strain *myo2(LQ)* carries the L1301P and Q1233R mutations in its genome at the *MYO2* locus linked to an *URA3* cassette conferring uracil prototrophy (lower panel). The corresponding control query strain (middle panel) has the same organization at its *MYO2* locus but carries a wild type copy of *MYO2*. **(C)** Strains from the SGA, which was performed as described in (A), were ordered according to their genetic interaction score with *myo2(LQ)*. **(D)** Comparison of the two screens in regards to the number of strains screened, mean score standard deviation (SD), the number of negative and positive interactors and their overlap in both replicates. **(E)** Analysis of GO term enrichments for bioprocesses among the negative interactors. The fold enrichment is the ratio of the GO term frequency among the negative interactors and among all the tested strains.

Genes can be categorized into so-called gene ontology (GO) terms indicating if the genes are involved in a particular process, function or are localized at a certain cellular component. Since the screen aimed at the identification of cellular processes contributing to mitochondrial inheritance, the negative and positive interactors were analyzed for an enrichment of GO terms for cellular processes with a p value $< 5\%$, as has been described in Boyle et al. (2004). Fold enrichment was calculated as the ratio of the frequency of genes with a given GO term among the hits (i.e., the negative and positive interactors, respectively) and the frequency of genes with this GO term among the background set (i.e., the screened strains). No significant functional enrichments were found among the positive interactors, however, Figure 23E shows that several bioprocesses were enriched many-fold among the negative interactors. These processes could be categorized into several classes mainly based on the localization of the process like mitochondrion or cytoskeleton or the overall function of the process like nuclear inheritance or mitosis. The GO terms 'mitochondrion inheritance', 'mitochondrion distribution' and 'mitochondrion localization' were identified, suggesting that the screen includes hits which are specific for mitochondrial functions and inheritance. Surprisingly, most of the functional enrichments concern the inheritance of the nucleus, which is consistent with the fact that Myo2 orients the mitotic spindle (Hwang et al., 2003). This can also explain the interactions with genes involved in microtubule-associated processes, which in yeast almost exclusively comprise the migration of the nucleus. Furthermore, components contributing to organelle organization in general, mitosis and cell polarity were found to be enriched among the negative interactors.

Among the reproducible, mitochondrion-related negative interactors was *YPT11*, as expected, since *myo2(LQ) Δypt11* cells have already been shown to be inviable due to a severe mitochondrial transport defect (Figure 22E; Förtsch et al., 2011). Furthermore, the genes encoding the ERMES subunits Gem1, Mmm1 and Mdm34 exhibited negative interactions with *myo2(LQ)*. ERMES mutants are known to have defects in mitochondrial inheritance (Burgess et al., 1994; Sogo and Yaffe, 1994; Berger et al., 1997; Frederick et al., 2004; Youngman et al., 2004; Förtsch et al., 2011). The genetic interaction with *myo2(LQ)* is consistent with the idea that the functionality of mitochondrial ER contacts is required for maintenance of a transportable morphology and loss of this morphology leads to inheritance defects (Förtsch et al., 2011). It is plausible that cells with such barely transportable mitochondria cannot tolerate certain mutations of the motor protein Myo2. *myo2(LQ)* also showed a genetic interaction with the phosphatase coding gene *PTC1*, the deletion of which has been reported to result in delayed inheritance of mitochondria, vacuoles, peroxisomes and cortical ER. Besides, loss of Ptc1 has effects on the steady-state levels of Mmr1, Vac17 and Inp2, which interact with Myo2 in order to promote organelle inheritance (Roeder et al., 1998; Du et al., 2006; Jin et al., 2009; Swayne et al., 2011). Ptc1 is required for the proper distribution of Mmr1, Myo2 itself and Myo4, which transports cortical ER (Jin et al., 2009; Swayne et al., 2011). Likely, if these processes fail in *Δptc1* and if the interaction of Myo2 with mitochondria is additionally affected by the *myo2(LQ)* mutation, mitochondrial inheritance is massively blocked and double mutants grow very poorly.

myo2(LQ) exhibited additional interactions with *NUM1*, which anchors mitochondria in the mother cell, and with genes encoding components of the mitochondrial fusion machinery. These interactions will be discussed in more detail below.

Taken together, the screening of more than 4000 yeast deletion strains with *myo2(LQ)* as a query mutation revealed about 200 strains growing surprisingly well or poorly. Several of the negative interactors can be explained easily, since these genes have already been shown to be involved in the inheritance of mitochondria. Although it is not known which interactors are specific for mitochondria, since Myo2 has diverse targets and may thus interact with genes unrelated to mitochondria, it is reasonable to assume that characterization of the interactors may yield new players involved in mitochondrial inheritance.

***myo2(LQ) Δnum1* mutants are synthetic sick**

The combination of the two mutations *myo2(LQ)* and *Δnum1* reproducibly showed a negative genetic interaction. This interaction has already been seen in two previous screens, where hypomorphic or conditional alleles of *myo2* showed a negative interaction with *Δnum1* (Tong et al., 2004; Costanzo et al., 2010). Num1 is a 313 kDa protein present at the cell cortex in mother cells, it interacts with dynein and microtubules and is important for nuclear migration (Farkasovsky and Kuntzel, 2001). It was also found to play a role in mitochondrial dynamics by facilitating mitochondrial division (Cervený et al., 2007). Recently, Num1 was shown to form a complex with Mdm36, a peripheral mitochondrial protein, which is thought to act as an adaptor between Num1 and mitochondria (Hammermeister et al., 2010; Lackner et al., 2013). This complex is thought to anchor mitochondria at the mother cell at sites opposite to the bud and to ensure that a portion of mitochondria remains in the mother cell (Klecker et al., 2013; Lackner et al., 2013).

The negative genetic interaction between *myo2(LQ)* and *Δnum1* is surprising since one would expect that mitochondrial transport into the bud in *myo2(LQ) Δnum1* cells would be relieved when the mitochondria are not retained in the mother. This relief is expected to result in a positive genetic interaction. In order to verify the negative interaction, *myo2(LQ)* cells were crossed with *Δnum1*. After sporulation, tetrads were dissected on rich medium. As anticipated from the screening results, the colony size of double mutants was very small compared to wild type and single mutants (Figure 24A). Quantification of colony size showed that *Δnum1* grew almost as good as WT and *myo2(LQ)* had less than 70% of fitness compared to WT (Figure 24B). This means that the double mutant *myo2(LQ) Δnum1* has an expected fitness almost identical to the fitness of *myo2(LQ)*, if the two genes work in unrelated pathways. However, the double mutant had a fitness of only about 5% compared to WT, which represents a negative genetic interaction and confirms the screening result. If the small colony size was due to problems of the double mutants of regrowing immediately after sporulation, the growth defect should not be observed in a drop dilution assay. Still, the *myo2(LQ) Δnum1* double mutants grew unexpectedly poorly (Figure 24C).

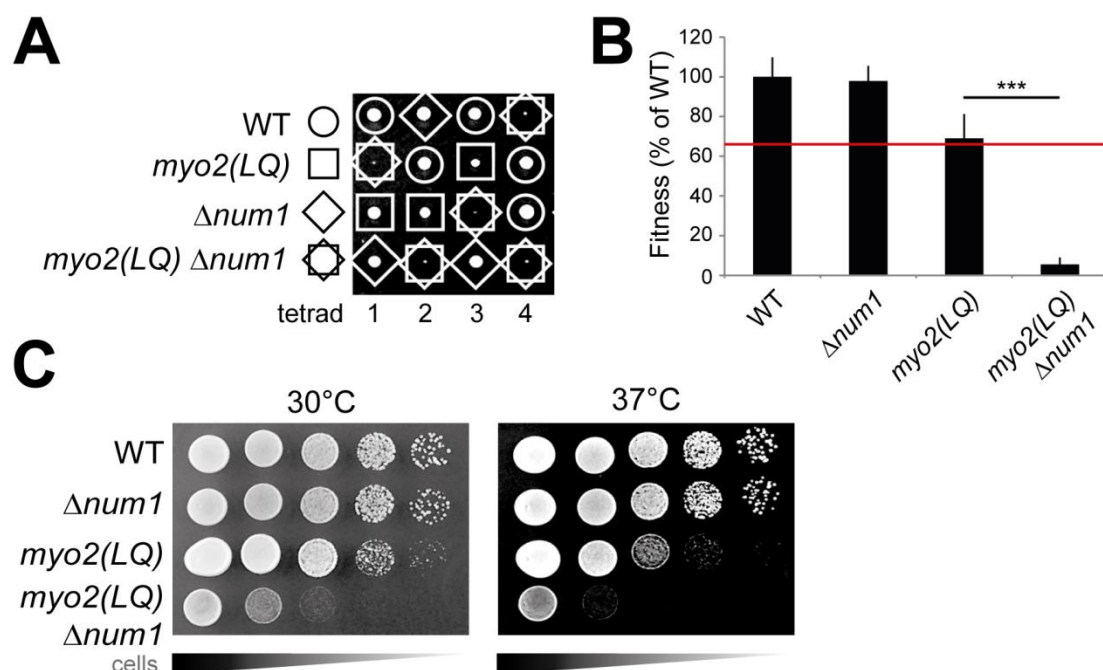


Figure 24. *myo2(LQ)* and $\Delta num1$ genetically interact. (A) *myo2(LQ)* and $\Delta num1$ cells were crossed, sporulated and tetrads were dissected on glucose-containing rich medium. After 3 days of incubation the genotypes were determined by plating the cells on medium lacking uracil and on medium containing geneticin. (B) Quantification of fitness. Colony size was determined after tetrad dissection and normalized to WT. Values represent the mean of 16 colonies per strain + SD. Asterisks indicate statistical significance (***) $p > 0,05\%$; two-tailed Student's t-test). The red line marks the expected fitness of the double mutant calculated by the product of the two single mutants' fitness. (C) Strains were adjusted to the same optical density, diluted in serial 1:10 steps and spotted on glucose-containing rich medium. Plates were incubated at 30°C and 37°C.

These results demonstrate that *myo2(LQ)* and $\Delta num1$ genetically interact and that the performed SGA screen produced results, which are reliable and consistent with previous observations (Tong et al., 2004; Costanzo et al., 2010).

The growth phenotype of *myo2(LQ) \Delta num1* is caused by a nuclear migration defect rather than a mitochondrial deficit

Although the genetic interaction of *myo2(LQ)* and $\Delta num1$ was confirmed, the origin of the interaction is not clear since Myo2 and Num1 are involved in multiple processes. In order to test whether the double mutant's growth deficit is caused by a mitochondria-specific effect, mtGFP expressing single and double mutants were analyzed with regard to mitochondrial morphology and mitochondrial inheritance. *myo2(LQ)* had mitochondria clumped mostly at the mother cell opposite to the bud (Figure 25A), which is consistent with previous observations (Förtsch et al., 2011). $\Delta num1$ mitochondria were also aberrant and their distribution was slightly shifted towards the bud, which is in agreement with the literature (Cervený et al., 2007; Klecker et al., 2013). The *myo2(LQ) \Delta num1* double mutants had mitochondrial networks which appeared very large, were distributed over the whole mother cell and often absent in the bud (Figure 25A). The inheritance defect of *myo2(LQ)* is

obviously epistatic to the bud-shifted mitochondrial distribution of $\Delta num1$, which is plausible since bud-directed movement depends on Myo2. The mitochondrial morphology of the double mutant resembles the one of $\Delta dnm1$ cells, in which the interaction of mitochondria with the actin cytoskeleton has been prevented either genetically by deletion of *MDM20* (Bleazard et al., 1999) or chemically by addition of latrunculin A (Cervený et al., 2001). Since $\Delta num1$ cells have a mitochondrial division defect similar to $\Delta dnm1$ and the *myo2(LQ)* mutation presumably leads to reduced attachment of mitochondria to actin, this phenotype might be common in cells with compromised mitochondrial fission as well as hampered mitochondria-actin interaction.

To determine whether the genetic interaction was based on a mitochondrial inheritance defect, it was quantified how many buds carried mitochondria in single and double mutants. When bud size and therefore cell cycle phase was ignored, almost all buds of WT and $\Delta num1$ contained mitochondria, whereas over 40% of buds were devoid of mitochondria in *myo2(LQ)* and *myo2(LQ) Δnum1* double mutants (Figure 25B, upper panel). Therefore, deletion of *NUM1* does not alleviate the mitochondrial inheritance defect in a *myo2(LQ)* background; indeed, it had no effect at all. Num1 is present at the bud tip only in large buds (Farkasovsky and Kuntzel, 1995; Heil-Chapdelaine et al., 2000) and might thus anchor mitochondria not only in the mother but also to the daughter's cell cortex at late cell cycle phases. If this was the case, retrograde transport of mitochondria from the daughter into the mother might be enhanced in *myo2(LQ) Δnum1* double mutants, since mitochondria would not be anchored in the daughter due to absence of Num1. Furthermore, retrograde transport would not be readily counteracted by anterograde movement because of the *myo2(LQ)* mutation. Consequently, it can be predicted that large buds are more often devoid of mitochondria, which would lead to the observed growth defect in *myo2(LQ) Δnum1* double mutants. However, no effect on mitochondrial inheritance was observed when large buds were quantified for presence of mitochondria (Figure 25B, lower panel). Accordingly, no evidence was found in support of the hypothesis that defective mitochondrial inheritance was the origin of the genetic interaction between *myo2(LQ)* and $\Delta num1$.

In order to address the question of a mitochondria-specific effect more directly, it was tested whether restoring anterograde mitochondrial movement by Myo2-Fis1 in the double mutant rescued the growth defect. Myo2-Fis1 is a mitochondria-specific Myo2 variant, the CBD of which was replaced by the mitochondrial membrane anchor of Fis1 and which restores anterograde mitochondrial movement in *myo2(LQ)* (Förtsch et al., 2011). Overexpression of Myo2-Fis1 leads to accumulation of mitochondria in the bud (Förtsch et al., 2011), which is toxic in $\Delta num1$ since mitochondria are not retained in the mother and are completely transferred into the bud (Kleckner et al., 2013), leading to the mother cell's death. This would supposedly also be the case in *myo2(LQ) Δnum1* double mutants and therefore *myo2-fis1* was put under control of a galactose-inducible promoter and double mutants carrying either an empty vector or a *myo2-fis1* expression plasmid were plated on media with different concentrations of glucose, which represses the *myo2-fis1* expression, and galactose, which induces the expression.

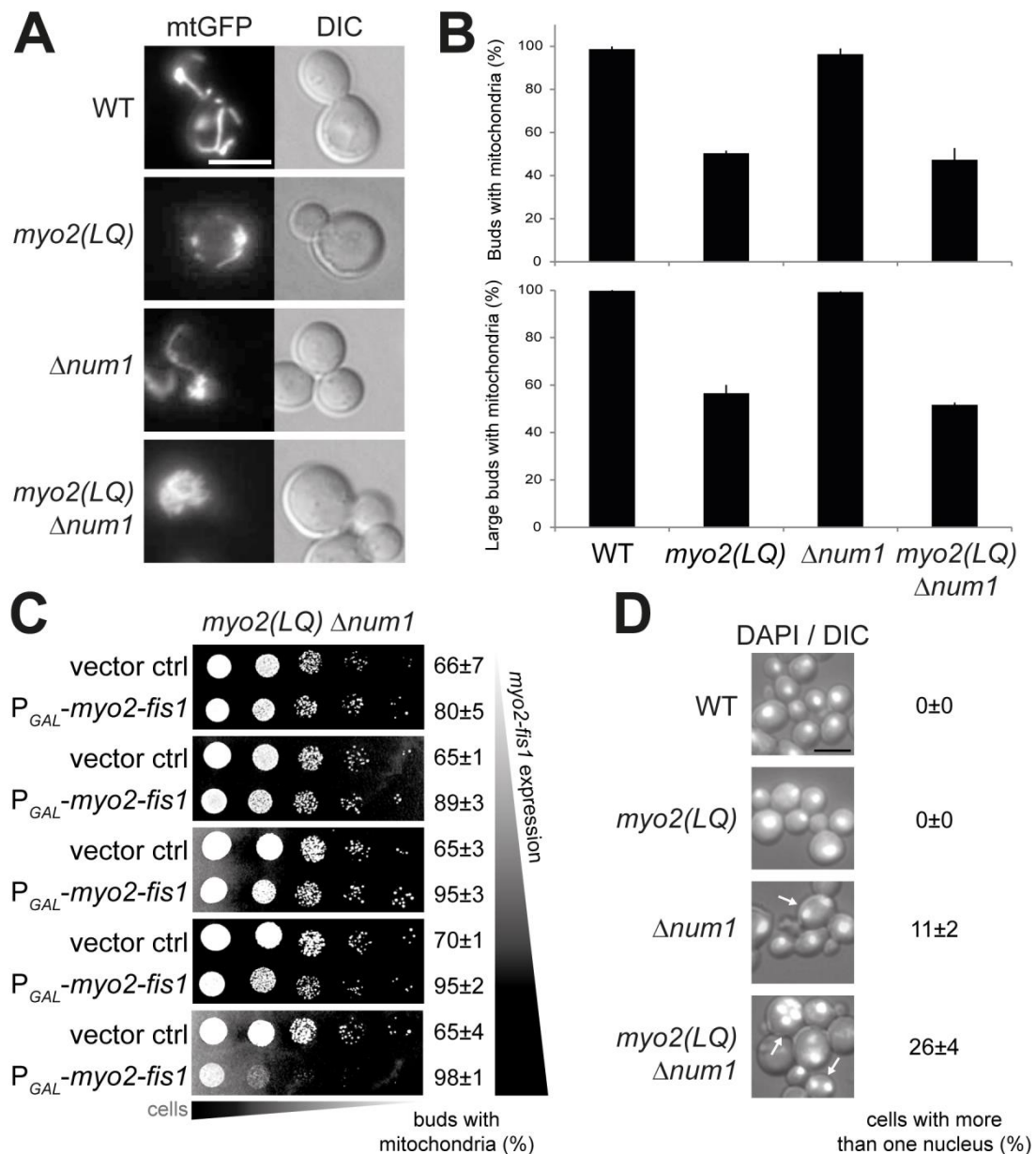


Figure 25. Phenotypic characterization of *myo2(LQ) Δnum1* mutants. (A) Cells expressing mtGFP were cultured in glucose-containing synthetic complete medium to logarithmic growth and analyzed by fluorescence microscopy. Representative images are shown. Bar, 5 μ m. (B) Cells expressing mtGFP were prepared as in (A) and the percentage of buds irrespective of bud size (upper panel) and the percentage of large buds (lower panel) containing mitochondria in at least 100 cells were determined. Values represent the mean of triplicate experiments \pm SD. (C) Cells expressing *myo2-fis1* from a galactose-inducible promoter or carrying a vector control were adjusted to the same optical density, diluted in serial 1:10 steps and spotted on different growth media (SCD, upper panel; SCGal + 2% glucose, second panel; SCGal + 1.5% glucose, third panel; SCGal + 1% glucose, fourth panel; SCGal + 0.5% glucose, fifth panel). For determination of the percentage of buds with mitochondria, cells were grown in the corresponding liquid media to logarithmic growth and scored for buds with mitochondria in at least 100 cells. Values represent the mean of triplicate experiments \pm SD. (D) Cells were grown in glucose-containing rich medium to logarithmic growth, fixed, stained with DAPI and analyzed by fluorescence microscopy. Representative images are shown. Arrows indicate cells with more than one nucleus. Bar, 5 μ m. Cells with at least two nuclei were scored in at least 100 cells per strain. Data represent the mean of triplicate experiments \pm SD.

Low expression of *myo2-fis1* did not lead to an improved growth of the double mutant, whereas high expression was toxic compared to the vector control as expected (Figure 25C). Quantification of buds with mitochondria showed that the double mutant's inheritance defect was indeed restored with increasing expression of *myo2-fis1* (Figure 25C). However, this did not result in improved growth, indicating that the growth deficit is not caused by the inheritance defect. The fact that inheritance was rescued already under conditions, which should repress Myo2-Fis1 expression, might be caused by a leakiness of the *GAL* promoter. The toxic effect of high Myo2-Fis1 concentrations was likely due to the transport of all mitochondria into the bud. In sum, no evidence favoring the hypothesis of a mitochondria-specific defect in *myo2(LQ) Δnum1* double mutants could be obtained.

Num1 and Myo2 are both involved in nuclear migration. Num1 serves as an anchor for dynein, which drives the mitotic spindle through the bud neck (Bloom, 2001; Farkasovsky and Kuntzel, 2001), and Myo2 orients the spindle towards the bud, serving as a molecular hinge between cytoplasmic microtubules, Bim1 and Kar9 on the one side and actin cables on the other side (Hwang et al., 2003). Thus, it appears plausible that *myo2(LQ) Δnum1* double mutants suffer from a severe nuclear migration defect. In order to test this idea, nuclei were stained with DAPI and the presence of multiple nuclei within one cell was quantified. WT and *myo2(LQ)* cells always showed only one nucleus per cell, whereas about one tenth of *Δnum1* cells contained more than one nucleus (Figure 25D). This fraction is increased more than twofold in double mutants, which is an unexpectedly high value compared to single mutants, demonstrating that combination of the two mutations results in a strong nuclear migration defect. It has been shown that the amino acid substitution L1301P of *myo2(LQ)* results in Myo2's inability to bind Kar9 (Eves et al., 2012) and therefore to bridge microtubules with the actin network. Consistently, *myo2(LQ)* reproducibly showed negative genetic interactions with *Δarp1*, *Δdyn1*, *Δldb18*, *Δbud6*, *Δjnm1*, *Δase1*, *Δkip2*, and *Δnip100*, which lack gene products that are mostly members of the yeast dynactin complex and that are all involved in establishment or orientation of the mitotic spindle.

In sum, a mitochondria-specific effect is not likely to be the cause for the growth defect in *myo2(LQ) Δnum1* double mutants, but this defect is reasonably due to disturbed nuclear migration. This highlights that screening with *myo2(LQ)* does not exclusively produce mitochondria-related hits and emphasizes the necessity to determine the origin of a genetic interaction when SGA is performed with query genes that are undoubtedly involved in more than one process.

Mutants with disturbed mitochondrial dynamics genetically interact with *myo2(LQ)*

The mutants *Δfzo1*, *Δmgm1* and *Δugo1* had mean genetic interaction scores – calculated from the two screening replicates – of -0.65, -0.48 and -0.41, respectively, indicating that these genes interact negatively with *myo2(LQ)*. These strains lack genes necessary for the fusion of mitochondria (reviewed in Westermann, 2010). To confirm the interaction, *myo2(LQ)* was crossed with *Δfzo1*, *Δmgm1* and *Δugo1*. After sporulation, tetrads were dissected on rich medium and genotypes were

determined. No double mutant was obtained in either case (Figure 26A), which demonstrates that combining *myo2(LQ)* with mutations leading to blocked mitochondrial fusion is synthetic lethal. Thereby, the screening results were confirmed.

Mitochondrial morphology is balanced by fusion and fission events. If blocking fusion leads to lethality in a *myo2(LQ)* background, obstructing the antagonistic pathway of fission might result in the opposite effect, i.e., a positive genetic interaction. To test this idea, *myo2(LQ)* was crossed with $\Delta dnm1$ and tetrads were dissected after sporulation. All spores were able to grow and colonies of double mutants appeared larger than *myo2(LQ)* colonies (Figure 26A). Quantification revealed that WT and $\Delta dnm1$ grew similarly well, while *myo2(LQ)* had a growth defect (Figure 26B). The calculated fitness of the double mutant almost equals the *myo2(LQ)* single mutant's fitness. However, the double mutants had colony sizes nearly as large as the WT and differed significantly from *myo2(LQ)* (Figure 26B). *DNM1* deletion therefore alleviates the compromised growth of *myo2(LQ)*, which represents a positive genetic interaction as predicted.

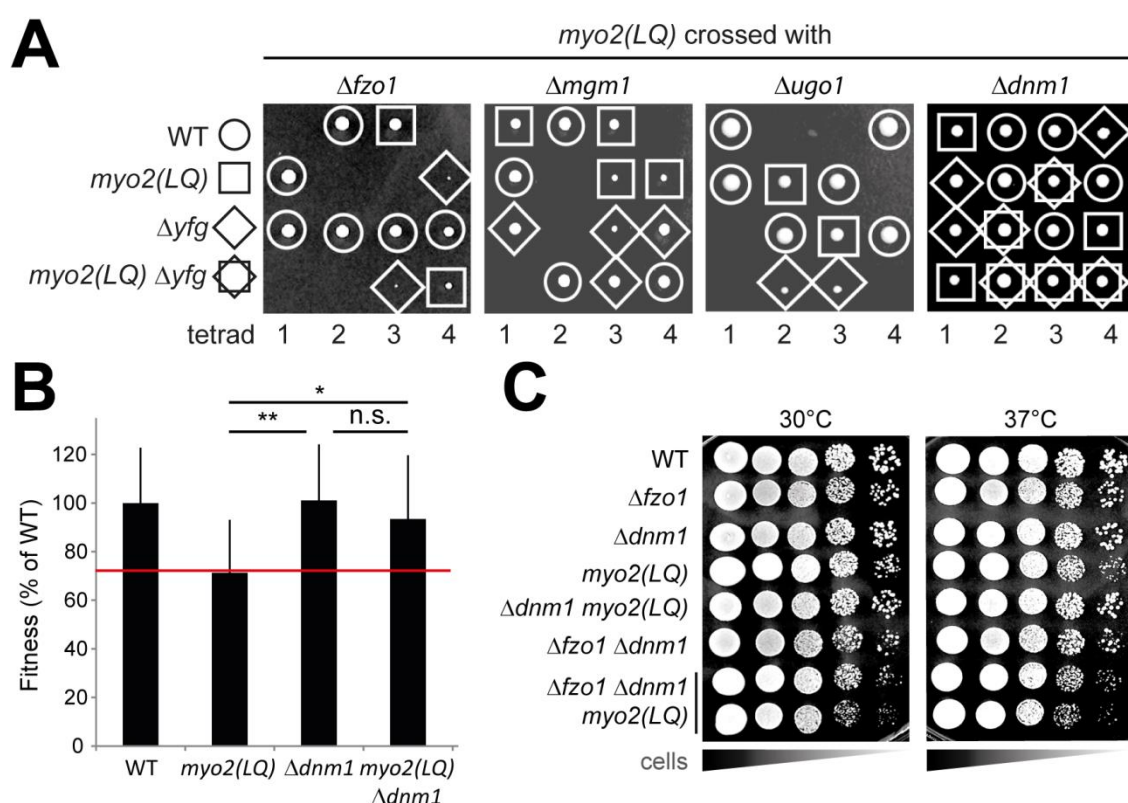


Figure 26. Genetic interactions of mitochondrial fusion and division components with *myo2(LQ)*. (A) *myo2(LQ)* cells were crossed with the indicated strains, sporulated and tetrads were dissected on glucose-containing rich medium. After 3 days of incubation the genotypes were determined by plating the cells on medium lacking uracil and on medium containing geneticin. (B) Quantification of fitness. Colony size was determined after tetrad dissection and normalized to WT. Values represent the mean of at least 14 colonies per strain + SD. Asterisks indicate statistical significance (* $p > 5\%$; ** $p > 0.5\%$; n. s., not significant; two-tailed Student's t-test). The red line marks the expected fitness of the double mutant calculated by the product of the two single mutants' fitness. (C) Strains were adjusted to the same optical density, diluted in serial 1:10 steps and spotted on glucose-containing rich medium. Plates were incubated at 30°C and 37°C.

If the genetic interactions of *myo2(LQ)* with components of mitochondrial fusion were caused by a compromised fusion activity itself, the synthetic lethality should not be rescued by additional deletion of *DNM1*. In *myo2(LQ) Δfzo1 Δdnm1* triple mutants, mitochondria are still not able to fuse, but can be expected to be static like in *Δfzo1 Δdnm1* double mutants (Sesaki and Jensen, 1999). If, however, the effect is caused by the fragmented mitochondrial morphology in *Δfzo1*, additional deletion of *DNM1* should rescue the cells, since *Δfzo1 Δdnm1* double mutants have a regularly shaped mitochondrial network (Sesaki and Jensen, 1999). In order to discriminate between the two possibilities, *myo2(LQ)* was crossed with a *Δfzo1 Δdnm1* double mutant and tetrads were dissected after sporulation. Apart from *myo2(LQ) Δfzo1* cells, all possible combinations of mutations could be obtained. A drop dilution assay revealed that *myo2(LQ) Δdnm1* cells grew better than *myo2(LQ)* as already expected (Figure 26C). But most importantly, *Δfzo1 Δdnm1 myo2(LQ)* triple mutants were viable. They grew slightly less well than *myo2(LQ)*, but this is possibly due to the fact that *Δfzo1 Δdnm1* double mutants grew also slightly worse than WT. This result suggests that the synthetic lethality between *myo2(LQ)* and fusion components is not caused by the loss of mitochondrial fusion activity but by the abnormal, fragmented mitochondrial morphology, which can be rescued by *DNM1* deletion.

Dnm1 depletion alleviates the mitochondrial inheritance defect of *myo2(LQ)*

Since *DNM1* deletion rescues the growth deficit of *myo2(LQ)* cells, it was tested whether mitochondrial inheritance was simultaneously restored. Single and double mutants expressing mtGFP were therefore analyzed with regard to mitochondrial morphology and inheritance. While *Δdnm1* cells had the characteristic mitochondrial nets, which can be seen at one side of the cell, *myo2(LQ)* cells exhibited an abnormal mitochondrial morphology and buds devoid of mitochondria (Figure 27A). In *myo2(LQ) Δdnm1* double mutants, however, mitochondria were organized in giant nets distributed all over the mother cell's cortex. Like in *myo2(LQ) Δnum1* double mutants, this phenotype appears typical for mitochondrial fission defective mutants with compromised mitochondria-actin association (Bleazard et al., 1999; Cervený et al., 2001).

Quantification of buds with mitochondria showed that *myo2(LQ) Δdnm1* double mutants have significantly more buds containing mitochondria than in *myo2(LQ)* single mutants (Figure 27B). This demonstrates that blocking mitochondrial division relieves the mitochondrial inheritance defect of *myo2(LQ)*.

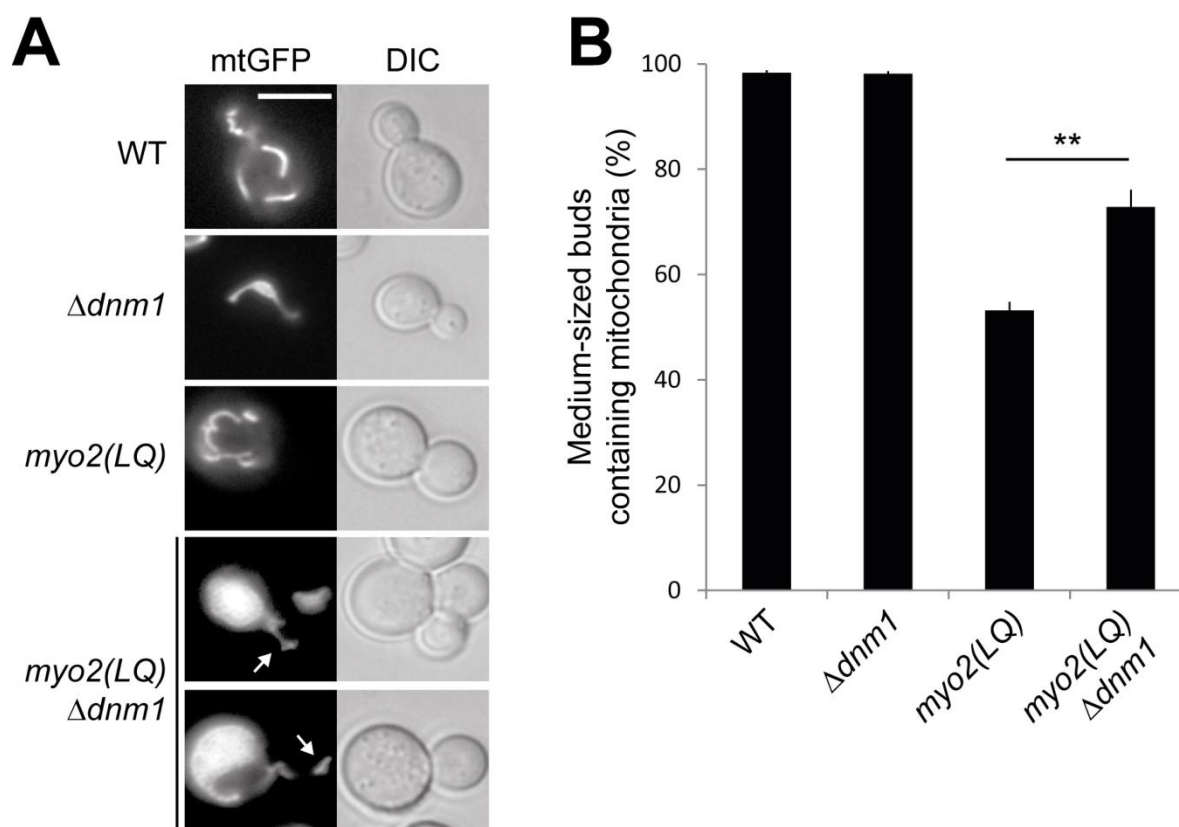


Figure 27. Deletion of *DNM1* in a *myo2(LQ)* background alleviates the transport defect. (A) Cells expressing mtGFP were cultured in glucose-containing synthetic complete medium to logarithmic growth and analyzed by fluorescence microscopy. Representative images are shown. Arrows indicate mitochondria in the buds of *myo2(LQ) Δdnm1* cells. Bar, 5 μ m. **(B)** Cells were prepared as in (A) and at least 100 medium-sized buds were scored for presence of mitochondria. Values represent the mean percentages + SD from triplicate experiments. Asterisks indicate statistical significance (** p > 0.5%; two-tailed Student's t-test).

Mitochondrial inheritance is blocked in *myo2(LQ) fzo1* mutants

Since $\Delta dnm1$ and *myo2(LQ)* show a positive genetic interaction in regard to both growth and mitochondrial inheritance, it was tested whether growth and inheritance also correlate in the case of *myo2(LQ)* and $\Delta fzo1$, i.e., whether *myo2(LQ) fzo1* double mutants have a severe inheritance defect. To circumvent the drawback of *myo2(LQ) Δfzo1* mutants being inviable, a temperature-sensitive *fzo1* allele, *fzo1-1*, was used (Hermann et al., 1998). This allele has three amino acid substitutions (K538I, N543I and P553Q) and leads to fragmentation of the mitochondrial network and the inability to grow on non-fermentable carbon sources at 37°C.

myo2(LQ) cells expressing mtGFP were mated with $\Delta fzo1$ cells complemented with a plasmid coding for either *FZO1* or *fzo1-1* under control of its endogenous promoter and *myo2(LQ) FZO1* or *fzo1-1* double mutants were obtained by tetrad dissection. A drop dilution assay showed that *myo2(LQ) FZO1* mutants are viable and grow well (Figure 28A), demonstrating that the observed growth defect can be prevented by plasmid-borne Fzo1, is specific for the *FZO1* deletion and not caused by a second site mutation. *myo2(LQ) fzo1-1* mutants grew already poorly at 25°C, which shows that the

fzo1-1 allele cannot completely complement the loss of wild type *FZO1* and therefore behaves as described (Hermann et al., 1998). At 37°C, however, the *myo2(LQ) fzo1-1* double mutant is almost dead and confirms the genetic interaction between *myo2(LQ)* and *fzo1*. Accordingly, the strains are suitable for further characterization.

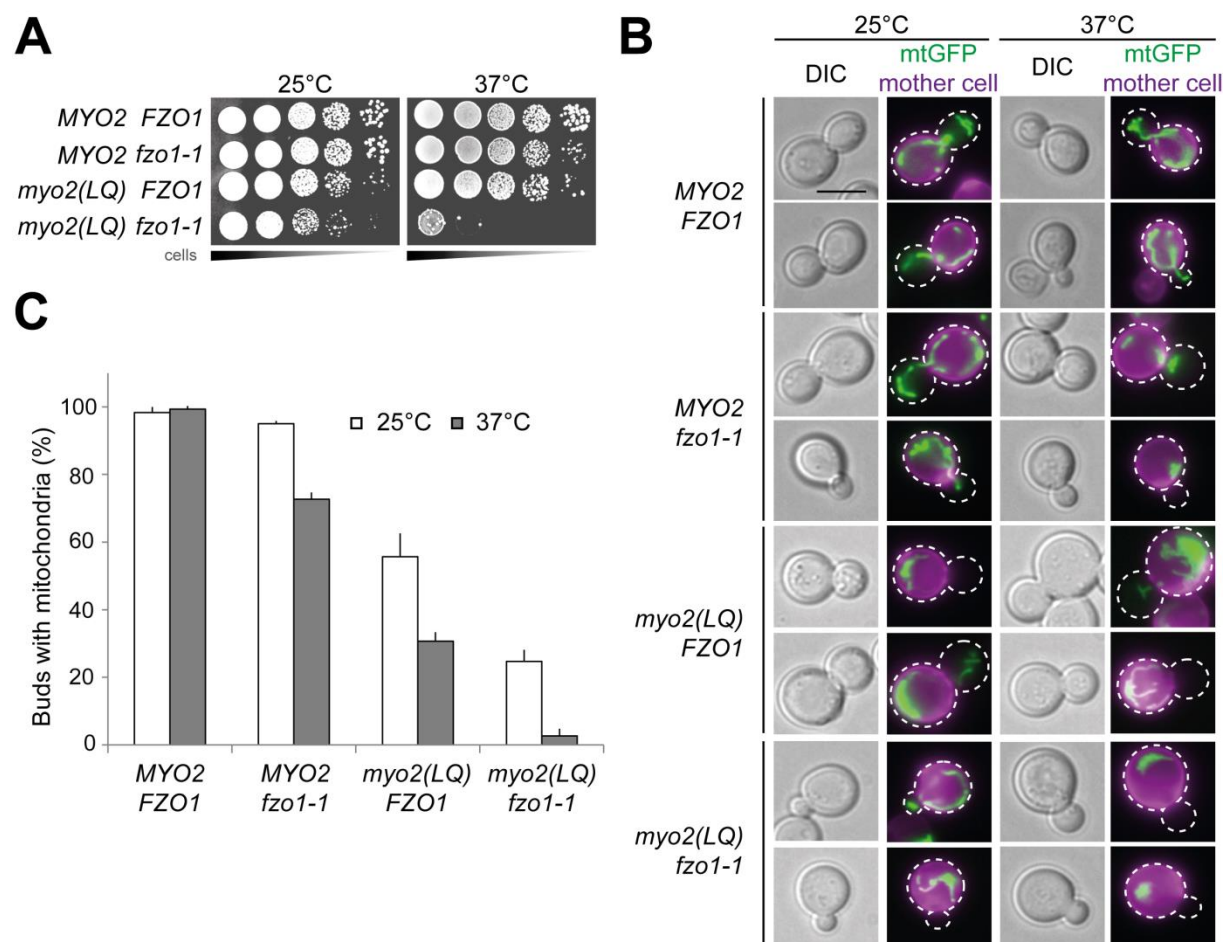


Figure 28. Mutation of *FZO1* enhances the mitochondrial inheritance defect in *myo2(LQ)* cells. (A) Strains were adjusted to the same optical density, diluted in serial 1:10 steps and spotted on glucose-containing selective medium. Plates were incubated at 25°C and 37°C. (B) Cells expressing mtGFP were grown to logarithmic growth at 25°C and stained with calcofluor. Cultures were splitted in half and either incubated for 1,5 h at 25°C or 37°C. Representative images are shown. The outlines of cells are indicated with dashed lines. Bar, 5 µm. (C) Cells from (B) were fixed with 3.7% formaldehyde and at least 100 buds (*not* stained with calcofluor) per strain were scored for presence of mitochondria. Data represent the mean values of triplicate experiments + SD.

Cells were then cultured at the permissive temperature of 25°C. Cells were pulsed with the cell wall stain calcofluor to allow the identification of mother cells. Eventually, one half of the culture was incubated at permissive and the other half at restrictive temperature. Cells were allowed to form new buds for 1.5 hours and mitochondrial inheritance was analyzed in cells, the mother of which showed a calcofluor signal and the bud did not. This staining pattern indicates that the bud was formed after the calcofluor pulse and therefore after the temperature shift. Microscopic analysis and quantification revealed that the *MYO2 fzo1-1* mutant has a slight mitochondrial inheritance defect at restrictive temperature (Figure 28B and C). The *myo2(LQ) FZO1* mutant had a substantial inheritance

defect already at 25°C, which was increased at 37°C and which is consistent with published observations (Förtsch et al., 2011). The *myo2(LQ) fzo1-1* mutant exhibited a pronounced defect already at permissive temperature, which is augmented at 37°C. At this temperature, almost no buds received mitochondria. Since mitochondrial inheritance is an essential process, this defect explains the observed synthetic lethality and shows that the maintenance of the mitochondrial network is vital when mitochondrial transport is hampered.

Fragmentation of mitochondria leads to impaired mitochondrial inheritance

Since mitochondria are not inherited by the bud in *myo2(LQ) fzo1* mutants, it was considered that fragmentation of mitochondria results in a mitochondrial inheritance defect per se, even if the transport machinery is not hampered. To this end, mutants lacking the mitochondrial fusion machinery were scored for mitochondrial inheritance. A $\Delta fzo1 \Delta dnm1$ double mutant served as a control, in which mitochondria are also unable to fuse, but form a wild type-like network (Sesaki and Jensen, 1999). The $\Delta mip1$ mutant lacking the mitochondrial DNA polymerase and consequently mtDNA was also included in the assay, given that mitochondrial fusion mutants cannot maintain their mitochondrial genome (Westermann, 2010).

Whilst wild type cells almost always managed to inherit mitochondria to the bud, about 20% of buds in fusion mutants were devoid of mitochondria (Figure 29A and B). This inheritance defect was statistically significant in $\Delta fzo1$ and $\Delta mgm1$, but not in $\Delta ugo1$. The defect was not caused by the absence of mtDNA in the fusion mutants since the $\Delta mip1$ mutant showed no inheritance deficit. Apparently, the defect is based on the fragmented mitochondrial morphology in fusion mutants because prevention of mitochondrial fission by deletion of *DNM1* in a $\Delta fzo1$ background restored mitochondrial inheritance.

Thus, mutants with fragmented mitochondria have problems in inheriting their mitochondria to the bud. This confirms the observation that *fzo1-1* mutants exhibit an inheritance defect under restrictive conditions (Figure 28C). Hence, the major objective of the *myo2(LQ)* SGA screen to uncover mutants with previously unknown mitochondrial inheritance defects was accomplished by the identification of mitochondrial fusion as a novel pathway contributing to the partitioning of mitochondria.

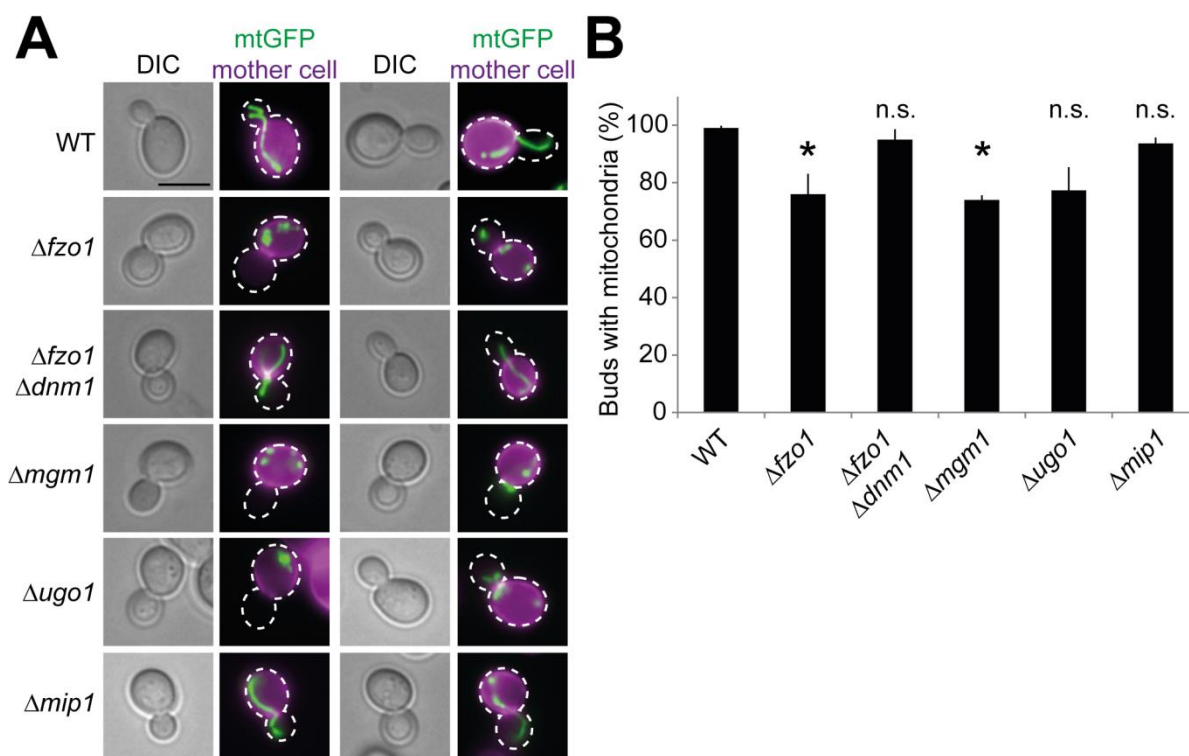


Figure 29. Analysis of mitochondrial inheritance in mitochondrial fusion mutants. (A) Strains expressing mtGFP were cultured to logarithmic growth; cells were pulsed with calcofluor and further incubated for 1.5 h to allow formation of new buds. Representative images are shown. The outlines of cells are indicated with dashed lines. Bar, 5 μ m. **(B)** Cells were prepared as in (A) and at least 100 buds (*not* stained with calcofluor) per strain were scored for presence of mitochondria. Data represent the mean values of triplicate experiments + SD. Asterisks indicate statistical significance in comparison to WT (* $p > 5\%$; n. s., not significant; two-tailed Student's t-test).

Discussion and outlook

The role of mitochondrial ER contacts in mitophagy

ERMES-mediated mitophagophore biogenesis

Screening mutants with compromised respiratory growth revealed that mutants lacking the mitochondrial ER tether ERMES fail to degrade their mitochondria by autophagy. Several lines of evidence suggest that ERMES has a pivotal role during growth of the phagophore, which occurs after initiation of mitophagophore growth at the phagophore assembly site (PAS). Assembly of the vacuole-isolation membrane contact site (VICS) before phagophore growth as marked by Atg14-GFP on mitochondria is not disturbed when ERMES is absent (Figure 18B). Moreover, Atg8 and Atg32 still colocalize in ERMES mutants (Figure 17B), indicating that mitochondrial recruitment of the core autophagic machinery works. Obvious defects occur only at later steps. The phagophore marker Atg5-GFP is present in several dots per mitochondrion in $\Delta mmm1$ (Figure 18C), suggesting that formation of excess mitophagophores is induced in cells missing ERMES. Furthermore, the staining pattern of Atg9-GFP marking the edges of the phagophore (Suzuki et al., 2013) is massively changed in $\Delta mmm1$ (Figure 20B), which confirms that phagophore biogenesis is affected.

In the wild type situation, the ERMES component Mmm1 and the phagophore constituent Atg8 interact in vivo on mitochondria (Figure 16). The fact that Mmm1-Atg8 interaction is not compromised in cells incapable of Atg8 lipidation indicates that Mmm1 interacts with Atg8 prior to its coupling to PE, which is essential for Atg8 accumulation at the PAS (Suzuki et al., 2001), further corroborating the idea that ERMES is specifically involved in phagophore biogenesis. Expression of the artificial ER-mitochondria tether chiMERA (Kornmann et al., 2009) rescues the Atg5 phenotype and the mitophagy defect (Figure 14 and Figure 19). This can also be achieved by expression of a mitochondria-specific variant of the peroxisomal ER tether protein Pex3 called Om45-Pex3 (Figure 21), which in sum demonstrates that loss of spatial proximity between mitochondria and ER is the main reason for the mitophagy defect.

Why is there a need for the ER at the sites of mitophagophore biogenesis? An obvious possibility is that the ER supplies lipids to the growing phagophore. The origin of the autophagosomal membrane has been discussed for a long time (Tooze and Yoshimori, 2010; Mari et al., 2011; Tooze, 2013). However, there is growing evidence for an involvement of the ER in this process in yeast. Blocking early steps of the secretory pathway results in defective autophagy (Ishihara et al., 2001; Reggiori et al., 2004). Moreover, ER exit sites (ERES), where secretory vesicles leave the ER, are present at the PAS and autophagosome formation relies on the functionality of these sites (Graef et al., 2013; Suzuki et al., 2013).

In sum, this points to a scenario in which ERMES tethers the mitochondrion destined for degradation, the phagophore expansion factor Atg8 and the ER in order to facilitate lipid flux from the ER to the phagophore (Figure 30). Biogenesis of surplus mitophagophores in ERMES mutants may therefore be

induced since mitophagophores cannot mature in the absence of ERMES presumably due to insufficient lipid supply. Consequently, mitophagophore biogenesis is induced at multiple sites on one mitochondrion. Since Mmm1 interacts with non-lipidated Atg8, ERMES may also be involved in the lipidation of Atg8 at mitochondria or in the insertion of Atg8 into the mitophagophore.

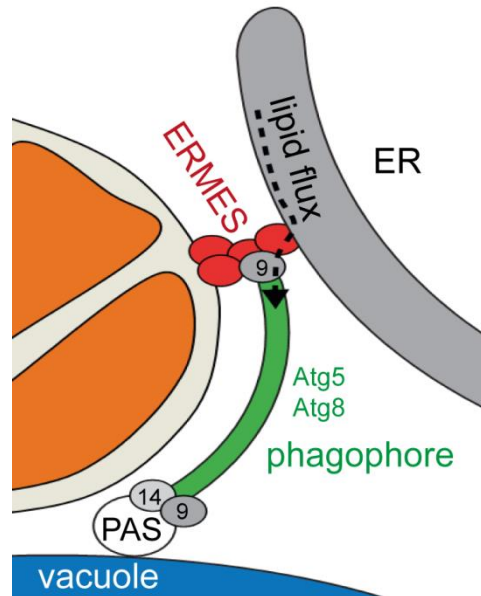


Figure 30. Model of ERMES-mediated mitophagophore biogenesis. ERMES facilitates spatial proximity between the phagophore assembly site (PAS), which is marked by Atg9 (9) and Atg14 (14), the phagophore marked by Atg5 and Atg8, and the ER. The putative lipid flux from the ER to ERMES to the phagophore is indicated by a dashed line. See text for details.

This model is consistent with results from previous studies that highlighted the importance of mitochondrial ER contacts for starvation-induced autophagosome biogenesis in mammals. Hailey et al. (2010) have proposed that mitochondria supply membrane material for autophagosomes. In this scenario, lipids are transported across Mfn2-mediated ER-mitochondria contacts and are then transferred to the growing autophagosome. However, it has been shown that autophagosomes arise from specialized subdomains of the ER, called omegasomes, in mammalian cells (Axe et al., 2008; Hayashi-Nishino et al., 2009). These conflicting results have been reconciled by the observation that the ER-resident SNARE protein syntaxin 17 (STX17) recruits ATG14 to the mitochondria-associated membranes (MAM), the contact sites between mitochondria and the ER in mammalian cells (Hamasaki et al., 2013). Omegasomes marked by the protein DFCP1 also relocate to the MAM under starvation, which depends on Mfn2 and PACS-2, both implicated in ER-mitochondria crosstalk (Simmen et al., 2005; de Brito and Scorrano, 2008). Furthermore, it has been shown that autophagosomes form at contacts between mitochondria and ER-derived omegasomes (Hamasaki et al., 2013), which does not exclude the possibility that mitochondria directly contribute lipids to the growing autophagosome as suggested by Hailey et al. (2010).

However, these results do not shed light on the process of mitophagy, since in mammalian cells mitochondria elongate under starvation conditions and hence are saved from degradation (Gomes et al., 2011). Instead, mitochondria are removed from the cell by mitophagy when they are damaged.

This damage can be triggered for example by chemical uncoupling of the electron transport chain (Narendra et al., 2008) or by light-induced activation of the mitochondria-targeted fluorescence protein KillerRed, which can be triggered to produce ROS (Bulina et al., 2006; Heo et al., 2013). Using the latter assay revealed that damaged mitochondrial pieces are removed from the network and degraded by mitophagy (Yang and Yang, 2013). Mitophagosomes form at sites that overlap with omegasomes marked by DFCP1. However, whether maintenance of mitochondrial ER contacts is functionally important for this process remains to be shown.

In conclusion, the results provided by this study demonstrate that in yeast mitochondrial ER contacts are not only the sites of mitophagosome biogenesis but that they have a vital function in mitophagy, presumably by ensuring a sufficient lipid supply from the ER to the mitophagophore. Given the fact that autophagosomes and mitophagosomes in mammalian cells also form at contacts between ER and mitochondria and that these contacts are functionally important at least in the case of general autophagy (Hailey et al., 2010; Hamasaki et al., 2013), it can be concluded that these contacts have retained their importance for this process during evolution.

ER-assisted mitochondrial division and mitophagy

During the mitochondrial life cycle, mitochondria frequently fuse and divide. Division events sometimes produce daughter units with decreased and increased membrane potential, respectively (Twig et al., 2008). Mitochondria with reduced membrane potential are less likely to rejoin with the mitochondrial network but are prone to degradation by mitophagy, which ultimately results in the maintenance of a healthy mitochondrial population. Blocking mitochondrial fission consequently reduces mitophagy and results in oxidized proteins and less respiratory capacity, highlighting the quality control aspect of mitophagy (Twig et al., 2008).

Recent studies revealed the importance of the ER in mitochondrial division. Dnm1 divides mitochondria by forming spirals around them. These spirals have a diameter of about 100 nm, which is too thin for a mitochondrion with a diameter of about 300 nm (Ingeman et al., 2005). Interestingly, constriction of mitochondrial tubules precedes recruitment of Dnm1 to these constrictions and even occurs in the absence of Dnm1 (Legesse-Miller et al., 2003). Friedman et al. (2011) have shown that the ER enwraps mitochondria in yeast and mammalian cells and that mitochondrial division ensues at these sites, which fit the diameter of Dnm1 spirals in vitro. This process has been termed ER-assisted mitochondrial division (ERMD) and was found to be important for the segregation of mitochondrial nucleoids to both mitochondrial daughter units (Murley et al., 2013; Friedman and Nunnari, 2014). Notably, the ER also determines the fission sites on endosomes in mammalian cells, suggesting that the ER is a common factor in organelle dynamics (Rowland et al., 2014).

Since compromised mitochondrial fission results in reduced mitophagy and fission requires the ER to surround mitochondria, it appears reasonable to assume that mutants lacking mitochondrial ER contacts have fission and consequently mitophagy defects. However, two lines of evidence suggest

that hampered mitochondrial fission is not the reason for the mitophagy defect in ERMES mutants. First, $\Delta dnm1 \Delta ermes$ double mutants show the same mitophagy rate as the ERMES single mutants (Figure 13). In other words, interfering with mitochondrial division in an ERMES mutant background does not enhance the mitophagy defect. Second, loss of ERMES leads to formation of excess mitophagophores as marked by Atg5-GFP (Figure 18C and D). This very pronounced phenotype cannot be seen when mitochondrial fission is absent, which demonstrates that a putative fission defect in ERMES mutants is not the cause of the mitophagy defect.

The fact that in this study $\Delta dnm1$ mutants did not have a mitophagy defect is in contrast to the results from Mao et al. (2013), who observed a mild deficiency, but it is in good agreement with observations from Mendl et al. (2011), who found no mitophagy defect in these mutants. Mao et al. (2013) propose that the diverging results can be explained as a result of different mitophagy induction protocols. Mao et al. (2013) starved the strains for nitrogen after culturing them on non-fermentable carbon sources, which is thought to be a very strong stimulus. Mendl et al. (2011) cultured the strains on non-fermentable carbon sources and induced mitophagy by addition of rapamycin, which mimics starvation but is perceived as a milder stimulus. The induction used here is not as strong as with non-fermentable carbon sources and nitrogen starvation (Figure 7C). In sum, this suggests that Dnm1-mediated division is important for efficient mitophagy when the stimulus is very strong and degradation of mitochondria has to be quick.

Mitophagy-specific fission is thought to act after mitophagy induction when the autophagy adaptor protein Atg11 recruits Dnm1 to mitochondria (Mao et al., 2013). It has been observed that ERMES subunits colocalize with these sites and therefore it has been proposed that ERMES functions during the process of mitophagy-specific division (Mao et al., 2013). Even if the main reason for the mitophagy defect in ERMES mutants is not the fission defect but the defective mitophagophore biogenesis, the results presented here do not exclude a role of ERMES in mitophagy-specific fission. It is plausible that ERMES is present at mitochondria destined for degradation, that ERMES supports mitophagy-specific fission and functions in the growth of the mitophagophore (Figure 31).

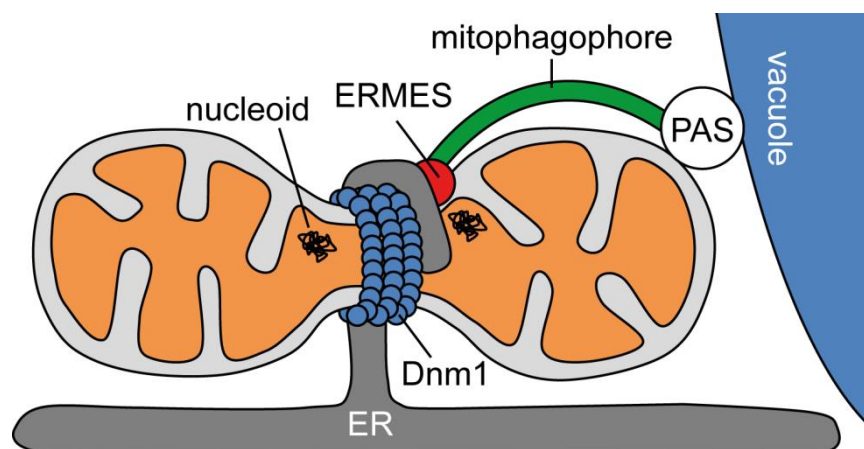


Figure 31. Involvement of ERMES in mitophagy-specific fission and mitophagophore biogenesis. See text for details. PAS, phagophore assembly site.

This scenario points to several interesting questions. First, what happens to ERMES after completion of mitophagy-specific fission? Does ERMES remain associated with the mitochondrial network and is available for another round of mitophagy-specific division, thereby isolating more mitochondrial pieces, which are then accessible for mitophagy?

Second, if ERMES remains on the mitochondrion separated for degradation, the contacts between ER-resident Mmm1 and the mitochondrial components should be resolved in order to not degrade part of the ER. It is currently unclear how this can be done. A candidate for this process is Gem1, which is a subunit of ERMES and acts as a negative regulator (Kornmann et al., 2011; Stroud et al., 2011; Murley et al., 2013).

The third fascinating question concerns the fate of mitochondrial DNA. Prior to ERMD, mitochondrial nucleoids are segregated to the daughter units (Murley et al., 2013). What happens to mtDNA during mitophagy-specific fission? One possibility is that mtDNA is spared from degradation and remains within the mitochondrial network. Alternatively, degrading mtDNA by mitophagy provides a plausible mechanism to adjust mtDNA content to mitochondrial mass, which declines during mitophagy. We already know from hepatocytes that mitochondrial fission and sequestration in autophagosomes are coordinated and that mtDNA is degraded alongside with mitochondria (Kim and Lemasters, 2011). Furthermore, it is tempting to speculate that mitophagy offers a mechanism for cells to get rid of defective mtDNA, which causes various diseases (Wallace, 2005, 2010).

ER association as a prerequisite for organellophagy

The autophagic degradation of different organelles, called organellophagy, shares common features like organelle-specific receptors, which interact with Atg8 and recruit the core autophagic machinery, thereby facilitating the sequestration of the organelle by an autophagosome and subsequent degradation (reviewed in Okamoto, 2014). It is an interesting question whether an association of the ER with the organelle destined for degradation is necessary for organellophagy in general like in mitophagy.

Pexophagy, the autophagic degradation of peroxisomes, together with mitophagy is the most intensively studied organellophagy pathway. Although mitochondria and peroxisomes do not share a common evolutionary heritage, they have common traits. Both organelles are engaged in β -oxidation of fatty acids and in detoxification of ROS. It is currently unclear whether direct contact sites between the two organelles exist, however, peroxisomes from rat liver cells co-sediment with mitochondria, suggesting that such contacts are indeed established (Islinger et al., 2006). Moreover, peroxisomes and mitochondria move in association with each other in fission yeast (Jourdain et al., 2008) and were found to be in close proximity by electron microscopy in baker's yeast (Rosenberger et al., 2009). Both organelles use the same signaling pathway to the nucleus in order to induce expression of mitochondrial or peroxisomal genes (Chelstowska and Butow, 1995) and, strikingly, fission of mitochondria and peroxisomes both rely on the same machinery in yeast and mammals (Schrader et al., 2012). This process is important for the degradation of both organelles when

organellophagy-specific division is initiated by Atg11-mediated recruitment of Dnm1 (Mao et al., 2013; Mao et al., 2014). Furthermore, the mitophagy-specific protein Atg32 can induce pexophagy when targeted to peroxisomes, and relocalization of the pexophagy machinery to mitochondria is sufficient to complement the absence of the mitophagy receptor Atg32 (Kondo-Okamoto et al., 2012; Motley et al., 2012). In addition, this relocalization rescues the mitophagophore defect in ERMES mutants presumably by restoring the contacts to the ER (Figure 21). These observations indicate that mitophagy and pexophagy share many common hallmarks.

Interestingly, mitochondria and peroxisomes both establish contacts with the ER, which are important for the organelles' behavior (Kornmann et al., 2009; Knoblach et al., 2013). While ERMES tethers mitochondria and ER, peroxisomal attachment to the ER relies on Pex3 anchored on peroxisomes and Pex3 residing in the ER membrane (Knoblach et al., 2013). Both are bridged by Inp1 acting as a molecular hinge. The absence of Pex3 results in defective pexophagy as expected, if peroxisomal ER contacts are supposed to be important for the degradation of peroxisomes, but this protein also recruits Atg36, which in turn recruits Atg8 and Atg11 during pexophagy (Motley et al., 2012). However, Inp1 was found to be dispensable for pexophagy (Motley et al., 2012), suggesting that these contacts are not essential for this process. However, no data demonstrating this has been presented.

Yet, peroxisomes destined for degradation were frequently found in close vicinity to mitochondria (Mao et al., 2014). Hence, the degradation of both, mitochondria and peroxisomes, may be coupled and initiated at the same sites within a cell. It is not clear whether peroxisomes and mitochondria share contacts with each other or if ERMES is in close proximity with peroxisomes during their degradation. Interestingly, it has been reported that during normal growth some peroxisomes are indeed close to mitochondrial ER contacts (Cohen et al., 2014), which strengthens the idea that pexophagy is executed at junctions between ER and mitochondria. It has not been tested yet, if ERMES is important for pexophagy, which would suggest that growth of phagophores sequestering peroxisomes relies on mitochondrial ER contacts. Furthermore, it is unknown whether the ER is involved in peroxisomal division as it is in the case of mitochondria. But Inp1 bridging ER and peroxisomes was proposed to be involved in peroxisomal fission, since it interacts with Vps1 (Fagarasanu et al., 2005), which in turn is redundant with Dnm1 in peroxisomal fission (Kuravi et al., 2006; Fagarasanu et al., 2010), suggesting that peroxisomal division happens at peroxisomal ER contacts. Interestingly, Vps1 was found to be important during pexophagy and to interact with Atg11 and Atg36 (Mao et al., 2014), which are part of the pexophagy machinery.

It will be interesting to see whether degradation of peroxisomes and mitochondria is coupled and if this degradation occurs at mitochondrial ER contacts. Moreover, it is of general interest whether fission of peroxisomes relies on contacts with the ER. Thus, the ER might have a general role in organelle dynamics and organellophagy.

Genetic interactions of *myo2(LQ)*

Organelle specificity of *myo2(LQ)*

The class V myosin Myo2 transports multiple cargos like peroxisomes, vacuoles, secretory vesicles, microtubule plus ends, Golgi cisternae, lipid droplets and mitochondria (reviewed in Pruyne et al., 2004; Knoblach and Rachubinski, 2015) and therefore has to cooperate with a variety of different adaptor molecules. It is plausible that *MYO2* genetically interacts with many different genes involved in the transport of diverse structures. In this study, a *myo2* mutant (Q1233R and L1301P) with a mitochondrial inheritance defect was used as a query strain and crossed to a yeast deletion library in order to screen for genetic interactions. About 200 reproducible interactions were detected. However, the *myo2(LQ)* mutant does not only have a mitochondrial but also a vacuolar inheritance defect, since both mutations lead to an inability of Myo2 to interact with the mitochondrial Myo2 interactor Mmr1 and the vacuolar Myo2 receptor Vac17 (Catlett et al., 2000; Förtsch et al., 2011; Eves et al., 2012). Moreover, the L1301P mutation of *myo2(LQ)* results in defective binding of Kar9 (Eves et al., 2012), which mediates the interaction of Myo2 with microtubule plus ends and is important for nuclear migration (Hwang et al., 2003). It is unlikely that *myo2(LQ)* has an effect on the transport of secretory vesicles or peroxisomes, as the two mutated residues do not lie in the corresponding binding regions (Pashkova et al., 2006; Fagarasanu et al., 2009). If the transport of Golgi structures is affected, has not been tested yet.

The transport and inheritance of vacuoles is not an essential process because vacuoles can be formed de novo by an unknown mechanism (Weisman, 2006). Additional mutations, which are blocking vacuolar inheritance completely in *myo2(LQ)* cells, are not expected to be detected by screening for unexpected growth behaviors in an SGA approach. The daughter cells lacking vacuoles will just rebuild vacuoles and multiply. Nuclear migration and mitochondrial inheritance are important for normal growth and are at least in part mediated by Myo2. Consequently, the genetic interactome of *myo2(LQ)* is expected to reveal genes involved in the inheritance of the nucleus and of mitochondria.

This was confirmed by the observation that most functional enrichments were found for the processes related to mitochondria and to the nucleus (Figure 23E). Moreover, the negative genetic interaction of *myo2(LQ)* and *NUM1* is caused by a strong disturbance of nuclear migration (Figure 25). This raises the question of how to filter out mitochondria-specific hits. A promising possibility is to test whether the expression of *myo2-fis1* rescues the growth defects of the negative interactors. Myo2-Fis1 is only able to restore the mitochondrial inheritance defect in the *myo2(LQ)* mutant, but not the defects of other organelles, as Myo2-Fis1 resides in the MOM (Förtsch et al., 2011). It has thus been shown that the synthetic lethality of *myo2(LQ)* Δ *ypt11* double mutants is based on a complete block of mitochondrial inheritance and that viability can be reinstated by *myo2-fis1* expression (Förtsch et al., 2011). Hence, a sublibrary containing all negative interactors can be crossed with a *myo2(LQ)* query strain carrying either an empty vector or a plasmid coding for *myo2-fis1*, and double mutants can be obtained by SGA technology. The double mutants carrying the empty vector are expected to exhibit growth defects as in the original screen, while mitochondria-

specific interactors should be rescued by *myo2-fis1* expression and the corresponding colonies should appear bigger than the ones with the control plasmid.

In contrast to the double mutants of negative interactors, which are barely growing or even inviable, mitochondrial inheritance can be assessed more directly in double mutants of positive interactors, which are growing better than expected. A sublibrary of positive interactors ($\Delta yfgX$) can be crossed with a *MYO2* and a *myo2(LQ)* query strain each carrying a plasmid coding for mtGFP. Double mutants can then be constructed by SGA technology and the fraction of buds with mitochondria can be quantified by fluorescence microscopy. The expectation is that in the wild type situation almost 100% of the buds have mitochondria in contrast to about 50% in the *myo2(LQ)* single mutant. If the other single mutant ($\Delta yfgX$) also would have about 100% of buds containing mitochondria, the calculated mitochondrial inheritance of the double mutant (*myo2(LQ)* $\Delta yfgX$) equals the one in the *myo2(LQ)* single mutant of 50%. If the fraction, however, would be higher than 50% in the double mutant, mitochondrial inheritance would be alleviated and the situation would be comparable to *myo2(LQ)* $\Delta dnm1$ double mutants. This double mutant grows surprisingly well and has more buds with mitochondria than expected (Figure 27). In double mutants identified by this approach, unexpected good growth and mitochondrial inheritance correlate and they are promising candidates for further characterization.

Possibly, these candidate genes code for components which are involved in the retrograde transport of mitochondria from the bud into the mother. If these genes are missing in a *myo2(LQ)* background, mitochondrial retrograde transport is expected to be reduced, inheritance of mitochondria to be alleviated and ultimately the double mutant is expected to grow better than the *myo2(LQ)* single mutant. If the gene products promote the backwards movement of mitochondria, their overexpression should result in a significant fraction of buds devoid of mitochondria in the wild type and be toxic in a *myo2(LQ)* background, since anterograde movement is hampered by the *myo2(LQ)* mutation and is at the same time heavily counteracted by the hyper-activation of retrograde transport. Thus, components of the retrograde transport of mitochondria can be identified.

Significance of genetic interactions between components of mitochondrial dynamics and *myo2(LQ)*

Screening for genetic interactors of *myo2(LQ)* revealed that mutations blocking mitochondrial fusion are synthetic lethal in a *myo2(LQ)* background (Figure 26). *myo2(LQ)* cells with the conditional *fzo1-1* allele show an almost complete block of mitochondrial inheritance under restrictive conditions (Figure 28), which explains the growth defect. The growth defect is rescued when mitochondrial fragmentation by mitochondrial division is prevented (Figure 26C), demonstrating that the fusion activity is not essential for *myo2(LQ)* mutants. Rather, these mutant cells depend on a wild type-like mitochondrial morphology. Blockage of mitochondrial division in *myo2(LQ)* mutant cells with fusion-competent mitochondria results in enhanced mitochondrial inheritance and augmented growth compared to *myo2(LQ)* single mutants (Figure 26 and Figure 27). Thus, components of two

antagonistic pathways, mitochondrial fusion and division, genetically interact with *myo2(LQ)* in divergent ways regarding growth and mitochondrial inheritance. Moreover, the temperature-sensitive *fzo1-1* allele and deletion of mitochondrial fusion components lead to many buds devoid of mitochondria in a wild type *MYO2* background (Figure 28B, C and Figure 29), indicating that fragmentation of mitochondria per se results in compromised inheritance. Notably, this is the first study observing an inheritance defect in yeast fusion mutants, although these have been characterized for more than 15 years (Hermann et al., 1998; Rapaport et al., 1998).

The question remains why mitochondrial morphology is important for inheritance. Possibly, a hyper-connected mitochondrial network alleviates the anterograde movement since much mitochondrial mass can be transported into the bud by pulling on a single mitochondrial tip. This would explain the effects of the *DNM1* knock-out. However, deletion of *NUM1*, which also results in net-like mitochondria (Cerveny et al., 2007), had no effect on mitochondrial inheritance in a *myo2(LQ)* background (Figure 25A and B), suggesting that the hyper-connection of the network alone is not sufficient to ease the transport. On the other hand, basal fission activity in $\Delta num1$ cells might be strong enough to slightly disconnect the mitochondrial network and thus to obscure the effect.

In the case of fragmented mitochondria many transport events of single mitochondria are required to ensure the inheritance of a large organellar volume. This might already be difficult for cells with a functional transport machinery and be further aggravated by compromising the machinery with the *myo2(LQ)* allele. However, it is counterintuitive that smaller mitochondria are harder to transport and that no mitochondrion at all is inherited by the bud in the *myo2(LQ) fzo1-1* mutant. Smaller mitochondria are expected to be the simpler cargo. Accordingly, secretory vesicles are transported by Myo2 with 3 $\mu\text{m/s}$ (Schott et al., 2002), whereas the bigger mitochondria move with a velocity of clearly below 1 $\mu\text{m/s}$ (Boldogh et al., 2004; Förtsch et al., 2011). One possible explanation for the defect is that the density of mitochondrial Myo2 receptors is too low on fragmented mitochondria in order to pull them into the bud. If this was the case, overexpression of the two proposed Myo2 receptors Mmr1 and Ypt11 might rescue the inheritance defect of fusion mutants and the growth defect of *myo2(LQ) fzo1-1* double mutants. Moreover, the growth defect of *myo2(LQ) fzo1-1* double mutants may prove valuable as a tool to search for additional mitochondrial Myo2 receptors. A screen comprising all yeast ORFs should be able to uncover genes the overexpression of which rescues the growth defect. Potentially, this screen can enable the identification of proteins that recruit Ypt11, Mmr1 or Myo2 itself to the mitochondrial surface and thereby promote anterograde transport.

Although the effects of mitochondrial dynamics on inheritance have not attracted much attention in yeast, it is known that mitochondrial distribution in neurons depends on fusion and fission (Hollenbeck and Saxton, 2005). Neurons are an ideal model to study mitochondrial transport since mitochondrial biogenesis occurs mainly in the cell body and mitochondria then have to be transported into the tips of dendrites and axons (reviewed in Sheng, 2014). These transport processes cover distances of up to one meter. Interestingly, there are conflicting results on the issue which morphologies are easier to transport. Defects in mitochondrial fusion and division have both

been shown to impact on mitochondrial motility and both pathways were demonstrated to be necessary for the transport of mitochondria to their destination (Li et al., 2004; Verstreken et al., 2005). Thus, a balance between fusion and division appears to ensure a mitochondrial morphology suitable for neuronal transport, which is highly important for the functionality of neurons. Miro, the human homolog of Gem1, connects mitochondria with kinesin and microtubules for mitochondrial transport. Remarkably, overexpression of Miro results in interconnection of mitochondria and boosts their transport, whereas compromising the functionality of Miro leads to mitochondrial fragmentation and less transport activity (summarized in Sheng, 2014), resembling the situation in *myo2(LQ)* cells. There, mitochondrial hyper-connection augments mobility, whilst fragmentation hampers transport. Furthermore, Miro directly interacts with the human homolog of Fzo1, Mfn2, and knock-down of Mfn2 results in less mitochondrial anterograde and retrograde movement (Misko et al., 2010).

Obviously, mitochondrial dynamics is an important factor for the movement of mitochondria. It is yet unclear, which role the dynamics exactly plays. One can speculate that fragmented mitochondria are less likely to be inherited to the daughter because this morphology is a hallmark of mitochondria with reduced functionality and these mitochondria would be detrimental to the daughter's health. Mitochondria undergo division and fragment in yeast and mammalian cells when they are damaged and stressed, for instance with H_2O_2 , and this results in heavily reduced mitochondrial motility in yeast (Baker et al., 2014; Zhou et al., 2014). Moreover, yeast cells accumulate fragmented, dysfunctional mitochondria concomitantly with replicative age (Scheckhuber et al., 2007; Hughes and Gottschling, 2012; Wang et al., 2014). Possibly, mitochondria with declined metabolic capacity adopt a shape by fragmentation that is less likely to be transported into the daughter cell, thus providing a potential quality control filter in addition to mitophagy. The biogenesis of Mgm1, the MIM component required for mitochondrial fusion, offers a putative mechanism, since the processing of Mgm1 by the protease Pcp1 depends on ATP (Herlan et al., 2004). Mitochondria with reduced oxidative phosphorylation and ATP thus might lack an Mgm1 isoform which is essential for fusion. Hence, these mitochondria cannot refuse with the mitochondrial network and are not inherited. In future experiments, this hypothesis can be tested by observation of mitochondrial motility via time-lapse fluorescence microscopy in stressed and aged yeast cells.

Materials and methods

Molecular biology

Plasmids and primers

Many of the plasmids used here were already described in Böckler and Westermann (2014). For a full list of primers and plasmids see Table 2 and Table 3 below. Standard procedures were used for cloning and amplification of plasmids (Green and Sambrook, 2012). PCR was performed using Pfu or phusion polymerase (Fermentas, St. Leon-Rot, Germany). For construction of pYX122-ssGFP-HDEL, ssGFP-HDEL was amplified using WP1055-ssGFP (Prinz et al., 2000) as a template and oligonucleotides WP1055fwdEcoRI and WP1055revXhoI and cloned into *EcoRI* and *XhoI* sites of pYX122 (R&D Systems, Abingdon, UK). To generate pYES-mtRosella, the *BamHI/NotI* fragment of pAS1NB-CS-RG (Rosado et al., 2008) was cloned into the *BamHI/NotI* sites of pYES-mtGFP (Westermann and Neupert, 2000). The *HindIII/XhoI* fragment of pYES-mtRosella was ligated into the *HindIII/XhoI* sites of pVT100U-mtGFP (Westermann and Neupert, 2000) to produce pVT100U-mtRosella. The *HindIII/SacI* fragment of pVT100U-mtRosella was cloned into the *HindIII/SacI* sites of pBN1001 to generate pBN-mtRosella. Rosella was amplified from pAS1NB-CS-RG with primers cytRosella-fwdBamHI and cytRosella-revXhoI and cloned into the *BamHI/XhoI* sites of pRS425-GPD resulting in pRS425-GPD-cytRosella. To generate pRS415-ADH-chiMERA and pRS415-TEF-chiMERA, the *BamHI/XhoI* fragment of pRS415-GPD-chiMERA (Kornmann et al., 2009) was cloned into the *BamHI/XhoI* sites of pRS415-ADH and pRS415-TEF (Mumberg et al., 1995), respectively. For cloning of pRS316-MMM1, pRS416-MDM12, and pRS416-MDM34, the genes were amplified from genomic DNA by using the primers MMM1fwdBamHI, MMM1revstopSpeI, MDM12fwdEcoRI, MDM12revXhoI, MDM34fwdHindIII and MDM34revXhoI, respectively. The genes were then cloned into pRS316 or pRS416 (Sikorski and Hieter, 1989; Christianson et al., 1992). yEmRFP (ERFP) was amplified from yEpGAP-Cherry (Keppler-Ross et al., 2008) using oligonucleotides MMM1eRFPfwd and MMM1eRFPprev and cloned into the *SacI/SpeI* sites of pRS316 to produce pRS316-ERFP. *MMM1* with its endogenous promoter was then amplified from genomic DNA using the primers MMM1F and MMM1R and subsequently ligated into the *XhoI/SpeI* sites of pRS316-ERFP to produce pRS316-MMM1-ERFP. pRS415-GFP-ATG8 was generated by ligating the *BamHI/XhoI* fragment of GFP-ATG8(414) (Abeliovich et al., 2003) into the *BamHI/XhoI* sites of pRS415 (Sikorski and Hieter, 1989; Christianson et al., 1992). ATG8-N-YN-425ADH was generated by amplifying *ATG8* from genomic DNA using the primers ATG8fwd and ATG8rev and cloning into the *SmaI/XhoI* sites of N-YN-425ADH (Skarp et al., 2008). MMM1-C-YC-426ADH was produced by amplifying *MMM1* from genomic DNA using the oligonucleotides MMM1fwd and MMM1revnostop and cloning into the *BamHI/ClaI* sites of C-YC-426ADH (Skarp et al., 2008). pRS415-MET-GFP-ATG32 and pRS415-MET-ERFP-ATG32 were generated by amplifying *ATG32* using the primers ATG32fwdApaI and ATG32revXhoI. *ATG32* was then cloned into the *ApaI/XhoI* sites of pRS415-MET-GFP-DNM1 and pRS415-MET-ERFP-DNM1, respectively. GFP-tagged versions of *ATG5*, *ATG9*, and *ATG14* were produced by amplifying the genes

from genomic DNA using the primers ATG5attBfwd, ATG5attBrev, ATG9attBfwd, ATG9attBrev, ATG14attBfwd, and ATG14attBrev, respectively. The genes were then cloned into pAG413-GPD-ccdB-GFP (Alberti et al., 2007) using the Gateway cloning system (Invitrogen, Carlsbad, CA). A DNA fragment coding for the mitochondrial presequence of *N. crassa* Su9 was amplified from pYES-mtGFP using primers GatewaySu9PSpYESmtGFPfwd and GatewaySu9PSpYESmtGFPrev. It was then cloned into pAG423-GPD-ccdB-dsRed using the Gateway cloning system to produce pAG423-GPD-mtdsRed. *FZO1* and *fzo1-1* with their endogenous promoter and terminator were amplified from genomic DNA coding either for *FZO1* or *fzo1-1* (Hermann et al., 1998) by using primers FZO1Xba1fwd and FZO1EcoRIrev and cloned into the *XbaI*/*EcoRI* sites of pRS313 resulting in pRS313-FZO1 and pRS313-fzo1-1. pRS316-3xmCherry was produced by amplifying 3xmCherry from pYM-3xmCherry(HIS3MX6)-2 using the primers 3xmCherryfwdSpeI and 3xmCherryrevNotI and cloning them into the *SpeI*/*NotI* sites of pRS316. Then *MMM1* was amplified from genomic DNA using the primers MMM1F and MMM1R and cloning it into the *SpeI*/*XhoI* sites of pRS316-3xmCherry thus generating pRS316-MMM1-3xmCherry. pAG415-GAL-myo2-fis1 was constructed as described in Klecker et al. (2013).

Table 2. Plasmids used in this study.

Name	Relevant characteristics	Source
ATG8-N-YN-425ADH	2 μ / LEU2 / ADH prom	this study; Böckler & Westermann, 2014
C-YC-426ADH	2 μ / URA3 / ADH prom	Skarp et al., 2008;
GFP-ATG8(414)	CEN / TRP1 / endogenous prom	Abeliovich et al., 2003
GFP-ATG8(416)	CEN / URA3 / endogenous prom	D. Klionsky, Michigan, USA
MMM1-C-YC-426ADH	2 μ / URA3 / ADH prom	this study; Böckler & Westermann, 2014
N-YN-425ADH	2 μ / LEU2 / ADH prom	Skarp et al., 2008
pAG413-GPD-ccdB-GFP	CEN / HIS3 / GPD prom	Alberti et al., 2007
pAG413-GPD-ATG14-GFP	CEN / HIS3 / GPD prom	this study; Böckler & Westermann, 2014
pAG413-GPD-ATG5-GFP	CEN / HIS3 / GPD prom	this study; Böckler & Westermann, 2014
pAG413-GPD-ATG9-GFP	CEN / HIS3 / GPD prom	this study; Böckler & Westermann, 2014
pAG415-GAL-ccdB	CEN / LEU2 / GAL prom	Alberti et al., 2007
pAG415-GAL-myo2-fis1	CEN / LEU2 / GAL prom	T. Klecker, Zellbiologie, Bayreuth
pAG423-GPD-ccdB-dsRed	2 μ / HIS3 / GPD prom	Alberti et al., 2007
pAG423-GPD-mtdsRed	2 μ / HIS3 / GPD prom	this study; Böckler & Westermann, 2014
pAS1NB-CS-RG	2 μ / LEU2 / PGK1 prom	Rosado et al., 2008
pBN1001	2 μ / LEU2 / ADH prom	B. Neumann, Zellbiologie, Bayreuth
pDONR221	gateway cloning vector	Invitrogen, Darmstadt
pJM14 (Om45-Pex3)	CEN / URA3 / OM45 prom	Motley et al., 2012
pRS313	CEN / HIS3	Sikorski & Hieter, 1989

Name	Relevant characteristics	Source
pRS313-FZO1	CEN / HIS3 / endogenous prom	this study
pRS313-fzo1-1	CEN / HIS3 / endogenous prom	this study
pRS316	CEN / URA3	Sikorski & Hieter, 1989
pRS316-3xmCherry	CEN / URA3	this study
pRS316-MMM1-3xmCherry	CEN / URA3 / endogenous prom	this study
pRS316-ERFP	CEN / URA3	this study; Böckler & Westermann, 2014
pRS316-MMM1	CEN / URA3 / endogenous prom	this study; Böckler & Westermann, 2014
pRS316-MMM1-ERFP	CEN / URA3 / endogenous prom	this study; Böckler & Westermann, 2014
pRS415	CEN / LEU2	Sikorski & Hieter, 1989
pRS415-ADH	CEN / LEU2 / ADH prom	Mumberg et al., 1995
pRS415-ADH-chiMERA	CEN / LEU2 / ADH prom	this study; Böckler & Westermann, 2014
pRS415-GFP-ATG8	CEN / LEU2 / endogenous prom	this study; Böckler & Westermann, 2014
pRS415-GPD-chiMERA	CEN / LEU2 / GPD prom	Kornmann et al., 2009
pRS415-MET-ERFP-ATG32	CEN / LEU2 / MET25 prom	this study
pRS415-MET-ERFP-DNM1	CEN / LEU2 / MET25 prom	D. Scholz, Zellbiologie, Bayreuth
pRS415-MET-GFP-ATG32	CEN / LEU2 / MET25 prom	this study; Böckler & Westermann, 2014
pRS415-MET-GFP-DNM1	CEN / LEU2 / MET25 prom	J. Nunnari, Davis, USA
pRS415-TEF	CEN / LEU2 / TEF prom	Mumberg et al., 1995
pRS415-TEF-chiMERA	CEN / LEU2 / TEF prom	this study; Böckler & Westermann, 2014
pRS416	CEN / URA3	Sikorski & Hieter, 1989
pRS416-MDM10	CEN / URA3 / endogenous prom	C. Meisinger, Freiburg
pRS416-MDM12	CEN / URA3 / endogenous prom	this study; Böckler & Westermann, 2014
pRS416-MDM34	CEN / URA3 / endogenous prom	this study; Böckler & Westermann, 2014
pRS425-GPD	2 μ / LEU2 / GPD prom	Mumberg et al., 1995
pRS425-GPD-cytRosella	2 μ / LEU2 / GPD prom	this study; Böckler & Westermann, 2014
pVT100U-mtGFP	2 μ / URA3 / ADH prom	Westermann & Neupert, 2000
pVT100U-mtRFP	2 μ / URA3 / ADH prom	Y. Brede, Zellbiologie, Bayreuth
pVT100U-mtRosella	2 μ / URA3 / ADH prom	this study; Böckler & Westermann, 2014
pYES-mtGFP	2 μ / URA3 / GAL prom	Westermann & Neupert, 2000
pYES-mtRosella	2 μ / URA3 / GAL prom	this study; Böckler & Westermann, 2014
pYM-3xmCherry (HIS3MX6)-2		C. Ungermann, Osnabrück
pYX122	CEN / HIS3	R&D systems, Abingdon, UK

Name	Relevant characteristics	Source
pYX122-ssGFP-HDEL	CEN / HIS3 / TPI prom	this study; Böckler & Westermann, 2014
pYX142	CEN / LEU2	R&D Systems, Abingdon, UK
pYX142-MCP1	CEN / LEU2 / TPI prom	Tan et al., 2013
pYX142-MCP2	CEN / LEU2 / TPI prom	Tan et al., 2013
pYX142-mtGFP	CEN / LEU2 / TPI prom	Westermann and Neupert, 2000
WP1055-ssGFP	CEN / URA3 / MET prom	Prinz et al., 2000
yEpGAP-Cherry	2 μ / URA3	Keppler-Ross et al., 2008

Table 3. Primers used for cloning in this study.

Name	Sequence (5' - 3')
3xmCherry fwd SpeI	TTTACTAGTCAGGTCGACATGGTGAGC
3xmCherry rev NotI	TTTGCGGCCGCTCACTTGTACAGCTCGTCCATGC
ATG14 attB rev	GGGGACCACTTTGTACAAGAAAGCTGGGTCGCCTACCACGTACCATCGGTCATG
ATG14 attB fwd	GGGGACAGTTTGTACAAAAAGCAGGCTTCATGCATTGCCCAATTGCCCACC
ATG32 fwd Apal	ATATGGGCCCCGTTTTGGAATACCAACAAAG
ATG32 rev XhoI	TAATACTCGAGTGAGTAGGAACGTGTATGTTTG
ATG5 attB fwd	GGGGACAAGTTTGTACAAAAAGCAGGCTTCATGAATGACATTAAACAACTACTTTG
ATG5 attB rev	GGGGACCACTTTGTACAAGAAAGCTGGGTCGAGCTCAGAGGAAGCTTTATCG
ATG8 fwd	TTTTCCCGGGATGAAGTCTACATTTAAGTCTGAATATC
ATG8 rev	TTTTCTCGAGCTACCTGCCAAATGTATTTTCTC
ATG9 attB fwd	GGGGACAAGTTTGTACAAAAAGCAGGCTTCATGGAGAGAGATGAATACAGTTACC
ATG9 attB rev	GGGGACCACTTTGTACAAGAAAGCTGGGTCTCTTCCGACGTCAGACTTCTTG
cytRosella fwd BamHI	TATGGATCCATGGCCTCCTCCGAGG
cytRosella rev XhoI	TATCTCGAGTCAGTGATCAGATTTGTATAGTTC
DsRedFP	AAAGGTAACATGGCCTCCTCCGAGGACGTC
DsRedRP	AAAGAGCTCCTACAGGAACAGGTGGTGGCG
FZO1 XbaI fwd	TTTTCTAGAGTGCTTGAGTATCAGGAGAAGG
FZO1 EcoRI rev	TTTGAATTCGAGCTATTACTTCCAGGGAC
Gateway Su9 PS pYESmtGFP fwd	GGGGACAAGTTTGTACAAAAAGCAGGCTCGAAAAAATGGCCTCCACTCGTGTCCCTCGC
Gateway Su9 PS pYESmtGFP rev	GGGGACCACTTTGTACAAGAAAGCTGGGTGTTCTTCTCCTTTACTCATA GATCTGG
MDM12 fwd EcoRI	TATGAATTCTGTTTGAAACCAACTCGAAGC
MDM12 rev XhoI	TATCTCGAGTGTTTCACAAACACAAGC
MDM34 fwd HindIII	TATAAGCTTTCGAAACACTGATCTGGAC
MDM34 rev XhoI	TATACTCGAGGTACGGTTGTGGTCAGTCG
MMM1 eRFP fwd	TATATAACTACTAGTATGGTTTCAAAAGGTGAAGAAGATA
MMM1 eRFP rev	TATATAGAGCTCCACAGCTGCTCGAGCG
MMM1 F	AAACTCGAGTGCTTATGCCGTTATTTGAGG
MMM1 fwd	TTTTGGATCCATGACTGATAGTGAGAATGAATCC

Name	Sequence (5' - 3')
MMM1 fwd BamHI	ATATATGGATCCTGCTTATGCCGTTATTTGAGG
MMM1 R	GAAGAAAAGCCTACAGAGTTAACTAGTTTT
MMM1 rev no stop	TTTTATCGATTAACCTCTGTAGGCTTTTCTTCTC
MMM1 rev stop SpeI	TAATACTAGTTTTGGAGAAGTCGTATCACC
pBN1001 fwd BglII	AATTATAGATCTCCTCAACATAACGAGAACAC
pBN1001 rev BglII	TATTATAGATCTTCGTCTACCCTATGAAC
WP1055 fwd EcoRI	GATACGAATTCATGAAAGCATTACACCAGTTTACTATG
WP1055 rev XhoI	ATATCTCGAGTTACAATTCGTCTGGCAGCCGGATC

Yeast genetics and cell biology

Yeast strains

Table 4. List of yeast strains used in this study. Strains derived from mating of BY4741 and BY4742 cells, sporulation and subsequent tetrad dissection of haploid cells are listed as isogenic to “BY”. Strains were transformed with plasmids listed in Table 2.

Isogenic	Name	Genotype	Source
BY4742	WT	<i>MATα his3Δ1 leu2Δ0 lys2Δ0 ura3Δ0</i>	Brachmann et al., 1998
BY4741	WT	<i>MATα his3Δ1 leu2Δ0 met15Δ0 ura3Δ0</i>	Brachmann et al., 1998
BY4742	<i>Δatg32</i>	<i>MATα his3Δ1 leu2Δ0 lys2Δ0 ura3Δ1 Δatg32::kanMX4</i>	Giaever et al., 2002
BY4742	WT (ρ^0)	<i>MATα his3Δ1 leu2Δ0 lys2Δ0 ura3Δ0 ρ^0</i>	T. Klecker, Zellbiologie, Bayreuth
BY4742	<i>Δmmm1</i>	<i>MATα his3Δ1 leu2Δ0 lys2Δ0 ura3Δ0 Δmmm1::kanMX4</i>	Giaever et al., 2002
BY4742	<i>Δmdm10</i>	<i>MATα his3Δ1 leu2Δ0 lys2Δ0 ura3Δ0 Δmdm10::kanMX4</i>	Giaever et al., 2002
BY4742	<i>Δmdm12</i>	<i>MATα his3Δ1 leu2Δ0 lys2Δ0 ura3Δ0 Δmdm12::kanMX4</i>	Giaever et al., 2002
BY4742	<i>Δmdm34</i>	<i>MATα his3Δ1 leu2Δ0 lys2Δ0 ura3Δ0 Δmdm34::kanMX4</i>	Giaever et al., 2002
BY4742	<i>Δatg1</i>	<i>MATα his3Δ1 leu2Δ0 lys2Δ0 ura3Δ0 Δatg1::kanMX4</i>	Giaever et al., 2002
BY4742	<i>Δmdm33</i>	<i>MATα his3Δ1 leu2Δ0 lys2Δ0 ura3Δ0 Δmdm33::kanMX4</i>	Giaever et al., 2002
BY4742	<i>Δsam37</i>	<i>MATα his3Δ1 leu2Δ0 lys2Δ0 ura3Δ0 Δsam37::kanMX4</i>	Giaever et al., 2002
BY4742	<i>Δdnm1</i>	<i>MATα his3Δ1 leu2Δ0 lys2Δ0 ura3Δ0 Δdnm1::kanMX4</i>	Giaever et al., 2002
BY4741	<i>Δmmm1</i>	<i>MATα his3Δ1 leu2Δ0 met15Δ0 ura3Δ0 Δmmm1::kanMX4</i>	Giaever et al., 2002
BY4741	<i>Δmdm10</i>	<i>MATα his3Δ1 leu2Δ0 met15Δ0 ura3Δ0 Δmdm10::kanMX4</i>	Giaever et al., 2002
BY4741	<i>Δmdm12</i>	<i>MATα his3Δ1 leu2Δ0 met15Δ0 ura3Δ0 Δmdm12::kanMX4</i>	Giaever et al., 2002
BY4741	<i>Δmdm34</i>	<i>MATα his3Δ1 leu2Δ0 met15Δ0 ura3Δ0 Δmdm34::kanMX4</i>	Giaever et al., 2002
BY	<i>Δmdm10 Δdnm1</i>	<i>MATα his3Δ1 leu2Δ0 met15Δ0 lys2Δ0 ura3Δ0 Δmdm10::kanMX4 Δdnm1::kanMX4</i>	this study
BY	<i>Δmdm12 Δdnm1</i>	<i>MATα his3Δ1 leu2Δ0 MET15 LYS2 ura3Δ0 Δmdm12::kanMX4 Δdnm1::kanMX4</i>	this study
BY	<i>Δmdm34 Δdnm1</i>	<i>MATα his3Δ1 leu2Δ0 MET15 lys2Δ0 ura3Δ0 Δdnm1::kanMX4 Δmdm34::kanMX4</i>	this study
BY	<i>Δatg32 Δmmm1</i>	<i>MATα his3Δ1 leu2Δ0 met15Δ0 lys2Δ0 ura3Δ0 Δatg32::kanMX4 Δmmm1::kanMX4</i>	this study
BY	<i>Δatg32 Δmdm10</i>	<i>MATα his3Δ1 leu2Δ0 met15Δ0 LYS2 ura3Δ0 Δatg32::kanMX4 Δmdm10::kanMX4</i>	this study

Isogenic	Name	Genotype	Source
BY	<i>Δatg32</i> <i>Δmdm12</i>	<i>MATα his3Δ1 leu2Δ0 met15Δ0 LYS2 ura3Δ0</i> <i>Δatg32::kanMX4 Δmdm12::kanMX4</i>	this study
BY	<i>Δatg32</i> <i>Δmdm34</i>	<i>MATα his3Δ1 leu2Δ0 met15Δ0 LYS2 ura3Δ0</i> <i>Δatg32::kanMX4 Δmdm34::kanMX4</i>	this study
YPH500	<i>Δmmm1</i>	<i>MATα ura3-52 lys2-801_amber ade2-101_ochre trp1-Δ63 his3-Δ200 leu2-Δ2 Δmmm1::HIS3MX6</i>	Dimmer et al., 2005
BY4741	ProtA-Mmm1	<i>MATα his3Δ1 leu2Δ0 met15Δ0 ura3Δ0 ProtA-MMM1 [HIS3]</i>	C. Meisinger, Freiburg
BY	Y7092	<i>MATα Δcan1::STE2pr-Sp_his5 Δlyp1 ura3Δ0 leu2Δ0 his3Δ1 met15Δ0</i>	Baryshnikova et al., 2010
BY	Y7092 <i>MYO2</i>	<i>MATα Δcan1::STE2pr-Sp_his5 Δlyp1 ura3Δ0 leu2Δ0 his3Δ1 met15Δ0 MYO2-URA3</i>	J. König, Zellbiologie, Bayreuth
BY	Y7092 <i>myo2(LQ)</i>	<i>MATα Δcan1::STE2pr-Sp_his5 Δlyp1 ura3Δ0 leu2Δ0 his3Δ1 met15Δ0 myo2(LQ)-URA3</i>	J. König, Zellbiologie, Bayreuth
BY4741	<i>Δypt11</i>	<i>MATα his3Δ1 leu2Δ0 met15Δ0 ura3Δ0 Δypt11::kanMX4</i>	Giaever et al., 2002
BY4741	<i>Δnum1</i>	<i>MATα his3Δ1 leu2Δ0 met15Δ0 ura3Δ0 Δnum1::kanMX4</i>	Giaever et al., 2002
BY	WT *	<i>MAT? ura3Δ0 leu2Δ0 met15Δ0 his3Δ1</i>	this study
BY	<i>Δnum1</i> *	<i>MAT? ura3Δ0 leu2Δ0 met15Δ0 his3Δ1 Δnum1::kanMX4</i>	this study
BY	<i>myo2(LQ)</i> *	<i>MAT? ura3Δ0 leu2Δ0 met15Δ0 his3Δ1 myo2(LQ)-URA3</i>	this study
BY	<i>myo2(LQ)</i> <i>Δnum1</i> *	<i>MAT? ura3Δ0 leu2Δ0 met15Δ0 his3Δ1 myo2(LQ)-URA3</i> <i>Δnum1::kanMX4</i>	this study
BY4741	<i>Δfzo1</i>	<i>MATα his3Δ1 leu2Δ0 met15Δ0 ura3Δ0 Δfzo1::kanMX4</i>	Giaever et al., 2002
BY4741	<i>Δmgm1</i>	<i>MATα his3Δ1 leu2Δ0 met15Δ0 ura3Δ0 Δmgm1::kanMX4</i>	Giaever et al., 2002
BY4741	<i>Δugo1</i>	<i>MATα his3Δ1 leu2Δ0 met15Δ0 ura3Δ0 Δugo1::kanMX4</i>	Giaever et al., 2002
BY4741	<i>Δdnm1</i>	<i>MATα his3Δ1 leu2Δ0 met15Δ0 ura3Δ0 Δdnm1::kanMX4</i>	Giaever et al., 2002
BY	<i>Δfzo1</i> *	<i>MAT? ura3Δ0 leu2Δ0 met15Δ0 his3Δ1 Δfzo1::kanMX4</i>	this study
BY	<i>Δdnm1</i> *	<i>MAT? ura3Δ0 leu2Δ0 met15Δ0 his3Δ1 Δdnm1::kanMX4</i>	this study
BY	<i>myo2(LQ)</i> *	<i>MAT? ura3Δ0 leu2Δ0 met15Δ0 his3Δ1 myo2(LQ)-URA3</i>	this study
BY	<i>myo2(LQ)</i> <i>Δdnm1</i> *	<i>MAT? ura3Δ0 leu2Δ0 met15Δ0 his3Δ1 myo2(LQ)-URA3</i> <i>Δdnm1::kanMX4</i>	this study
BY4741	<i>Δfzo1</i> <i>Δdnm1</i>	<i>MATα his3Δ1 leu2Δ0 met15Δ0 ura3Δ0 Δfzo1::kanMX4</i> <i>Δdnm1::kanMX4</i>	M. Dürr, Zellbiologie, Bayreuth
BY	<i>Δfzo1</i> <i>Δdnm1</i> *	<i>MAT? ura3Δ0 leu2Δ0 met15Δ0 his3Δ1 Δfzo1::kanMX4</i> <i>Δdnm1::kanMX4</i>	this study
BY	<i>myo2(LQ)</i> <i>Δfzo1</i> <i>Δdnm1</i> *	<i>MAT? ura3Δ0 leu2Δ0 met15Δ0 his3Δ1 myo2(LQ)-URA3</i> <i>Δfzo1::kanMX4 Δdnm1::kanMX4</i>	this study
BY	<i>myo2(LQ)</i> <i>Δfzo1</i> */**	<i>MAT? ura3Δ0 leu2Δ0 met15Δ0 his3Δ1 myo2(LQ)-URA3</i> <i>Δfzo1::kanMX4</i>	this study

* Strains were constructed by mating the Y7092 *myo2(LQ)* strain with BY4741 *Δyfg1::kanMX4* strains. *Δcan1::STE2pr-Sp_his5*, *Δlyp1* alleles and mating type have not been tested.

** Strain was complemented with either pRS313-FZO1 or pRS313-fzo1-1.

Culturing and media

Yeast cells were cultured on rich medium, selective minimal (SM) or selective complete (SC) medium as described in Sherman (2002) with 0.67% yeast nitrogen base (YNB) with ammonium sulfate and without amino acids as nitrogen source and with 2% glucose (dextrose; D), 2% galactose (Gal) or 3% glycerol as carbon sources, respectively. 2% agar was added to the above mentioned media in order to produce medium plates. If geneticin (G418) was added to plates, YNB was omitted, since

ammonium sulfate inhibits the action of G418. Instead, 0.1% monosodium glutamate (MSG) was used as a nitrogen source and 0.17% YNB without amino acids and without ammonium sulfate was added in addition. The standard temperature was 30°C, if not indicated otherwise, and agitation was 150 rpm for tubes and flasks and 280 rpm for deep-well plates. For culturing cells prior to starvation, cells were cultured on SGalRD (0.67% YNB with ammonium sulfate and without amino acids, 2% galactose, 2% raffinose, and 0.1% glucose, supplemented with adenine, lysine, methionine, tryptophan and additional supplements depending on the strain). Yeasts were starved in SD-N (0.17% YNB without amino acids and without ammonium sulfate, 2% glucose, without further supplements). For screening the *pet* library, cells were inoculated in 200 µl SGalRD and incubated overnight in deep-well plates (96 format; 30°C, 280 rpm). 300 µl fresh medium was added, cells were grown for additional six hours and washed four times with water before resuspending them in 300 µl SD-N and starvation for two days. Sporulation of diploids was carried out either in liquid medium (1% potassium acetate, 0.005% zinc acetate) or on plates (1% potassium acetate, 2% agar) for up to two weeks at 22°C. For sporulation during SGA, enriched sporulation medium (1% potassium acetate, 0.1% yeast extract, 0.05% glucose, 0.000025% histidine, 0.000025% lysine, 0.000125% leucine, 2% agar) was used. For long-time storage of yeast, cells were resuspended in 15% glycerol and frozen at -80°C.

Transformation of plasmids

Cells were cultured to logarithmic growth either in liquid medium or on plates. Plasmids were transformed into yeast by resuspending cells in 360 µl transformation mixture (33% PEG4000, 0.1 M lithium acetate (pH 7.5), 0.42 mg/ml single stranded carrier DNA from salmon sperm, 0.5 – 1 µg of plasmid DNA). After an 1 h heat shock at 42°C, cells were pelleted by centrifugation and resuspended in 100 µl water and plated on appropriate synthetic selection medium. For transformation of pAS1NB-CS-RG into the *pet* library, the library was plated on glucose-containing rich medium and incubated for two days at 30°C. Cells were then resuspended in 150 µl of water, pelleted and resuspended in 150 µl of transformation mixture per well in a microtiter plate (96 format) and heat-shocked for 1 h at 42°C. After pelleting the cells they were resuspended in 50 µl water and plated by using sterile pinning tools on SMD plates lacking leucine for selection of transformants.

Drop dilution assay

Different strains were cultured to stationary phase, adjusted to the same optical density (OD₆₀₀ between 0.5 and 2) and diluted in serial 1:10 steps in water. 5 µl of cell suspension from the dilutions were dropped on agar plates and incubated for several days at the required temperatures.

Construction of diploid cells and tetrad dissection

Approximately equal amounts of haploid yeast cells of opposite mating types were taken from agar plates and resuspended in glucose-containing liquid rich medium and allowed to mate (30°C, 150 rpm) for up to 8 h. 100 µl of culture were then plated on appropriate selection medium and incubated overnight (30°C). Diploids were transferred to fresh selection plates to get rid of remaining haploids and again incubated overnight. After sporulation, a small amount of cells was resuspended in water and 2 mg/ml zymolyase was added (10 min, room temperature). 50 µl of cell suspension were plated at the edge of an agar plate and allowed to dry. Tetrads were dissected by using a micromanipulator (Singer MSM Series 300 with Acer n30 pocket PC; Singer Instruments, Roadwater, UK). After growth for several days, single colonies were transferred to appropriate selection medium and genotypes were determined by colony-PCR if necessary.

Quantification of colony size

Sizes of colonies generated by tetrad dissection were determined by using ImageJ software (version 1.43; National Institutes of Health, Bethesda, USA). An image of the plate with the colonies was opened and converted to a binary picture. Colonies were selected by using the wand (tracing) tool and the colony size in pixels was measured by using the shortcut 'ctrl + m'.

Synthetic genetic array

SGA was essentially performed as described in Baryshnikova et al. (2010) and a ROTOR HDA robot (Singer Instruments) was used for plating. Query strains were plated on PlusPlates (Singer Instruments) containing YPD solid medium and incubated for two days at 30°C. The *MATa* deletion library was plated in a 384 format on YPD and incubated for 2 to 3 days at ambient temperature. The library was then arrayed to a high-density of $4 \times 384 = 1536$ strains on one YPD plate. Then, every deletion strain was present in four replicates on the plate. The query strains were mixed with this high-density array (HDA) by plating the query strains on the HDA and using the target mix option. Cells were allowed to mate for one day at room temperature. Colonies were then plated on diploid selection medium (SCD[MSG] containing 200 mg/l G418, but lacking uracil, 2% agar) and grown for 1 day at 30°C. This selection was repeated once. Then cells were plated on enriched sporulation medium using the target mix option and incubated at 22°C for 5 to 10 days. Sporulated yeast cells were then plated on *MATa* selection medium (SCD lacking histidine, arginine and lysine; containing 50 mg/l canavanine and 50 mg/l thialysine, 2% agar) and incubated for 2 days at 30°C. Colonies were plated on *MATa*/kanR selection medium (SCD[MSG] lacking histidine, arginine and lysine; containing 50 mg/l canavanine and 50 mg/l thialysine as well as 200 mg/l G418, 2% agar) and incubated for 1 day at 30°C. Cells were replica-plated on *MATa*/kanR/*URA3* selection medium (SCD[MSG] lacking histidine, arginine, lysine and uracil; containing 50 mg/l canavanine and 50 mg/l thialysine as well as 200 mg/l G418, 2% agar) and incubated for 1 to 2 days until colonies grew to a substantial size. This was repeated once. Finally, colonies were replica-plated on *MATa*/kanR/*URA3* selection medium and

incubated for 20 h at 30°C. Then plate images were acquired from 40 cm distance by using a Kodak EasyShare DX7590 camera.

SGA data acquisition

Data were acquired using the web browser-based SGAtools (<http://sgatools.ccb.utoronto.ca>; Wagih et al., 2013). Images were named according to the instructions and loaded for image analysis (1536 format). Autorotation of images was allowed, colonies were assigned as 'bright' and images were processed. Correct identification of colonies by the software was confirmed by visual inspection. A table with the information about the position of every strain on the plates was uploaded. In the options section, '4 (2 x 2) replicates' was chosen and the software was told to score the normalized output. The normalized and scored results were downloaded as an Excel file.

Functional enrichment analysis of GO terms

Functional enrichment analysis of GO terms was carried out using the web browser tool 'GO term finder' from the 'Saccharomyces Genome Database' (SGD; <http://www.yeastgenome.org/cgi-bin/GO/goTermFinder.pl>; Boyle et al., 2004). The list of negative or positive interactors, respectively, was uploaded as well as the background set of screened strains and functional enrichments of GO terms for process, function and component with a p value < 5% were searched. Subsequently, the ratio of the cluster frequency and the background frequency was determined.

Fluorescence microscopy

Microscopy procedures have already been described in Böckler and Westermann (2014). Epifluorescence microscopy was performed using an Axioplan 2 or an Axiophot microscope (Carl Zeiss, Jena) equipped with an Evolution VF Mono Cooled monochrome camera (Intas, Göttingen) with Image ProPlus 5.0 and Scope Pro4.5 software (Media Cybernetics, Rockville, US) or a Leica DCF360FX Camera with Leica LAF AF Version 2.2.1 software (Leica Microsystems, Wetzlar), respectively. Images were acquired using a Plan Neofluar 1003/1.30 Ph3 oil objective (Carl Zeiss).

For confocal microscopy, a Leica TCS SP5 system (Leica) was used in combination with an inverted Leica DMI 6000 CS Trino microscope equipped with an HCX PL APO CS 63.0×/1.40 oil UV objective and LAS AF SP5 MicroLab software (Leica). This system is equipped with an Argon laser (458 nm/5 mW, 476 nm/5 mW, 488 nm/20 mW, 496 nm/5 mW, 514 nm/20 mW), a DPSS laser (561 nm/20 mW) and the respective acusto-optical tunable filters (AOTF).

Staining of cellular structures

Vacuoles were stained by addition of 100 μ M CellTracker Blue CMAC to cells. After incubation for 30 min under agitation, cells were washed at least three times and subjected to fluorescence microscopy. In order to visualize mitochondria, 5 μ M rhodamine-b-hexylester was added to cells. Cells were immediately subjected to fluorescence microscopy. For staining of DNA, cells were fixed with 100% methanol for five minutes, washed once with PBS and resuspended in PBS. 1 μ g/ml DAPI was added and cells were incubated for five minutes at room temperature. After washing the cells four times with PBS and resuspending them in 200 μ l PBS they were either stored at 4°C or immediately subjected to fluorescence microscopy. To stain cell walls, cell suspensions were mixed 1:1 with 10 mM HEPES/2% glucose buffer (pH 7.2), pelleted and resuspended in HEPES/glucose buffer. 25 μ M calcofluor was added and cells were incubated for 30 min under agitation. After washing once with water cells were resuspended in fresh medium and further cultured as required.

Protein biochemistry

Preparation of cell extracts

Cells were incubated in 200 μ l 0.1 M NaOH for 10 min at room temperature, pelleted and boiled for 5 min in SDS sample buffer (600 mM Tris-HCl, pH 6.8; 5% glycerol, 2% SDS, 4% β -mercaptoethanol, 0.0025% bromophenol blue).

SDS-PAGE, Western blotting, immuno-detection and antibodies

Proteins were separated by SDS-PAGE. Stacking gels (10 x 150 x 1 mm) contained 5% acrylamide-bisacrylamide mixture (Roth, Karlsruhe, Germany), 60 mM Tris-HCl (pH 6.8), 0.1% SDS, 0.05% APS and 0.1% TEMED. Resolving gels (90 x 150 x 1 mm) contained either 8% or 10% acrylamide-bisacrylamide, 385 mM Tris-HCl (pH 8.8), 0.1% SDS, 0.05% APS and 0.035% TEMED. 8% acrylamide-bisacrylamide mixture was used for resolution of ProtA-Mmm1, 10% acrylamide-bisacrylamide mixture for Ape1, chiMERA, cytRosella, GFP-Atg8, Hexokinase, Ilv5, mtRosella, Ndi1, and Tom40. Electrophoresis was performed at a constant current of 15 – 20 mA in a vertical chamber (Mini-PROTEAN Tetra Electrophoresis System, BioRad, München) in running buffer (0.1% SDS, 192 mM glycine, 25 mM Tris). Proteins were transferred to a nitrocellulose membrane (Amersham Biosciences, Piscataway, USA) by semi-dry Western blotting. The gel was placed on three filter sheets (Whatman, Kent, UK) and the membrane soaked in transfer buffer (11.26 g/l glycine, 2.42 g/l Tris, 0.2 g/l SDS, 200 ml/l methanol) and covered with three filter sheets soaked in transfer buffer. With a constant current of ca. 1.5 mA/cm² of membrane, the proteins were blotted between 30 min and 1 h. Successful blotting was confirmed by soaking the blots for 1 – 5 min in Ponceau staining solution (0.5% PonceauS, 3% TCA) and destaining with water. The blot was then incubated in TBST buffer (6% Tris, 8.8% NaCl, 0.5% Tween20; pH 7.5) with 5% milk powder for 30 min under agitation. After incubation with primary antibody for 1 h at room temperature or overnight at 4°C, the blot was

washed three times with TBST, the secondary antibody coupled to horseradish peroxidase (HRP) was added for 1 h and the blot was again washed with TBST three times. For decoration of ProtA-Mmm1, PAP antibody was added for 2.5 h, washed three times with TBST and detection followed without prior addition of a secondary antibody. For detection, 2 ml of solution 1 (12.1 g/l Tris, 250 mg/l luminol), 800 µl of solution 2 (1.1 g/l coumaric acid in DMSO) and 2.4 µl 30% H₂O₂ were mixed in a final volume of 5 ml and 100 µl of solution A and B from ECL Ultra TMA-6 (Lumigen, Southfield, USA) were added. The blot was covered with the solution and luminescence was detected using the ImageQuant LAS-4000 gel documentation (GE Healthcare Europe GmbH, Freiburg).

Table 5. Antibodies used in this study. Antibodies were diluted in TBST with 5% milk powder with the exception of anti-Ape1 diluted in TBST without milk.

Antibody	Organism	Dilution	Source
anti-Ape1 (sc-26740)	goat	1 : 200	Santa Cruz Biotechnology, Dallas, USA
anti-GFP (ab6556)	rabbit	1 : 3,000	Abcam, Cambridge, UK
anti-Hxk	rabbit	1 : 15,000	unknown
anti-Ilv5	rabbit	1 : 500	J. Herrmann, Kaiserslautern, Germany
anti-Ndi1	rabbit	1 : 1,000	Seo et al., 1998
anti-Tom40	rabbit	1 : 2,000	W. Neupert, München
Peroxidase Anti-Peroxidase (PAP) Soluble Complex antibody (P1291)	rabbit	1 : 2,000	Sigma-Aldrich, St. Louis, USA
anti-rabbit HRP (w4011)	goat	1 : 10,000	Promega, Mannheim
anti-goat HRP (sc-2033)	donkey	1 : 1,000	Santa Cruz Biotechnology, Dallas, USA

Shock-freezing of cells and cryo-grinding

Cells were grown overnight (30°C, 150 rpm) in 20 ml of synthetic medium containing 3% glycerol and 0.1% glucose supplemented with methionine, tryptophan, lysine, leucine, histidine and adenine (concentrations according to Sherman, 2002). 100 ml of fresh medium were added and the culture was grown during the day. 500 ml fresh medium were inoculated for overnight incubation and the OD_{600} was 0.2 on the next day. Cells were washed twice with 500 ml water and starved (30°C, 150 rpm) for 1 h in 500 ml SD-N. Cells were pelleted and resuspended in 8 ml SD-N. The suspension was transferred to a syringe closed with a luer plug and pelleted. The supernatant was discarded and the pellet in the syringe was pressed into a vial filled with liquid nitrogen. After discarding the liquid nitrogen, the shock-frozen yeast cells were stored for at least one day at -80°C. Frozen cells were transferred to a precooled 10 ml grinding jar (Retsch, Düsseldorf) containing a 10 mm steel ball. The jar was subsequently introduced into the CryoMill (Retsch) and cooled automatically with liquid nitrogen. The sample was precooled for 5 min with 5 Hz and then grinded for 15 min with 25 Hz. The yeast powder was then transferred to a precooled vial to avoid thawing. The powder was stored at -80°C.

Immuno-precipitation

200 mg of frozen yeast powder were transferred to ice-cold SS34 tubes and allowed to semi-thaw on ice for several minutes. The powder was resuspended in 2 ml solubilization buffer (20 mM Tris, pH 7.4; 50 mM NaCl, 10% glycerol, 0.1 mM EDTA, 1% digitonin, 2 mM PMSF, 30 mg/l DNaseI, 10x EDTA-free protease inhibitors [Roche, Mannheim]) and incubated for 45 min under agitation at 4°C. After centrifugation (10 min, 17.000 rcf, 4°C), the supernatant (input fraction) was transferred to a 15 ml vial. 18 µl of sepharose beads covered with camelid-derived single-domain antibodies against GFP (provided by M. Hermann and O. Stemmann, Genetics, Bayreuth; see also Rothbauer et al., 2008) were equilibrated with 500 µl equilibration buffer (20 mM Tris, pH 7.4; 50 mM NaCl, 10% glycerol, 0.1 mM EDTA) and with 500 µl solubilization buffer in Mobicol Mini Columns (Boca Scientific, Boca Raton, USA). Beads were transferred to the solubilized material and incubated for 90 min at 4°C under agitation. Beads were pelleted (5 min, 7 rcf, 4°C) and transferred to the columns. Beads were washed twice (30 sec, 4°C, 500 rpm, eppendorf F45-30-11) with washing buffer (20 mM Tris, pH 7.4; 60 mM NaCl, 10% glycerol, 0.5 mM EDTA, 0.3% digitonin). 100 µl of SDS sample buffer were added to the beads, boiled for 10 min at 99°C and elution was performed (1 min, 2000 rcf).

References

- Abeliovich, H., Zarei, M., Rigbolt, K.T., Youle, R.J., and Dengjel, J. (2013). Involvement of mitochondrial dynamics in the segregation of mitochondrial matrix proteins during stationary phase mitophagy. *Nat Commun* 4, 2789.
- Abeliovich, H., Zhang, C., Dunn, W.A., Jr., Shokat, K.M., and Klionsky, D.J. (2003). Chemical genetic analysis of Apg1 reveals a non-kinase role in the induction of autophagy. *Mol Biol Cell* 14, 477-490.
- Achleitner, G., Gaigg, B., Krasser, A., Kainersdorfer, E., Kohlwein, S.D., Perktold, A., Zellnig, G., and Daum, G. (1999). Association between the endoplasmic reticulum and mitochondria of yeast facilitates interorganelle transport of phospholipids through membrane contact. *Eur J Biochem* 264, 545-553.
- Alberti, S., Gitler, A.D., and Lindquist, S. (2007). A suite of Gateway cloning vectors for high-throughput genetic analysis in *Saccharomyces cerevisiae*. *Yeast* 24, 913-919.
- Altmann, K., Frank, M., Neumann, D., Jakobs, S., and Westermann, B. (2008). The class V myosin motor protein, Myo2, plays a major role in mitochondrial motility in *Saccharomyces cerevisiae*. *J Cell Biol* 181, 119-130.
- Altmann, K., and Westermann, B. (2005). Role of essential genes in mitochondrial morphogenesis in *Saccharomyces cerevisiae*. *Mol Biol Cell* 16, 5410-5417.
- Amchenkova, A.A., Bakeeva, L.E., Chentsov, Y.S., Skulachev, V.P., and Zorov, D.B. (1988). Coupling membranes as energy-transmitting cables. I. Filamentous mitochondria in fibroblasts and mitochondrial clusters in cardiomyocytes. *J Cell Biol* 107, 481-495.
- Anton, F., Dittmar, G., Langer, T., and Escobar-Henriques, M. (2013). Two deubiquitylases act on mitofusin and regulate mitochondrial fusion along independent pathways. *Mol Cell* 49, 487-498.
- Aoki, Y., Kanki, T., Hirota, Y., Kurihara, Y., Saigusa, T., Uchiumi, T., and Kang, D. (2011). Phosphorylation of Serine 114 on Atg32 mediates mitophagy. *Mol Biol Cell* 22, 3206-3217.
- Arai, S., Noda, Y., Kainuma, S., Wada, I., and Yoda, K. (2008). Ypt11 functions in bud-directed transport of the Golgi by linking Myo2 to the coatomer subunit Ret2. *Curr Biol* 18, 987-991.
- Axe, E.L., Walker, S.A., Manifava, M., Chandra, P., Roderick, H.L., Habermann, A., Griffiths, G., and Ktistakis, N.T. (2008). Autophagosome formation from membrane compartments enriched in phosphatidylinositol 3-phosphate and dynamically connected to the endoplasmic reticulum. *J Cell Biol* 182, 685-701.
- Baker, M.J., Lampe, P.A., Stojanovski, D., Korwitz, A., Anand, R., Tatsuta, T., and Langer, T. (2014). Stress-induced OMA1 activation and autocatalytic turnover regulate OPA1-dependent mitochondrial dynamics. *EMBO J* 33, 578-593.
- Baryshnikova, A., Costanzo, M., Dixon, S., Vizeacoumar, F.J., Myers, C.L., Andrews, B., and Boone, C. (2010). Synthetic genetic array (SGA) analysis in *Saccharomyces cerevisiae* and *Schizosaccharomyces pombe*. *Methods Enzymol* 470, 145-179.
- Berger, K.H., Sogo, L.F., and Yaffe, M.P. (1997). Mdm12p, a component required for mitochondrial inheritance that is conserved between budding and fission yeast. *J Cell Biol* 136, 545-553.
- Bevis, B.J., and Glick, B.S. (2002). Rapidly maturing variants of the Discosoma red fluorescent protein (DsRed). *Nat Biotechnol* 20, 83-87.

- Bleazard, W., McCaffery, J.M., King, E.J., Bale, S., Mozdy, A., Tieu, Q., Nunnari, J., and Shaw, J.M. (1999). The dynamin-related GTPase Dnm1 regulates mitochondrial fission in yeast. *Nat Cell Biol* **1**, 298-304.
- Bloom, K. (2001). Nuclear migration: cortical anchors for cytoplasmic dynein. *Curr Biol* **11**, R326-329.
- Böckler, S., and Westermann, B. (2014). Mitochondrial ER contacts are crucial for mitophagy in yeast. *Dev Cell* **28**, 450-458.
- Boldogh, I.R., Nowakowski, D.W., Yang, H.C., Chung, H., Karmon, S., Royes, P., and Pon, L.A. (2003). A protein complex containing Mdm10p, Mdm12p, and Mmm1p links mitochondrial membranes and DNA to the cytoskeleton-based segregation machinery. *Mol Biol Cell* **14**, 4618-4627.
- Boldogh, I.R., Ramcharan, S.L., Yang, H.C., and Pon, L.A. (2004). A type V myosin (Myo2p) and a Rab-like G-protein (Ypt11p) are required for retention of newly inherited mitochondria in yeast cells during cell division. *Mol Biol Cell* **15**, 3994-4002.
- Boyle, E.I., Weng, S., Gollub, J., Jin, H., Botstein, D., Cherry, J.M., and Sherlock, G. (2004). GO::TermFinder--open source software for accessing Gene Ontology information and finding significantly enriched Gene Ontology terms associated with a list of genes. *Bioinformatics* **20**, 3710-3715.
- Brachmann, C.B., Davies, A., Cost, G.J., Caputo, E., Li, J., Hieter, P., and Boeke, J.D. (1998). Designer deletion strains derived from *Saccharomyces cerevisiae* S288C: a useful set of strains and plasmids for PCR-mediated gene disruption and other applications. *Yeast* **14**, 115-132.
- Breker, M., Gymrek, M., and Schuldiner, M. (2013). A novel single-cell screening platform reveals proteome plasticity during yeast stress responses. *J Cell Biol* **200**, 839-850.
- Breslow, D.K., Cameron, D.M., Collins, S.R., Schuldiner, M., Stewart-Ornstein, J., Newman, H.W., Braun, S., Madhani, H.D., Krogan, N.J., and Weissman, J.S. (2008). A comprehensive strategy enabling high-resolution functional analysis of the yeast genome. *Nat Methods* **5**, 711-718.
- Bulina, M.E., Chudakov, D.M., Britanova, O.V., Yanushevich, Y.G., Staroverov, D.B., Chepurnykh, T.V., Merzlyak, E.M., Shkrob, M.A., Lukyanov, S., and Lukyanov, K.A. (2006). A genetically encoded photosensitizer. *Nat Biotechnol* **24**, 95-99.
- Burgess, S.M., Delannoy, M., and Jensen, R.E. (1994). *MMM1* encodes a mitochondrial outer membrane protein essential for establishing and maintaining the structure of yeast mitochondria. *J Cell Biol* **126**, 1375-1391.
- Buvelot Frei, S., Rahl, P.B., Nussbaum, M., Briggs, B.J., Calero, M., Janeczko, S., Regan, A.D., Chen, C.Z., Barral, Y., Whittaker, G.R., *et al.* (2006). Bioinformatic and comparative localization of Rab proteins reveals functional insights into the uncharacterized GTPases Ypt10p and Ypt11p. *Mol Cell Biol* **26**, 7299-7317.
- Catlett, N.L., Duex, J.E., Tang, F., and Weisman, L.S. (2000). Two distinct regions in a yeast myosin-V tail domain are required for the movement of different cargoes. *J Cell Biol* **150**, 513-526.
- Cebollero, E., Reggiori, F., and Kraft, C. (2012a). Reticulophagy and ribophagy: regulated degradation of protein production factories. *Int J Cell Biol* **2012**, 182834.
- Cebollero, E., van der Vaart, A., Zhao, M., Rieter, E., Klionsky, D.J., Helms, J.B., and Reggiori, F. (2012b). Phosphatidylinositol-3-phosphate clearance plays a key role in autophagosome completion. *Curr Biol* **22**, 1545-1553.
- Cervený, K.L., McCaffery, J.M., and Jensen, R.E. (2001). Division of mitochondria requires a novel *DMN1*-interacting protein, Net2p. *Mol Biol Cell* **12**, 309-321.
- Cervený, K.L., Studer, S.L., Jensen, R.E., and Sesaki, H. (2007). Yeast mitochondrial division and distribution require the cortical num1 protein. *Dev Cell* **12**, 363-375.

- Chelstowska, A., and Butow, R.A. (1995). *RTG* genes in yeast that function in communication between mitochondria and the nucleus are also required for expression of genes encoding peroxisomal proteins. *J Biol Chem* 270, 18141-18146.
- Chernyakov, I., Santiago-Tirado, F., and Bretscher, A. (2013). Active segregation of yeast mitochondria by Myo2 is essential and mediated by Mmr1 and Ypt11. *Curr Biol* 23, 1818-1824.
- Christianson, T.W., Sikorski, R.S., Dante, M., Shero, J.H., and Hieter, P. (1992). Multifunctional yeast high-copy-number shuttle vectors. *Gene* 110, 119-122.
- Cohen, M.M., Leboucher, G.P., Livnat-Levanon, N., Glickman, M.H., and Weissman, A.M. (2008). Ubiquitin-proteasome-dependent degradation of a mitofusin, a critical regulator of mitochondrial fusion. *Mol Biol Cell* 19, 2457-2464.
- Cohen, Y., Klug, Y.A., Dimitrov, L., Erez, Z., Chuartzman, S.G., Elinger, D., Yofe, I., Soliman, K., Gartner, J., Thoms, S., *et al.* (2014). Peroxisomes are juxtaposed to strategic sites on mitochondria. *Mol Biosyst* 10, 1742-1748.
- Collins, S.R., Miller, K.M., Maas, N.L., Roguev, A., Fillingham, J., Chu, C.S., Schuldiner, M., Gebbia, M., Recht, J., Shales, M., *et al.* (2007). Functional dissection of protein complexes involved in yeast chromosome biology using a genetic interaction map. *Nature* 446, 806-810.
- Costanzo, M., Baryshnikova, A., Bellay, J., Kim, Y., Spear, E.D., Sevier, C.S., Ding, H., Koh, J.L., Toufighi, K., Mostafavi, S., *et al.* (2010). The genetic landscape of a cell. *Science* 327, 425-431.
- Csordas, G., Varnai, P., Golenar, T., Roy, S., Purkins, G., Schneider, T.G., Balla, T., and Hajnoczky, G. (2010). Imaging interorganelle contacts and local calcium dynamics at the ER-mitochondrial interface. *Mol Cell* 39, 121-132.
- Darsow, T., Rieder, S.E., and Emr, S.D. (1997). A multispecificity syntaxin homologue, Vam3p, essential for autophagic and biosynthetic protein transport to the vacuole. *J Cell Biol* 138, 517-529.
- de Brito, O.M., and Scorrano, L. (2008). Mitofusin 2 tethers endoplasmic reticulum to mitochondria. *Nature* 456, 605-610.
- De Vos, K.J., Morotz, G.M., Stoica, R., Tudor, E.L., Lau, K.F., Ackerley, S., Warley, A., Shaw, C.E., and Miller, C.C. (2012). VAPB interacts with the mitochondrial protein PTP1P51 to regulate calcium homeostasis. *Hum Mol Genet* 21, 1299-1311.
- Deffieu, M., Bhatia-Kissova, I., Salin, B., Galinier, A., Manon, S., and Camougrand, N. (2009). Glutathione participates in the regulation of mitophagy in yeast. *J Biol Chem* 284, 14828-14837.
- Dimmer, K.S., Fritz, S., Fuchs, F., Messerschmitt, M., Weinbach, N., Neupert, W., and Westermann, B. (2002). Genetic basis of mitochondrial function and morphology in *Saccharomyces cerevisiae*. *Mol Biol Cell* 13, 847-853.
- Dimmer, K.S., Jakobs, S., Vogel, F., Altmann, K., and Westermann, B. (2005). Mdm31 and Mdm32 are inner membrane proteins required for maintenance of mitochondrial shape and stability of mitochondrial DNA nucleoids in yeast. *J Cell Biol* 168, 103-115.
- Dixon, S.J., Costanzo, M., Baryshnikova, A., Andrews, B., and Boone, C. (2009). Systematic mapping of genetic interaction networks. *Annu Rev Genet* 43, 601-625.
- Drubin, D.G., Jones, H.D., and Wertman, K.F. (1993). Actin structure and function: roles in mitochondrial organization and morphogenesis in budding yeast and identification of the phalloidin-binding site. *Mol Biol Cell* 4, 1277-1294.
- Du, Y., Walker, L., Novick, P., and Ferro-Novick, S. (2006). Ptc1p regulates cortical ER inheritance via Sit2p. *EMBO J* 25, 4413-4422.
- Elbaz-Alon, Y., Rosenfeld-Gur, E., Shinder, V., Futerman, A.H., Geiger, T., and Schuldiner, M. (2014). A dynamic interface between vacuoles and mitochondria in yeast. *Dev Cell* 30, 95-102.

- Eppler, U.D., Suriapranata, I., Eskelinen, E.L., and Thumm, M. (2001). Aut5/Cvt17p, a putative lipase essential for disintegration of autophagic bodies inside the vacuole. *J Bacteriol* **183**, 5942-5955.
- Estrada, P., Kim, J., Coleman, J., Walker, L., Dunn, B., Takizawa, P., Novick, P., and Ferro-Novick, S. (2003). Myo4p and She3p are required for cortical ER inheritance in *Saccharomyces cerevisiae*. *J Cell Biol* **163**, 1255-1266.
- Eves, P.T., Jin, Y., Brunner, M., and Weisman, L.S. (2012). Overlap of cargo binding sites on myosin V coordinates the inheritance of diverse cargoes. *J Cell Biol* **198**, 69-85.
- Fagarasanu, A., Fagarasanu, M., Eitzen, G.A., Aitchison, J.D., and Rachubinski, R.A. (2006). The peroxisomal membrane protein Inp2p is the peroxisome-specific receptor for the myosin V motor Myo2p of *Saccharomyces cerevisiae*. *Dev Cell* **10**, 587-600.
- Fagarasanu, A., Mast, F.D., Knoblach, B., Jin, Y., Brunner, M.J., Logan, M.R., Glover, J.N., Eitzen, G.A., Aitchison, J.D., Weisman, L.S., *et al.* (2009). Myosin-driven peroxisome partitioning in *S. cerevisiae*. *J Cell Biol* **186**, 541-554.
- Fagarasanu, A., Mast, F.D., Knoblach, B., and Rachubinski, R.A. (2010). Molecular mechanisms of organelle inheritance: lessons from peroxisomes in yeast. *Nat Rev Mol Cell Biol* **11**, 644-654.
- Fagarasanu, M., Fagarasanu, A., Tam, Y.Y., Aitchison, J.D., and Rachubinski, R.A. (2005). Inp1p is a peroxisomal membrane protein required for peroxisome inheritance in *Saccharomyces cerevisiae*. *J Cell Biol* **169**, 765-775.
- Fannjiang, Y., Cheng, W.C., Lee, S.J., Qi, B., Pevsner, J., McCaffery, J.M., Hill, R.B., Basanez, G., and Hardwick, J.M. (2004). Mitochondrial fission proteins regulate programmed cell death in yeast. *Genes Dev* **18**, 2785-2797.
- Farkasovsky, M., and Kuntzel, H. (1995). Yeast Num1p associates with the mother cell cortex during S/G2 phase and affects microtubular functions. *J Cell Biol* **131**, 1003-1014.
- Farkasovsky, M., and Kuntzel, H. (2001). Cortical Num1p interacts with the dynein intermediate chain Pac11p and cytoplasmic microtubules in budding yeast. *J Cell Biol* **152**, 251-262.
- Fehrenbacher, K.L., Boldogh, I.R., and Pon, L.A. (2005). A role for Jsn1p in recruiting the Arp2/3 complex to mitochondria in budding yeast. *Mol Biol Cell* **16**, 5094-5102.
- Fehrenbacher, K.L., Yang, H.C., Gay, A.C., Huckaba, T.M., and Pon, L.A. (2004). Live cell imaging of mitochondrial movement along actin cables in budding yeast. *Curr Biol* **14**, 1996-2004.
- Förtsch, J., Hummel, E., Krist, M., and Westermann, B. (2011). The myosin-related motor protein Myo2 is an essential mediator of bud-directed mitochondrial movement in yeast. *J Cell Biol* **194**, 473-488.
- Fowler, S.L., Akins, M., Zhou, H., Figeys, D., and Bennett, S.A. (2013). The liver connexin32 interactome is a novel plasma membrane-mitochondrial signaling nexus. *J Proteome Res* **12**, 2597-2610.
- Frederick, R.L., McCaffery, J.M., Cunningham, K.W., Okamoto, K., and Shaw, J.M. (2004). Yeast Miro GTPase, Gem1p, regulates mitochondrial morphology via a novel pathway. *J Cell Biol* **167**, 87-98.
- Frederick, R.L., Okamoto, K., and Shaw, J.M. (2008). Multiple pathways influence mitochondrial inheritance in budding yeast. *Genetics* **178**, 825-837.
- Frey, T.G., and Mannella, C.A. (2000). The internal structure of mitochondria. *Trends Biochem Sci* **25**, 319-324.
- Friedman, J.R., Lackner, L.L., West, M., Dibenedetto, J.R., Nunnari, J., and Voeltz, G.K. (2011). ER Tubules Mark Sites of Mitochondrial Division. *Science* **334**, 358-62.
- Friedman, J.R., and Nunnari, J. (2014). Mitochondrial form and function. *Nature* **505**, 335-343.

- Fritz, S., Weinbach, N., and Westermann, B. (2003). Mdm30 is an F-box protein required for maintenance of fusion-competent mitochondria in yeast. *Mol Biol Cell* **14**, 2303-2313.
- Gancedo, J.M. (1998). Yeast carbon catabolite repression. *Microbiol Mol Biol Rev* **62**, 334-361.
- Garcia-Rodriguez, L.J., Gay, A.C., and Pon, L.A. (2007). Puf3p, a Pumilio family RNA binding protein, localizes to mitochondria and regulates mitochondrial biogenesis and motility in budding yeast. *J Cell Biol* **176**, 197-207.
- Geisler, S., Holmstrom, K.M., Skujat, D., Fiesel, F.C., Rothfuss, O.C., Kahle, P.J., and Springer, W. (2010). PINK1/Parkin-mediated mitophagy is dependent on VDAC1 and p62/SQSTM1. *Nat Cell Biol* **12**, 119-131.
- Giaever, G., Chu, A.M., Ni, L., Connelly, C., Riles, L., Veronneau, S., Dow, S., Lucau-Danila, A., Anderson, K., Andre, B., *et al.* (2002). Functional profiling of the *Saccharomyces cerevisiae* genome. *Nature* **418**, 387-391.
- Giaever, G., and Nislow, C. (2014). The Yeast deletion collection: a decade of functional genomics. *Genetics* **197**, 451-465.
- Goffeau, A., Barrell, B.G., Bussey, H., Davis, R.W., Dujon, B., Feldmann, H., Galibert, F., Hoheisel, J.D., Jacq, C., Johnston, M., *et al.* (1996). Life with 6000 genes. *Science* **274**, 546, 563-547.
- Gomes, L.C., Di Benedetto, G., and Scorrano, L. (2011). During autophagy mitochondria elongate, are spared from degradation and sustain cell viability. *Nat Cell Biol* **13**, 589-598.
- Gomes, L.C., and Dikic, I. (2014). Autophagy in antimicrobial immunity. *Mol Cell* **54**, 224-233.
- Goode, B.L., and Eck, M.J. (2007). Mechanism and function of formins in the control of actin assembly. *Annu Rev Biochem* **76**, 593-627.
- Gorsich, S.W., and Shaw, J.M. (2004). Importance of mitochondrial dynamics during meiosis and sporulation. *Mol Biol Cell* **15**, 4369-4381.
- Graef, M., Friedman, J.R., Graham, C., Babu, M., and Nunnari, J. (2013). ER exit sites are physical and functional core autophagosome biogenesis components. *Mol Biol Cell* **24**, 2918-2931.
- Graef, M., and Nunnari, J. (2011). Mitochondria regulate autophagy by conserved signalling pathways. *EMBO J* **30**, 2101-2114.
- Gray, M.W., Burger, G., and Lang, B.F. (1999). Mitochondrial evolution. *Science* **283**, 1476-1481.
- Green, M.R., and Sambrook, J. (2012). Molecular cloning : a laboratory manual, 4th edn (Cold Spring Harbor, N.Y.: Cold Spring Harbor Laboratory Press).
- Hailey, D.W., Rambold, A.S., Satpute-Krishnan, P., Mitra, K., Sougrat, R., Kim, P.K., and Lippincott-Schwartz, J. (2010). Mitochondria supply membranes for autophagosome biogenesis during starvation. *Cell* **141**, 656-667.
- Hamasaki, M., Furuta, N., Matsuda, A., Nezu, A., Yamamoto, A., Fujita, N., Oomori, H., Noda, T., Haraguchi, T., Hiraoka, Y., *et al.* (2013). Autophagosomes form at ER-mitochondria contact sites. *Nature* **495**, 389-393.
- Hammermeister, M., Schodel, K., and Westermann, B. (2010). Mdm36 is a mitochondrial fission-promoting protein in *Saccharomyces cerevisiae*. *Mol Biol Cell* **21**, 2443-2452.
- Harner, M., Korner, C., Walther, D., Mokranjac, D., Kaesmacher, J., Welsch, U., Griffith, J., Mann, M., Reggiori, F., and Neupert, W. (2011). The mitochondrial contact site complex, a determinant of mitochondrial architecture. *EMBO J* **30**, 4356-4370.
- Hayashi-Nishino, M., Fujita, N., Noda, T., Yamaguchi, A., Yoshimori, T., and Yamamoto, A. (2009). A subdomain of the endoplasmic reticulum forms a cradle for autophagosome formation. *Nat Cell Biol* **11**, 1433-1437.

- Heil-Chapdelaine, R.A., Oberle, J.R., and Cooper, J.A. (2000). The cortical protein Num1p is essential for dynein-dependent interactions of microtubules with the cortex. *J Cell Biol* 151, 1337-1344.
- Heo, J.M., Livnat-Levanon, N., Taylor, E.B., Jones, K.T., Dephoure, N., Ring, J., Xie, J., Brodsky, J.L., Madeo, F., Gygi, S.P., *et al.* (2010). A stress-responsive system for mitochondrial protein degradation. *Mol Cell* 40, 465-480.
- Heo, J.M., Nielson, J.R., Dephoure, N., Gygi, S.P., and Rutter, J. (2013). Intramolecular interactions control Vms1 translocation to damaged mitochondria. *Mol Biol Cell* 24, 1263-1273.
- Herlan, M., Bornhovd, C., Hell, K., Neupert, W., and Reichert, A.S. (2004). Alternative topogenesis of Mgm1 and mitochondrial morphology depend on ATP and a functional import motor. *J Cell Biol* 165, 167-173.
- Hermann, G.J., Thatcher, J.W., Mills, J.P., Hales, K.G., Fuller, M.T., Nunnari, J., and Shaw, J.M. (1998). Mitochondrial fusion in yeast requires the transmembrane GTPase Fzo1p. *J Cell Biol* 143, 359-373.
- Higuchi, R., Vevea, J.D., Swayne, T.C., Chojnowski, R., Hill, V., Boldogh, I.R., and Pon, L.A. (2013). Actin dynamics affect mitochondrial quality control and aging in budding yeast. *Curr Biol* 23, 2417-2422.
- Hobbs, A.E., Srinivasan, M., McCaffery, J.M., and Jensen, R.E. (2001). Mmm1p, a mitochondrial outer membrane protein, is connected to mitochondrial DNA (mtDNA) nucleoids and required for mtDNA stability. *J Cell Biol* 152, 401-410.
- Hollenbeck, P.J., and Saxton, W.M. (2005). The axonal transport of mitochondria. *J Cell Sci* 118, 5411-5419.
- Honscher, C., Mari, M., Auffarth, K., Bohnert, M., Griffith, J., Geerts, W., van der Laan, M., Cabrera, M., Reggiori, F., and Ungermann, C. (2014). Cellular metabolism regulates contact sites between vacuoles and mitochondria. *Dev Cell* 30, 86-94.
- Hoppins, S., Collins, S.R., Cassidy-Stone, A., Hummel, E., Devay, R.M., Lackner, L.L., Westermann, B., Schuldiner, M., Weissman, J.S., and Nunnari, J. (2011). A mitochondrial-focused genetic interaction map reveals a scaffold-like complex required for inner membrane organization in mitochondria. *J Cell Biol im Druck*.
- Hu, C.D., Chinenov, Y., and Kerppola, T.K. (2002). Visualization of interactions among bZIP and Rel family proteins in living cells using bimolecular fluorescence complementation. *Mol Cell* 9, 789-798.
- Hughes, A.L., and Gottschling, D.E. (2012). An early age increase in vacuolar pH limits mitochondrial function and lifespan in yeast. *Nature* 492, 261-265.
- Huh, W.K., Falvo, J.V., Gerke, L.C., Carroll, A.S., Howson, R.W., Weissman, J.S., and O'Shea, E.K. (2003). Global analysis of protein localization in budding yeast. *Nature* 425, 686-691.
- Hwang, E., Kusch, J., Barral, Y., and Huffaker, T.C. (2003). Spindle orientation in *Saccharomyces cerevisiae* depends on the transport of microtubule ends along polarized actin cables. *J Cell Biol* 161, 483-488.
- Ichimura, Y., Kirisako, T., Takao, T., Satomi, Y., Shimonishi, Y., Ishihara, N., Mizushima, N., Tanida, I., Kominami, E., Ohsumi, M., *et al.* (2000). A ubiquitin-like system mediates protein lipidation. *Nature* 408, 488-492.
- Ingerman, E., Perkins, E.M., Marino, M., Mears, J.A., McCaffery, J.M., Hinshaw, J.E., and Nunnari, J. (2005). Dnm1 forms spirals that are structurally tailored to fit mitochondria. *J Cell Biol* 170, 1021-1027.
- Inoue, Y., and Klionsky, D.J. (2010). Regulation of macroautophagy in *Saccharomyces cerevisiae*. *Semin Cell Dev Biol* 21, 664-670.

- Ishihara, N., Hamasaki, M., Yokota, S., Suzuki, K., Kamada, Y., Kihara, A., Yoshimori, T., Noda, T., and Ohsumi, Y. (2001). Autophagosome requires specific early Sec proteins for its formation and NSF/SNARE for vacuolar fusion. *Mol Biol Cell* 12, 3690-3702.
- Ishikawa, K., Catlett, N.L., Novak, J.L., Tang, F., Nau, J.J., and Weisman, L.S. (2003). Identification of an organelle-specific myosin V receptor. *J Cell Biol* 160, 887-897.
- Islinger, M., Luers, G.H., Zischka, H., Ueffing, M., and Volkl, A. (2006). Insights into the membrane proteome of rat liver peroxisomes: microsomal glutathione-S-transferase is shared by both subcellular compartments. *Proteomics* 6, 804-816.
- Ito, T., Chiba, T., Ozawa, R., Yoshida, M., Hattori, M., and Sakaki, Y. (2001). A comprehensive two-hybrid analysis to explore the yeast protein interactome. *Proc Natl Acad Sci U S A* 98, 4569-4574.
- Itoh, T., Toh, E.A., and Matsui, Y. (2004). Mmr1p is a mitochondrial factor for Myo2p-dependent inheritance of mitochondria in the budding yeast. *EMBO J* 23, 2520-2530.
- Itoh, T., Watabe, A., Toh, E.A., and Matsui, Y. (2002). Complex formation with Ypt11p, a rab-type small GTPase, is essential to facilitate the function of Myo2p, a class V myosin, in mitochondrial distribution in *Saccharomyces cerevisiae*. *Mol Cell Biol* 22, 7744-7757.
- Iwasawa, R., Mahul-Mellier, A.L., Datler, C., Pazarentzos, E., and Grimm, S. (2011). Fis1 and Bap31 bridge the mitochondria-ER interface to establish a platform for apoptosis induction. *EMBO J* 30, 556-568.
- Jin, Y., Taylor Eves, P., Tang, F., and Weisman, L.S. (2009). *PTC1* is required for vacuole inheritance and promotes the association of the myosin-V vacuole-specific receptor complex. *Mol Biol Cell* 20, 1312-1323.
- Jourdain, I., Sontam, D., Johnson, C., Dillies, C., and Hyams, J.S. (2008). Dynamin-dependent biogenesis, cell cycle regulation and mitochondrial association of peroxisomes in fission yeast. *Traffic* 9, 353-365.
- Kanki, T., and Klionsky, D.J. (2010). The molecular mechanism of mitochondria autophagy in yeast. *Mol Microbiol* 75, 795-800.
- Kanki, T., Kurihara, Y., Jin, X., Goda, T., Ono, Y., Aihara, M., Hirota, Y., Saigusa, T., Aoki, Y., Uchiumi, T., *et al.* (2013). Casein kinase 2 is essential for mitophagy. *EMBO Rep* 14, 788-794.
- Kanki, T., Wang, K., Baba, M., Bartholomew, C.R., Lynch-Day, M.A., Du, Z., Geng, J., Mao, K., Yang, Z., Yen, W.L., *et al.* (2009a). A genomic screen for yeast mutants defective in selective mitochondria autophagy. *Mol Biol Cell* 20, 4730-4738.
- Kanki, T., Wang, K., Cao, Y., Baba, M., and Klionsky, D.J. (2009b). Atg32 is a mitochondrial protein that confers selectivity during mitophagy. *Dev Cell* 17, 98-109.
- Kashatus, D.F., Lim, K.H., Brady, D.C., Pershing, N.L., Cox, A.D., and Counter, C.M. (2011). RALA and RALBP1 regulate mitochondrial fission at mitosis. *Nat Cell Biol* 13, 1108-1115.
- Keppler-Ross, S., Noffz, C., and Dean, N. (2008). A new purple fluorescent color marker for genetic studies in *Saccharomyces cerevisiae* and *Candida albicans*. *Genetics* 179, 705-710.
- Kerppola, T.K. (2008a). Bimolecular fluorescence complementation (BiFC) analysis as a probe of protein interactions in living cells. *Annu Rev Biophys* 37, 465-487.
- Kerppola, T.K. (2008b). Bimolecular fluorescence complementation: visualization of molecular interactions in living cells. *Methods Cell Biol* 85, 431-470.
- Kihara, A., Noda, T., Ishihara, N., and Ohsumi, Y. (2001). Two distinct Vps34 phosphatidylinositol 3-kinase complexes function in autophagy and carboxypeptidase Y sorting in *Saccharomyces cerevisiae*. *J Cell Biol* 152, 519-530.

- Kikyo, M., Tanaka, K., Kamei, T., Ozaki, K., Fujiwara, T., Inoue, E., Takita, Y., Ohya, Y., and Takai, Y. (1999). An FH domain-containing Bnr1p is a multifunctional protein interacting with a variety of cytoskeletal proteins in *Saccharomyces cerevisiae*. *Oncogene* 18, 7046-7054.
- Kim, I., and Lemasters, J.J. (2011). Mitochondrial degradation by autophagy (mitophagy) in GFP-LC3 transgenic hepatocytes during nutrient deprivation. *Am J Physiol Cell Physiol* 300, C308-317.
- Kim, J., Huang, W.P., Stromhaug, P.E., and Klionsky, D.J. (2002). Convergence of multiple autophagy and cytoplasm to vacuole targeting components to a perivacuolar membrane compartment prior to de novo vesicle formation. *J Biol Chem* 277, 763-773.
- Kirisako, T., Baba, M., Ishihara, N., Miyazawa, K., Ohsumi, M., Yoshimori, T., Noda, T., and Ohsumi, Y. (1999). Formation process of autophagosome is traced with Apg8/Aut7p in yeast. *J Cell Biol* 147, 435-446.
- Kirisako, T., Ichimura, Y., Okada, H., Kabeya, Y., Mizushima, N., Yoshimori, T., Ohsumi, M., Takao, T., Noda, T., and Ohsumi, Y. (2000). The reversible modification regulates the membrane-binding state of Apg8/Aut7 essential for autophagy and the cytoplasm to vacuole targeting pathway. *J Cell Biol* 151, 263-276.
- Klecker, T., Böckler, S., and Westermann, B. (2014). Making connections: interorganelle contacts orchestrate mitochondrial behavior. *Trends Cell Biol* 24, 537-45.
- Klecker, T., Scholz, D., Fortsch, J., and Westermann, B. (2013). The yeast cell cortical protein Num1 integrates mitochondrial dynamics into cellular architecture. *J Cell Sci* 126, 2924-2930.
- Klionsky, D.J., Abdalla, F.C., Abeliovich, H., Abraham, R.T., Acevedo-Arozena, A., Adeli, K., Agholme, L., Agnello, M., Agostinis, P., Aguirre-Ghiso, J.A., *et al.* (2012). Guidelines for the use and interpretation of assays for monitoring autophagy. *Autophagy* 8, 445-544.
- Klionsky, D.J., Cueva, R., and Yaver, D.S. (1992). Aminopeptidase I of *Saccharomyces cerevisiae* is localized to the vacuole independent of the secretory pathway. *J Cell Biol* 119, 287-299.
- Knoblauch, B., and Rachubinski, R.A. (2015). Sharing the cell's bounty - organelle inheritance in yeast. *J Cell Sci*.
- Knoblauch, B., Sun, X., Coquelle, N., Fagarasanu, A., Poirier, R.L., and Rachubinski, R.A. (2013). An ER-peroxisome tether exerts peroxisome population control in yeast. *EMBO J* 32, 2439-2453.
- Kondo-Okamoto, N., Noda, N.N., Suzuki, S.W., Nakatogawa, H., Takahashi, I., Matsunami, M., Hashimoto, A., Inagaki, F., Ohsumi, Y., and Okamoto, K. (2012). Autophagy-related protein 32 acts as autophagic degron and directly initiates mitophagy. *J Biol Chem* 287, 10631-10638.
- Kopeck, K.O., Alva, V., and Lupas, A.N. (2010). Homology of SMP domains to the TULIP superfamily of lipid-binding proteins provides a structural basis for lipid exchange between ER and mitochondria. *Bioinformatics* 26, 1927-1931.
- Kornmann, B. (2013). The molecular hug between the ER and the mitochondria. *Curr Opin Cell Biol* 25, 443-448.
- Kornmann, B., Currie, E., Collins, S.R., Schuldiner, M., Nunnari, J., Weissman, J.S., and Walter, P. (2009). An ER-mitochondria tethering complex revealed by a synthetic biology screen. *Science* 325, 477-481.
- Kornmann, B., Osman, C., and Walter, P. (2011). The conserved GTPase Gem1 regulates endoplasmic reticulum-mitochondria connections. *Proc Natl Acad Sci U S A* 108, 14151-14156.
- Kraft, C., Deplazes, A., Sohrmann, M., and Peter, M. (2008). Mature ribosomes are selectively degraded upon starvation by an autophagy pathway requiring the Ubp3p/Bre5p ubiquitin protease. *Nat Cell Biol* 10, 602-610.

- Krogan, N.J., Cagney, G., Yu, H., Zhong, G., Guo, X., Ignatchenko, A., Li, J., Pu, S., Datta, N., Tikuisis, A.P., *et al.* (2006). Global landscape of protein complexes in the yeast *Saccharomyces cerevisiae*. *Nature* **440**, 637-643.
- Kunau, W.H., Dommes, V., and Schulz, H. (1995). beta-oxidation of fatty acids in mitochondria, peroxisomes, and bacteria: a century of continued progress. *Prog Lipid Res* **34**, 267-342.
- Kundu, M., Lindsten, T., Yang, C.Y., Wu, J., Zhao, F., Zhang, J., Selak, M.A., Ney, P.A., and Thompson, C.B. (2008). Ulk1 plays a critical role in the autophagic clearance of mitochondria and ribosomes during reticulocyte maturation. *Blood* **112**, 1493-1502.
- Kuravi, K., Nagotu, S., Krikken, A.M., Sjollem, K., Deckers, M., Erdmann, R., Veenhuis, M., and van der Klei, I.J. (2006). Dynamin-related proteins Vps1p and Dnm1p control peroxisome abundance in *Saccharomyces cerevisiae*. *J Cell Sci* **119**, 3994-4001.
- Kurihara, Y., Kanki, T., Aoki, Y., Hirota, Y., Saigusa, T., Uchiumi, T., and Kang, D. (2012). Mitophagy plays an essential role in reducing mitochondrial production of reactive oxygen species and mutation of mitochondrial DNA by maintaining mitochondrial quantity and quality in yeast. *J Biol Chem* **287**, 3265-3272.
- Lackner, L.L., Ping, H., Graef, M., Murley, A., and Nunnari, J. (2013). Endoplasmic reticulum-associated mitochondria-cortex tether functions in the distribution and inheritance of mitochondria. *Proc Natl Acad Sci U S A* **110**, E458-467.
- Lahiri, S., Chao, J.T., Tavassoli, S., Wong, A.K., Choudhary, V., Young, B.P., Loewen, C.J., and Prinz, W.A. (2014). A conserved endoplasmic reticulum membrane protein complex (EMC) facilitates phospholipid transfer from the ER to mitochondria. *PLoS Biol* **12**, e1001969.
- Lamark, T., and Johansen, T. (2012). Aggrephagy: selective disposal of protein aggregates by macroautophagy. *Int J Cell Biol* **2012**, 736905.
- Lander, E.S., Linton, L.M., Birren, B., Nusbaum, C., Zody, M.C., Baldwin, J., Devon, K., Dewar, K., Doyle, M., FitzHugh, W., *et al.* (2001). Initial sequencing and analysis of the human genome. *Nature* **409**, 860-921.
- Lawrence, E., and Mandato, C. (2013). Mitochondrial inheritance is mediated by microtubules in mammalian cell division. *Commun Integr Biol* **6**, e27557.
- Lee, T.I., Causton, H.C., Holstege, F.C., Shen, W.C., Hannett, N., Jennings, E.G., Winston, F., Green, M.R., and Young, R.A. (2000). Redundant roles for the TFIID and SAGA complexes in global transcription. *Nature* **405**, 701-704.
- Legesse-Miller, A., Massol, R.H., and Kirchhausen, T. (2003). Constriction and Dnm1p recruitment are distinct processes in mitochondrial fission. *Mol Biol Cell* **14**, 1953-1963.
- Lewandowska, A., Macfarlane, J., and Shaw, J.M. (2013). Mitochondrial association, protein phosphorylation, and degradation regulate the availability of the active Rab GTPase Ypt11 for mitochondrial inheritance. *Mol Biol Cell* **24**, 1185-1195.
- Li, Z., Okamoto, K., Hayashi, Y., and Sheng, M. (2004). The importance of dendritic mitochondria in the morphogenesis and plasticity of spines and synapses. *Cell* **119**, 873-887.
- Lill, R., and Mühlenhoff, U. (2005). Iron-sulfur-protein biogenesis in eukaryotes. *Trends Biochem Sci* **30**, 133-141.
- Liu, L., Sakakibara, K., Chen, Q., and Okamoto, K. (2014). Receptor-mediated mitophagy in yeast and mammalian systems. *Cell Res* **24**, 787-795.
- Loewith, R., and Hall, M.N. (2011). Target of rapamycin (TOR) in nutrient signaling and growth control. *Genetics* **189**, 1177-1201.

- Luban, C., Beutel, M., Stahl, U., and Schmidt, U. (2005). Systematic screening of nuclear encoded proteins involved in the splicing metabolism of group II introns in yeast mitochondria. *Gene* 354, 72-79.
- Lynch-Day, M.A., Bhandari, D., Menon, S., Huang, J., Cai, H., Bartholomew, C.R., Brumell, J.H., Ferro-Novick, S., and Klionsky, D.J. (2010). Trs85 directs a Ypt1 GEF, TRAPPIII, to the phagophore to promote autophagy. *Proc Natl Acad Sci U S A* 107, 7811-7816.
- Lynch-Day, M.A., and Klionsky, D.J. (2010). The Cvt pathway as a model for selective autophagy. *FEBS Lett* 584, 1359-1366.
- Manjithaya, R., Nazarko, T.Y., Farre, J.C., and Subramani, S. (2010). Molecular mechanism and physiological role of pexophagy. *FEBS Lett* 584, 1367-1373.
- Mao, K., Liu, X., Feng, Y., and Klionsky, D.J. (2014). The progression of peroxisomal degradation through autophagy requires peroxisomal division. *Autophagy* 10, 652-661.
- Mao, K., Wang, K., Liu, X., and Klionsky, D.J. (2013). The scaffold protein Atg11 recruits fission machinery to drive selective mitochondria degradation by autophagy. *Dev Cell* 26, 9-18.
- Mao, K., Wang, K., Zhao, M., Xu, T., and Klionsky, D.J. (2011). Two MAPK-signaling pathways are required for mitophagy in *Saccharomyces cerevisiae*. *J Cell Biol* 193, 755-767.
- Mari, M., Griffith, J., Rieter, E., Krishnappa, L., Klionsky, D.J., and Reggiori, F. (2010). An Atg9-containing compartment that functions in the early steps of autophagosome biogenesis. *J Cell Biol* 190, 1005-1022.
- Mari, M., Tooze, S.A., and Reggiori, F. (2011). The puzzling origin of the autophagosomal membrane. *F1000 Biol Rep* 3, 25.
- Matsuda, N., Sato, S., Shiba, K., Okatsu, K., Saisho, K., Gautier, C.A., Sou, Y.S., Saiki, S., Kawajiri, S., Sato, F., *et al.* (2010). PINK1 stabilized by mitochondrial depolarization recruits Parkin to damaged mitochondria and activates latent Parkin for mitophagy. *J Cell Biol* 189, 211-221.
- Matsuura, A., Tsukada, M., Wada, Y., and Ohsumi, Y. (1997). Apg1p, a novel protein kinase required for the autophagic process in *Saccharomyces cerevisiae*. *Gene* 192, 245-250.
- McBride, H.M., Neuspiel, M., and Wasiak, S. (2006). Mitochondria: more than just a powerhouse. *Curr Biol* 16, R551-560.
- Meeusen, S., and Nunnari, J. (2003). Evidence for a two membrane-spanning autonomous mitochondrial DNA replisome. *J Cell Biol* 163, 503-510.
- Meisinger, C., Pfannschmidt, S., Rissler, M., Milenkovic, D., Becker, T., Stojanovski, D., Youngman, M.J., Jensen, R.E., Chacinska, A., Guiard, B., *et al.* (2007). The morphology proteins Mdm12/Mmm1 function in the major beta-barrel assembly pathway of mitochondria. *EMBO J* 26, 2229-2239.
- Meisinger, C., Rissler, M., Chacinska, A., Szklarz, L.K., Milenkovic, D., Kozjak, V., Schonfisch, B., Lohaus, C., Meyer, H.E., Yaffe, M.P., *et al.* (2004). The mitochondrial morphology protein Mdm10 functions in assembly of the preprotein translocase of the outer membrane. *Dev Cell* 7, 61-71.
- Mendl, N., Occhipinti, A., Müller, M., Wild, P., Dikic, I., and Reichert, A.S. (2011). Mitophagy in yeast is independent of mitochondrial fission and requires the stress response gene *WHI2*. *J Cell Sci* 124, 1339-1350.
- Merz, S., and Westermann, B. (2009). Genome-wide deletion mutant analysis reveals genes required for respiratory growth, mitochondrial genome maintenance and mitochondrial protein synthesis in *Saccharomyces cerevisiae*. *Genome Biol* 10, R95.
- Messerschmitt, M., Jakobs, S., Vogel, F., Fritz, S., Dimmer, K.S., Neupert, W., and Westermann, B. (2003). The inner membrane protein Mdm33 controls mitochondrial morphology in yeast. *J Cell Biol* 160, 553-564.

- Miesenböck, G., De Angelis, D.A., and Rothman, J.E. (1998). Visualizing secretion and synaptic transmission with pH-sensitive green fluorescent proteins. *Nature* 394, 192-195.
- Mijaljica, D., Prescott, M., and Devenish, R.J. (2012). A late form of nucleophagy in *Saccharomyces cerevisiae*. *PLoS One* 7, e40013.
- Misko, A., Jiang, S., Wegorzewska, I., Milbrandt, J., and Baloh, R.H. (2010). Mitofusin 2 is necessary for transport of axonal mitochondria and interacts with the Miro/Milton complex. *J Neurosci* 30, 4232-4240.
- Mizushima, N., Yoshimori, T., and Ohsumi, Y. (2011). The role of Atg proteins in autophagosome formation. *Annu Rev Cell Dev Biol* 27, 107-132.
- Mnaimneh, S., Davierwala, A.P., Haynes, J., Moffat, J., Peng, W.T., Zhang, W., Yang, X., Pootoolal, J., Chua, G., Lopez, A., *et al.* (2004). Exploration of essential gene functions via titratable promoter alleles. *Cell* 118, 31-44.
- Mohanty, A., and McBride, H.M. (2013). Emerging roles of mitochondria in the evolution, biogenesis, and function of peroxisomes. *Front Physiol* 4, 268.
- Motley, A.M., Nuttall, J.M., and Hettema, E.H. (2012). Pex3-anchored Atg36 tags peroxisomes for degradation in *Saccharomyces cerevisiae*. *EMBO J* 31, 2852-2868.
- Mozdy, A.D., McCaffery, J.M., and Shaw, J.M. (2000). Dnm1p GTPase-mediated mitochondrial fission is a multi-step process requiring the novel integral membrane component Fis1p. *J Cell Biol* 151, 367-380.
- Mumberg, D., Muller, R., and Funk, M. (1995). Yeast vectors for the controlled expression of heterologous proteins in different genetic backgrounds. *Gene* 156, 119-122.
- Murley, A., Lackner, L.L., Osman, C., West, M., Voeltz, G.K., Walter, P., and Nunnari, J. (2013). ER-associated mitochondrial division links the distribution of mitochondria and mitochondrial DNA in yeast. *Elife* 2, e00422.
- Nagai, T., Ibata, K., Park, E.S., Kubota, M., Mikoshiba, K., and Miyawaki, A. (2002). A variant of yellow fluorescent protein with fast and efficient maturation for cell-biological applications. *Nat Biotechnol* 20, 87-90.
- Nakada, K., Inoue, K., Ono, T., Isobe, K., Ogura, A., Goto, Y.I., Nonaka, I., and Hayashi, J.I. (2001). Inter-mitochondrial complementation: Mitochondria-specific system preventing mice from expression of disease phenotypes by mutant mtDNA. *Nat Med* 7, 934-940.
- Nakatogawa, H., Ichimura, Y., and Ohsumi, Y. (2007). Atg8, a ubiquitin-like protein required for autophagosome formation, mediates membrane tethering and hemifusion. *Cell* 130, 165-178.
- Nakatogawa, H., Suzuki, K., Kamada, Y., and Ohsumi, Y. (2009). Dynamics and diversity in autophagy mechanisms: lessons from yeast. *Nat Rev Mol Cell Biol* 10, 458-467.
- Narendra, D., Tanaka, A., Suen, D.F., and Youle, R.J. (2008). Parkin is recruited selectively to impaired mitochondria and promotes their autophagy. *J Cell Biol* 183, 795-803.
- Narendra, D.P., Jin, S.M., Tanaka, A., Suen, D.F., Gautier, C.A., Shen, J., Cookson, M.R., and Youle, R.J. (2010). PINK1 is selectively stabilized on impaired mitochondria to activate Parkin. *PLoS Biol* 8, e1000298.
- Neuspiel, M., Schauss, A.C., Braschi, E., Zunino, R., Rippstein, P., Rachubinski, R.A., Andrade-Navarro, M.A., and McBride, H.M. (2008). Cargo-selected transport from the mitochondria to peroxisomes is mediated by vesicular carriers. *Curr Biol* 18, 102-108.
- Nguyen, T.T., Lewandowska, A., Choi, J.Y., Markgraf, D.F., Junker, M., Bilgin, M., Ejsing, C.S., Voelker, D.R., Rapoport, T.A., and Shaw, J.M. (2012). Gem1 and ERMES do not directly affect

- phosphatidylserine transport from ER to mitochondria or mitochondrial inheritance. *Traffic* **13**, 880-890.
- Noda, T., Kim, J., Huang, W.P., Baba, M., Tokunaga, C., Ohsumi, Y., and Klionsky, D.J. (2000). Apg9p/Cvt7p is an integral membrane protein required for transport vesicle formation in the Cvt and autophagy pathways. *J Cell Biol* **148**, 465-480.
- Nowikovsky, K., Reipert, S., Devenish, R.J., and Schweyen, R.J. (2007). Mdm38 protein depletion causes loss of mitochondrial K⁺/H⁺ exchange activity, osmotic swelling and mitophagy. *Cell Death Differ* **14**, 1647-1656.
- Obara, K., Sekito, T., and Ohsumi, Y. (2006). Assortment of phosphatidylinositol 3-kinase complexes--Atg14p directs association of complex I to the pre-autophagosomal structure in *Saccharomyces cerevisiae*. *Mol Biol Cell* **17**, 1527-1539.
- Ohsumi, Y. (2001). Molecular dissection of autophagy: two ubiquitin-like systems. *Nat Rev Mol Cell Biol* **2**, 211-216.
- Okamoto, K. (2014). Organellophagy: Eliminating cellular building blocks via selective autophagy. *J Cell Biol* **205**, 435-445.
- Okamoto, K., Kondo-Okamoto, N., and Ohsumi, Y. (2009). Mitochondria-anchored receptor Atg32 mediates degradation of mitochondria via selective autophagy. *Dev Cell* **17**, 87-97.
- Ono, T., Isobe, K., Nakada, K., and Hayashi, J.I. (2001). Human cells are protected from mitochondrial dysfunction by complementation of DNA products in fused mitochondria. *Nat Genet* **28**, 272-275.
- Osman, C., Haag, M., Potting, C., Rodenfels, J., Dip, P.V., Wieland, F.T., Brugger, B., Westermann, B., and Langer, T. (2009). The genetic interactome of prohibitins: coordinated control of cardiolipin and phosphatidylethanolamine by conserved regulators in mitochondria. *J Cell Biol* **184**, 583-596.
- Ozaki-Kuroda, K., Yamamoto, Y., Nohara, H., Kinoshita, M., Fujiwara, T., Irie, K., and Takai, Y. (2001). Dynamic localization and function of Bni1p at the sites of directed growth in *Saccharomyces cerevisiae*. *Mol Cell Biol* **21**, 827-839.
- Pankiv, S., Clausen, T.H., Lamark, T., Brech, A., Bruun, J.A., Outzen, H., Overvatn, A., Bjorkoy, G., and Johansen, T. (2007). p62/SQSTM1 binds directly to Atg8/LC3 to facilitate degradation of ubiquitinated protein aggregates by autophagy. *J Biol Chem* **282**, 24131-24145.
- Pashkova, N., Jin, Y., Ramaswamy, S., and Weisman, L.S. (2006). Structural basis for myosin V discrimination between distinct cargoes. *EMBO J* **25**, 693-700.
- Peraza-Reyes, L., Crider, D.G., and Pon, L.A. (2010). Mitochondrial manoeuvres: latest insights and hypotheses on mitochondrial partitioning during mitosis in *Saccharomyces cerevisiae*. *Bioessays* **32**, 1040-1049.
- Pon, L.A. (2008). Golgi inheritance: rab rides the coat-tails. *Curr Biol* **18**, R743-R745.
- Priault, M., Salin, B., Schaeffer, J., Vallette, F.M., di Rago, J.P., and Martinou, J.C. (2005). Impairing the bioenergetic status and the biogenesis of mitochondria triggers mitophagy in yeast. *Cell Death Differ* **12**, 1613-1621.
- Prinz, W.A., Grzyb, L., Veenhuis, M., Kahana, J.A., Silver, P.A., and Rapoport, T.A. (2000). Mutants affecting the structure of the cortical endoplasmic reticulum in *Saccharomyces cerevisiae*. *J Cell Biol* **150**, 461-474.
- Pruyne, D., Legesse-Miller, A., Gao, L., Dong, Y., and Bretscher, A. (2004). Mechanisms of polarized growth and organelle segregation in yeast. *Annu Rev Cell Dev Biol* **20**, 559-591.
- Rapaport, D., Brunner, M., Neupert, W., and Westermann, B. (1998). Fzo1p is a mitochondrial outer membrane protein essential for the biogenesis of functional mitochondria in *Saccharomyces cerevisiae*. *J Biol Chem* **273**, 20150-20155.

- Reck-Peterson, S.L., Provance, D.W., Jr., Mooseker, M.S., and Mercer, J.A. (2000). Class V myosins. *Biochim Biophys Acta* 1496, 36-51.
- Reggiori, F., and Klionsky, D.J. (2013). Autophagic processes in yeast: mechanism, machinery and regulation. *Genetics* 194, 341-361.
- Reggiori, F., Wang, C.W., Nair, U., Shintani, T., Abeliovich, H., and Klionsky, D.J. (2004). Early stages of the secretory pathway, but not endosomes, are required for Cvt vesicle and autophagosome assembly in *Saccharomyces cerevisiae*. *Mol Biol Cell* 15, 2189-2204.
- Reichert, A.S., and Neupert, W. (2004). Mitochondriomics or what makes us breathe. *Trends Genet* 20, 555-562.
- Richard, V.R., Leonov, A., Beach, A., Burstein, M.T., Koupaki, O., Gomez-Perez, A., Levy, S., Pluska, L., Mattie, S., Rafesh, R., *et al.* (2013). Macromitophagy is a longevity assurance process that in chronologically aging yeast limited in calorie supply sustains functional mitochondria and maintains cellular lipid homeostasis. *Aging (Albany NY)* 5, 234-269.
- Rizzuto, R., De Stefani, D., Raffaello, A., and Mammucari, C. (2012). Mitochondria as sensors and regulators of calcium signalling. *Nat Rev Mol Cell Biol* 13, 566-578.
- Rizzuto, R., Pinton, P., Carrington, W., Fay, F.S., Fogarty, K.E., Lifshitz, L.M., Tuft, R.A., and Pozzan, T. (1998). Close contacts with the endoplasmic reticulum as determinants of mitochondrial Ca²⁺ responses. *Science* 280, 1763-1766.
- Roeder, A.D., Hermann, G.J., Keegan, B.R., Thatcher, S.A., and Shaw, J.M. (1998). Mitochondrial inheritance is delayed in *Saccharomyces cerevisiae* cells lacking the serine/threonine phosphatase *PTC1*. *Mol Biol Cell* 9, 917-930.
- Rosado, C.J., Mijaljica, D., Hatzinisiriou, I., Prescott, M., and Devenish, R.J. (2008). Rosella: a fluorescent pH-biosensor for reporting vacuolar turnover of cytosol and organelles in yeast. *Autophagy* 4, 205-213.
- Rosenberger, S., Connerth, M., Zellnig, G., and Daum, G. (2009). Phosphatidylethanolamine synthesized by three different pathways is supplied to peroxisomes of the yeast *Saccharomyces cerevisiae*. *Biochim Biophys Acta* 1791, 379-387.
- Rothbauer, U., Zolghadr, K., Muyldermans, S., Schepers, A., Cardoso, M.C., and Leonhardt, H. (2008). A versatile nanotrap for biochemical and functional studies with fluorescent fusion proteins. *Mol Cell Proteomics* 7, 282-289.
- Rowland, A.A., Chitwood, P.J., Phillips, M.J., and Voeltz, G.K. (2014). ER Contact Sites Define the Position and Timing of Endosome Fission. *Cell* 159, 1027-1041.
- Rowland, A.A., and Voeltz, G.K. (2012). Endoplasmic reticulum-mitochondria contacts: function of the junction. *Nat Rev Mol Cell Biol* 13, 607-625.
- Sandoval, H., Thiagarajan, P., Dasgupta, S.K., Schumacher, A., Prchal, J.T., Chen, M., and Wang, J. (2008). Essential role for Nix in autophagic maturation of erythroid cells. *Nature* 454, 232-235.
- Schauss, A.C., Bewersdorf, J., and Jakobs, S. (2006). Fis1p and Caf4p, but not Mdv1p, determine the polar localization of Dnm1p clusters on the mitochondrial surface. *J Cell Sci* 119, 3098-3106.
- Scheckhuber, C.Q., Erjavec, N., Tinazli, A., Hamann, A., Nystrom, T., and Osiewacz, H.D. (2007). Reducing mitochondrial fission results in increased life span and fitness of two fungal ageing models. *Nat Cell Biol* 9, 99-105.
- Schmidt, O., Pfanner, N., and Meisinger, C. (2010). Mitochondrial protein import: from proteomics to functional mechanisms. *Nat Rev Mol Cell Biol* 11, 655-667.
- Schott, D.H., Collins, R.N., and Bretscher, A. (2002). Secretory vesicle transport velocity in living cells depends on the myosin-V lever arm length. *J Cell Biol* 156, 35-39.

- Schrader, M., Bonekamp, N.A., and Islinger, M. (2012). Fission and proliferation of peroxisomes. *Biochim Biophys Acta* 1822, 1343-1357.
- Schrader, M., Grille, S., Fahimi, H.D., and Islinger, M. (2013). Peroxisome interactions and cross-talk with other subcellular compartments in animal cells. *Subcell Biochem* 69, 1-22.
- Schuck, S., Gallagher, C.M., and Walter, P. (2014). ER-phagy mediates selective degradation of endoplasmic reticulum independently of the core autophagy machinery. *J Cell Sci* 127, 4078-4088.
- Seo, B.B., Kitajima-Ihara, T., Chan, E.K., Scheffler, I.E., Matsuno-Yagi, A., and Yagi, T. (1998). Molecular remedy of complex I defects: rotenone-insensitive internal NADH-quinone oxidoreductase of *Saccharomyces cerevisiae* mitochondria restores the NADH oxidase activity of complex I-deficient mammalian cells. *Proc Natl Acad Sci U S A* 95, 9167-9171.
- Sesaki, H., and Jensen, R.E. (1999). Division versus fusion: Dnm1p and Fzo1p antagonistically regulate mitochondrial shape. *J Cell Biol* 147, 699-706.
- Sesaki, H., and Jensen, R.E. (2004). Ugo1p links the Fzo1p and Mgm1p GTPases for mitochondrial fusion. *J Biol Chem* 279, 28298-28303.
- Sheng, Z.H. (2014). Mitochondrial trafficking and anchoring in neurons: New insight and implications. *J Cell Biol* 204, 1087-1098.
- Sherman, F. (2002). Getting started with yeast. *Methods Enzymol* 350, 3-41.
- Shintani, T., and Klionsky, D.J. (2004). Cargo proteins facilitate the formation of transport vesicles in the cytoplasm to vacuole targeting pathway. *J Biol Chem* 279, 29889-29894.
- Sikorski, R.S., and Hieter, P. (1989). A system of shuttle vectors and yeast host strains designed for efficient manipulation of DNA in *Saccharomyces cerevisiae*. *Genetics* 122, 19-27.
- Simmen, T., Aslan, J.E., Blagoveshchenskaya, A.D., Thomas, L., Wan, L., Xiang, Y., Feliciangeli, S.F., Hung, C.H., Crump, C.M., and Thomas, G. (2005). PACS-2 controls endoplasmic reticulum-mitochondria communication and Bid-mediated apoptosis. *EMBO J* 24, 717-729.
- Simon, V.R., Swayne, T.C., and Pon, L.A. (1995). Actin-dependent mitochondrial motility in mitotic yeast and cell-free systems: identification of a motor activity on the mitochondrial surface. *J Cell Biol* 130, 345-354.
- Skarp, K.P., Zhao, X., Weber, M., and Jantti, J. (2008). Use of bimolecular fluorescence complementation in yeast *Saccharomyces cerevisiae*. *Methods Mol Biol* 457, 165-175.
- Sogo, L.F., and Yaffe, M.P. (1994). Regulation of mitochondrial morphology and inheritance by Mdm10p, a protein of the mitochondrial outer membrane. *J Cell Biol* 126, 1361-1373.
- Soubannier, V., McLelland, G.L., Zunino, R., Braschi, E., Rippstein, P., Fon, E.A., and McBride, H.M. (2012). A vesicular transport pathway shuttles cargo from mitochondria to lysosomes. *Curr Biol* 22, 135-141.
- Steinberg, G., and Schliwa, M. (1993). Organelle movements in the wild type and wall-less *fgsg;os-1* mutants of *Neurospora crassa* are mediated by cytoplasmic microtubules. *J Cell Sci* 106 (Pt 2), 555-564.
- Stroud, D.A., Oeljeklaus, S., Wiese, S., Bohnert, M., Lewandrowski, U., Sickmann, A., Guiard, B., van der Laan, M., Warscheid, B., and Wiedemann, N. (2011). Composition and topology of the endoplasmic reticulum-mitochondria encounter structure. *J Mol Biol* 413, 743-750.
- Sugiura, A., McLelland, G.L., Fon, E.A., and McBride, H.M. (2014). A new pathway for mitochondrial quality control: mitochondrial-derived vesicles. *EMBO J*.

- Surma, M.A., Klose, C., Peng, D., Shales, M., Mrejen, C., Stefanko, A., Braberg, H., Gordon, D.E., Vorkel, D., Ejlsing, C.S., *et al.* (2013). A lipid E-MAP identifies Ubx2 as a critical regulator of lipid saturation and lipid bilayer stress. *Mol Cell* 51, 519-530.
- Suzuki, K., Akioka, M., Kondo-Kakuta, C., Yamamoto, H., and Ohsumi, Y. (2013). Fine mapping of autophagy-related proteins during autophagosome formation in *Saccharomyces cerevisiae*. *J Cell Sci* 126, 2534-2544.
- Suzuki, K., Kirisako, T., Kamada, Y., Mizushima, N., Noda, T., and Ohsumi, Y. (2001). The pre-autophagosomal structure organized by concerted functions of APG genes is essential for autophagosome formation. *EMBO J* 20, 5971-5981.
- Suzuki, K., Kubota, Y., Sekito, T., and Ohsumi, Y. (2007). Hierarchy of Atg proteins in pre-autophagosomal structure organization. *Genes Cells* 12, 209-218.
- Swayne, T.C., Zhou, C., Boldogh, I.R., Charalel, J.K., McFaline-Figueroa, J.R., Thoms, S., Yang, C., Leung, G., McInnes, J., Erdmann, R., *et al.* (2011). Role for cER and Mmr1p in anchorage of mitochondria at sites of polarized surface growth in budding yeast. *Curr Biol* 21, 1994-1999.
- Szabadkai, G., Bianchi, K., Varnai, P., De Stefani, D., Wieckowski, M.R., Cavagna, D., Nagy, A.I., Balla, T., and Rizzuto, R. (2006). Chaperone-mediated coupling of endoplasmic reticulum and mitochondrial Ca²⁺ channels. *J Cell Biol* 175, 901-911.
- Taguchi, N., Ishihara, N., Jofuku, A., Oka, T., and Mihara, K. (2007). Mitotic phosphorylation of dynamin-related GTPase Drp1 participates in mitochondrial fission. *J Biol Chem* 282, 11521-11529.
- Tait, S.W., and Green, D.R. (2010). Mitochondria and cell death: outer membrane permeabilization and beyond. *Nat Rev Mol Cell Biol* 11, 621-632.
- Tamura, Y., Onguka, O., Hobbs, A.E., Jensen, R.E., Iijima, M., Claypool, S.M., and Sesaki, H. (2012). Role for two conserved intermembrane space proteins, Ups1p and Ups2p, in intra-mitochondrial phospholipid trafficking. *J Biol Chem* 287, 15205-15218.
- Tan, T., Ozbalci, C., Brugger, B., Rapaport, D., and Dimmer, K.S. (2013). Mcp1 and Mcp2, two novel proteins involved in mitochondrial lipid homeostasis. *J Cell Sci* 126, 3563-3574.
- Tarassov, K., Messier, V., Landry, C.R., Radinovic, S., Serna Molina, M.M., Shames, I., Malitskaya, Y., Vogel, J., Bussey, H., and Michnick, S.W. (2008). An in vivo map of the yeast protein interactome. *Science* 320, 1465-1470.
- Teter, S.A., and Klionsky, D.J. (1999). How to get a folded protein across a membrane. *Trends Cell Biol* 9, 428-431.
- Tieu, Q., and Nunnari, J. (2000). Mdv1p is a WD repeat protein that interacts with the dynamin-related GTPase, Dnm1p, to trigger mitochondrial division. *J Cell Biol* 151, 353-366.
- Tieu, Q., Okreglak, V., Naylor, K., and Nunnari, J. (2002). The WD repeat protein, Mdv1p, functions as a molecular adaptor by interacting with Dnm1p and Fis1p during mitochondrial fission. *J Cell Biol* 158, 445-452.
- Tong, A.H., Evangelista, M., Parsons, A.B., Xu, H., Bader, G.D., Page, N., Robinson, M., Raghibizadeh, S., Hogue, C.W., Bussey, H., *et al.* (2001). Systematic genetic analysis with ordered arrays of yeast deletion mutants. *Science* 294, 2364-2368.
- Tong, A.H., Lesage, G., Bader, G.D., Ding, H., Xu, H., Xin, X., Young, J., Berriz, G.F., Brost, R.L., Chang, M., *et al.* (2004). Global mapping of the yeast genetic interaction network. *Science* 303, 808-813.
- Tooze, S.A. (2013). Current views on the source of the autophagosome membrane. *Essays Biochem* 55, 29-38.
- Tooze, S.A., and Yoshimori, T. (2010). The origin of the autophagosomal membrane. *Nat Cell Biol* 12, 831-835.

- Tsukada, M., and Ohsumi, Y. (1993). Isolation and characterization of autophagy-defective mutants of *Saccharomyces cerevisiae*. *FEBS Lett* 333, 169-174.
- Twig, G., Elorza, A., Molina, A.J., Mohamed, H., Wikstrom, J.D., Walzer, G., Stiles, L., Haigh, S.E., Katz, S., Las, G., *et al.* (2008). Fission and selective fusion govern mitochondrial segregation and elimination by autophagy. *EMBO J* 27, 433-446.
- Unal, E., Kinde, B., and Amon, A. (2011). Gametogenesis eliminates age-induced cellular damage and resets life span in yeast. *Science* 332, 1554-1557.
- Vance, J.E. (1990). Phospholipid synthesis in a membrane fraction associated with mitochondria. *J Biol Chem* 265, 7248-7256.
- Verstreken, P., Ly, C.V., Venken, K.J., Koh, T.W., Zhou, Y., and Bellen, H.J. (2005). Synaptic mitochondria are critical for mobilization of reserve pool vesicles at *Drosophila* neuromuscular junctions. *Neuron* 47, 365-378.
- Vevea, J.D., Swayne, T.C., Boldogh, I.R., and Pon, L.A. (2014). Inheritance of the fittest mitochondria in yeast. *Trends Cell Biol* 24, 53-60.
- Vogel, F., Bornhvd, C., Neupert, W., and Reichert, A.S. (2006). Dynamic subcompartmentalization of the mitochondrial inner membrane. *J Cell Biol* 175, 237-247.
- von der Malsburg, K., Muller, J.M., Bohnert, M., Oeljeklaus, S., Kwiatkowska, P., Becker, T., Loniewska-Lwowska, A., Wiese, S., Rao, S., Milenkovic, D., *et al.* (2011). Dual role of mitofilin in mitochondrial membrane organization and protein biogenesis. *Dev Cell* 21, 694-707.
- Wagih, O., Usaj, M., Baryshnikova, A., VanderSluis, B., Kuzmin, E., Costanzo, M., Myers, C.L., Andrews, B.J., Boone, C.M., and Parts, L. (2013). SGAtools: One-stop analysis and visualization of array-based genetic interaction screens. *Nucleic Acids Res* 41, W591-596.
- Wagner, W., Bielli, P., Wacha, S., and Ragnini-Wilson, A. (2002). Mlc1p promotes septum closure during cytokinesis via the IQ motifs of the vesicle motor Myo2p. *EMBO J* 21, 6397-6408.
- Wallace, D.C. (2005). A mitochondrial paradigm of metabolic and degenerative diseases, aging, and cancer: a dawn for evolutionary medicine. *Annu Rev Genet* 39, 359-407.
- Wallace, D.C. (2010). Mitochondrial DNA mutations in disease and aging. *Environ Mol Mutagen* 51, 440-450.
- Wang, I.H., Chen, H.Y., Wang, Y.H., Chang, K.W., Chen, Y.C., and Chang, C.R. (2014). Resveratrol modulates mitochondria dynamics in replicative senescent yeast cells. *PLoS One* 9, e104345.
- Wang, K., Jin, M., Liu, X., and Klionsky, D.J. (2013). Proteolytic processing of Atg32 by the mitochondrial i-AAA protease Yme1 regulates mitophagy. *Autophagy* 9, 1828-1836.
- Warren, G., and Wickner, W. (1996). Organelle inheritance. *Cell* 84, 395-400.
- Weisman, L.S. (2006). Organelles on the move: insights from yeast vacuole inheritance. *Nat Rev Mol Cell Biol* 7, 243-252.
- Westermann, B. (2010). Mitochondrial fusion and fission in cell life and death. *Nat Rev Mol Cell Biol* 11, 872-884.
- Westermann, B. (2014). Mitochondrial inheritance in yeast. *Biochim Biophys Acta* 1837, 1039-1046.
- Westermann, B., and Neupert, W. (2000). Mitochondria-targeted green fluorescent proteins: convenient tools for the study of organelle biogenesis in *Saccharomyces cerevisiae*. *Yeast* 16, 1421-1427.
- Winzeler, E.A., Shoemaker, D.D., Astromoff, A., Liang, H., Anderson, K., Andre, B., Bangham, R., Benito, R., Boeke, J.D., Bussey, H., *et al.* (1999). Functional characterization of the *S. cerevisiae* genome by gene deletion and parallel analysis. *Science* 285, 901-906.

- Wong, E.D., Wagner, J.A., Gorsich, S.W., McCaffery, J.M., Shaw, J.M., and Nunnari, J. (2000). The dynamin-related GTPase, Mgm1p, is an intermembrane space protein required for maintenance of fusion competent mitochondria. *J Cell Biol* 151, 341-352.
- Wong, Y.C., and Holzbaur, E.L. (2014). Optineurin is an autophagy receptor for damaged mitochondria in parkin-mediated mitophagy that is disrupted by an ALS-linked mutation. *Proc Natl Acad Sci U S A*.
- Wu, X., Wang, F., Rao, K., Sellers, J.R., and Hammer, J.A., 3rd (2002). Rab27a is an essential component of melanosome receptor for myosin Va. *Mol Biol Cell* 13, 1735-1749.
- Wurm, C.A., and Jakobs, S. (2006). Differential protein distributions define two sub-compartments of the mitochondrial inner membrane in yeast. *FEBS Lett* 580, 5628-5634.
- Yaffe, M.P., Harata, D., Verde, F., Eddison, M., Toda, T., and Nurse, P. (1996). Microtubules mediate mitochondrial distribution in fission yeast. *Proc Natl Acad Sci U S A* 93, 11664-11668.
- Yang, J.Y., and Yang, W.Y. (2013). Bit-by-bit autophagic removal of parkin-labelled mitochondria. *Nat Commun* 4, 2428.
- Yang, Z., Geng, J., Yen, W.L., Wang, K., and Klionsky, D.J. (2010). Positive or negative roles of different cyclin-dependent kinase Pho85-cyclin complexes orchestrate induction of autophagy in *Saccharomyces cerevisiae*. *Mol Cell* 38, 250-264.
- Yang, Z., and Klionsky, D.J. (2010). Eaten alive: a history of macroautophagy. *Nat Cell Biol* 12, 814-822.
- Yin, H., Pruyne, D., Huffaker, T.C., and Bretscher, A. (2000). Myosin V orientates the mitotic spindle in yeast. *Nature* 406, 1013-1015.
- Youle, R.J., and Karbowski, M. (2005). Mitochondrial fission in apoptosis. *Nat Rev Mol Cell Biol* 6, 657-663.
- Youle, R.J., and Narendra, D.P. (2011). Mechanisms of mitophagy. *Nat Rev Mol Cell Biol* 12, 9-14.
- Youngman, M.J., Hobbs, A.E., Burgess, S.M., Srinivasan, M., and Jensen, R.E. (2004). Mmm2p, a mitochondrial outer membrane protein required for yeast mitochondrial shape and maintenance of mtDNA nucleoids. *J Cell Biol* 164, 677-688.
- Zhou, C., Slaughter, B.D., Unruh, J.R., Guo, F., Yu, Z., Mickey, K., Narkar, A., Ross, R.T., McClain, M., and Li, R. (2014). Organelle-based aggregation and retention of damaged proteins in asymmetrically dividing cells. *Cell* 159, 530-542.

Acknowledgments

I am grateful to ...

- ... Benedikt Westermann for giving me the opportunity to work in his lab as a fast-track student as well as for his support and ideas.
- ... Prof. Ruth Freitag and Prof. Olaf Stemmann for scientific advice.
- ... all former and recent members of the Westermann group.
- ... Charles Boone, Ralf Braun, Kai Dimmer, Mark Dürr, Hannes Herrmann, Ewald Hettema, Jussi Jääntti, Till Klecker, Daniel Klionsky, Johannes König, Chris Meisinger, Despina Mikropoulou, Alison Motley, Brigitte Neumann, Karin Nowikovsky, Doron Rapaport, Dirk Scholz, Chris Ungermann and Peter Walter for providing strains, plasmids or antibodies.
- ... the students Fabienne Benz, Xenia Chelius, Jana Deisel, Sarah Grosche, Markus Spindler, Maria Stenger and Madita Wolter for their great work, their contributions to some experiments and for teaching me how to tutor.
- ... Vera Bahle, Nadine Hock and Maria Stenger for helpful comments on the manuscript.
- ... Stefan Geimer, Rita Grotjahn and Ann-Katrin Unger for help with electron microscopy.
- ... Annette Suske for her support during lab routine.
- ... Petra Helies for providing absolutely clean flasks and tubes.
- ... the DFG for funding.
- ... my girlfriend Ines, my family and my friends for their continuous support.

Appendix

The *pet* library

Table 6. List of deletion strains contained in the *pet* library (Merz and Westermann, 2009), which has been screened for mitophagy defects.

Systematic name	Standard name	Systematic name	Standard name	Systematic name	Standard name
YAL044C	GCV3	YHR116W	COX23	YGR222W	PET54
YAL026C	DRS2	YCL007C		YGR243W	FMP43
YAL013W	DEP1	YLR204W	QRI1	YBL019W	APN2
YAL010C	MDM10	YLR226W	BUR2	YBL021C	HAP3
YAL009W	SPO7	YKL040C	NFU1	YBL031W	SHE1
YLL041C	SDH2	YKL054C	DEF1	YBL032W	HEK2
YLR055C	SPT8	YKL055C	OAR1	YBL036C	
YLR056W	ERG3	YKL080W	VMA5	YBL045C	COR1
YLR125W		YKL109W	HAP4	YBL046W	PSY4
YML087C		YKL119C	VPH2	YBL053W	
YMR188C	MRPS17	YKL148C	SDH1	YBL057C	PTH2
YOR036W	PEP12	YKL155C	RSM22	YBL062W	
YER070W	RNR1	YGR105W	VMA21	YBL080C	PET112
YOR332W	VMA4	YGR112W	SHY1	YBL082C	ALG3
YOR350C	MNE1	YOR135C	IRC14	YBL090W	MRP21
YOR358W	HAP5	YOR196C	LIP5	YGL066W	SGF73
YOR380W	RDR1	YOR200W		YGL070C	RBP9
YOL004W	SIN3	YOR221C	MCT1	YGL071W	AFT1
YOL008W	COQ10	YJL176C	SWI3	YNL185C	MRPL19
YOL051W	GAL11	YLR393W	ATP10	YNL184C	
YOL071W	EMI5	YLR403W	SFP1	YNL177C	MRPL22
YPL262W	FUM1	YDR148C	KGD2	YNL170W	
YPL254W	HFI1	YDR162C	NBP2	YNL159C	ASI2
YPL234C	TFP3	YDR195W	REF2	YKL208W	CBT1
YPL188W	POS5	YDR204W	COQ4	YKL212W	SAC1
YPL136W		YDR216W	ADR1	YKR001C	VPS1
YPL097W	MSY1	YDR237W	MRPL7	YKR006C	MRPL13
YDR065W		YOR305W		YDR264C	AKR1
YDR079W	PET100	YER061C	CEM1	YDR270W	CCC2
YDR116C	MRPL1	YLR260W	LCB5	YDR276C	PMP3
YDR129C	SAC6	YLR270W	DCS1	YDR296W	MHR1
YDR349C	YPS7	YLR294C		YDR298C	ATP5
YDR364C	CDC40	YLR295C	ATP14	YDR337W	MRPS28
YDR378C	LSM6	YLR304C	ACO1	YHR039C-B	VMA10
YDR392W	SPT3	YLR312W-A	MRPL15	YIR021W	MRS1
YEL003W	GIM4	YGL215W		YMR064W	AEP1
YEL007W		YGL237C	HAP2	YMR070W	MOT3
YEL024W	RIP1	YGL244W	RTF1	YMR072W	ABF2
YEL027W	CUP5	YGL251C	HFM1	YMR077C	VPS20
YEL050C	RML2	YGR020C	VMA7	YMR089C	YTA12
YEL051W	VMA8	YPL059W	GRX5	YOL095C	HMI1
YEL061C	CIN8	YPL045W	VPS16	YOL096C	COQ3
YER058W	PET117	YPL031C	PHO85	YHR168W	MTG2

Systematic name	Standard name	Systematic name	Standard name	Systematic name	Standard name
YER087W		YPL013C	MRPS16	YLR038C	COX12
YHR030C	SLT2	YPR116W		YMR158W	MRPS8
YHR038W	RRF1	YPR123C		YNL252C	MRPL17
YHR039C	MSC7	YPR134W	MSS18	YPL132W	COX11
YHR049C-A		YPR191W	QCR2	YML110C	COQ5
YHR060W	VMA22	YGR220C	MRPL9	YML120C	NDI1
YMR097C	MTG1	YBR026C	ETR1	YGL129C	RSM23
YMR098C		YBR044C	TCM62	YGL135W	RPL1B
YPR036W	VMA13	YNL005C	MRP7	YGL143C	MRF1
YPR066W	UBA3	YNL037C	IDH1	YGL165C	
YPR099C		YNR020C		YER114C	BOI2
YJL120W		YNR025C		YER131W	RPS26B
YJL121C	RPE1	YNR037C	RSM19	YER145C	FRT1
YJL063C	MRPL8	YNR041C	COQ2	YER154W	OXA1
YJL046W		YNR042W		YER155C	BEM2
YHR006W	STP2	YNR045W	PET494	YLR377C	FBP1
YHR009C		YNL081C	SWS2	YOL148C	SPT20
YHR026W	PPA1	YIL125W	KGD1	YER017C	AFG3
YHR067W	HTD2	YIL153W	RRD1	YER050C	RSM18
YHR194W	MDM31	YIL155C	GUT2	YAL039C	CYC3
YLL018C-A	COX19	YIL157C	FMP35	YML061C	PIF1
YLR447C	VMA6	YOR331C		YMR015C	ERG5
YML081C-A	ATP18	YOR150W	MRPL23	YMR021C	MAC1
YAL047C	SPC72	YOR187W	TUF1	YMR035W	IMP2
YAL054C	ACS1	YNL052W	COX5A	YMR151W	YIM2
YJR077C	MIR1	YNL071W	LAT1	YMR150C	IMP1
YJR113C	RSM7	YNL073W	MSK1	YMR193W	MRPL24
YJR120W		YKL194C	MST1	YMR228W	MTF1
YJR121W	ATP2	YBR289W	SNF5	YMR256C	COX7
YJR122W	CAF17	YCR028C-A	RIM1	YMR257C	PET111
YJR144W	MGM101	YCR046C	IMG1	YMR267W	PPA2
YDL192W	ARF1	YGR155W	CYS4	YMR282C	AEP2
YDR010C		YLR382C	NAM2	YMR286W	MRPL33
YDR025W	RPS11A	YPL148C	PPT2	YMR287C	DSS1
YBR282W	MRPL27	YNL315C	ATP11	YMR293C	
YBR283C	SSH1	YPL078C	ATP4	YHL038C	CBP2
YCL001W-A		YJL101C	GSH1	YHR011W	DIA4
YCR020W-B	HTL1	YKR085C	MRPL20	YPL271W	ATP15
YCR024C		YLR439W	MRPL4	YPL215W	CBP3
YCR071C	IMG2	YBR081C	SPT7	YJL209W	CBP1
YJL003W	COX16	YBR128C	ATG14	YJL180C	ATP12
YJR033C	RAV1	YBR146W	MRPS9	YLL027W	ISA1
YJR040W	GEF1	YDL012C		YLL033W	
YJR048W	CYC1	YDL032W		YLL042C	ATG10
YDL099W	BUG1	YDL033C	SLM3	YOR318C	
YDL107W	MSS2	YDL039C	PRM7	YOR330C	MIP1
YDL128W	VCX1	YDL044C	MTF2	YOR375C	GDH1
YDL114W		YDL045W-A	MRP10	YOL009C	MDM12
YDL129W		YDL056W	MBP1	YOL033W	MSE1
YDL133W		YDL067C	COX9	YOL083W	
YDL157C		YDL068W		YOR065W	CYT1
YDR269C		YDL077C	VMA6	YHR051W	COX6
YDR271C		YDL091C	UBX3	YHR091C	MSR1

Systematic name	Standard name	Systematic name	Standard name	Systematic name	Standard name
YGL017W	ATE1	YDR448W	ADA2	YHR120W	MSH1
YGL218W		YDR458C	HEH2	YPL173W	MRPL40
YBL099W	ATP1	YDR491C		YPL172C	COX10
YBL100C		YDR523C	SPS1	YPL104W	MSD1
YBR003W	COQ1	YDR529C	QCR7	YOR127W	RGA1
YOR155C	ISN1	YNL213C			
YOR158W	PET123	YML095C-A		YDR375C	BCS1
YOR241W	MET7	YJL127C	SPT10	YGR062C	COX18
YOR211C	MGM1	YJL124C	LSM1	YGR076C	MRPL25
YLR067C	PET309	YJL102W	MEF2	YGR102C	
YLR069C	MEF1	YJL096W	MRPL49	YGR150C	
YLR070C	XYL2	YAL016W	TPD3	YGR167W	CLC1
YLR091W		YGL218W		YGR171C	MSM1
YHR147C	MRPL6	YBR039W	ATP3	YGR174C	CBP4
YBR179C	FZO1	YJL184W	GON7	YGR180C	RNR4
YBR251W	MRPS5	YNL138W	SRV2	YGR215W	RSM27
YBR268W	MRPL37	YPR067W	ISA2	YKL003C	MRP17
YCL010C	SGF29	YBR097W	VPS15	YKL016C	ATP7
YCR003W	MRPL32	YGL206C	CHC1	YKL114C	APN1
YDR175C	RSM24	YGL240W	DOC1	YKL134C	OCT1
YDR194C	MSS116	YGR262C	BUD32	YKL138C	MRPL31
YDR197W	CBS2	YBL093C	ROX3	YKL169C	
YDR230W		YER014C-A	BUD25	YKL170W	MRPL38
YDR114C		YLR239C	LIP2	YMR231W	PEP5
YDR115W		YLR337C	VRP1	YLL006W	MMM1
YLR139C	SLS1	YLR369W	SSQ1	YLR148W	PEP3
YLR144C	ACF2	YFL016C	MDJ1	YKL002W	DID4
YLR201C	COQ9	YDR079C-A	TFB5	YKL087C	CYT2
YLR202C		YDR379C-A		YDR377W	ATP17
YLR203C	MSS51	YEL059C-A	SOM1	YLR240W	VPS34
YDR347W	MRP1	YHR050W-A		YNL243W	SLA2
YDR350C	ATP22				

Genetic interactors of *myo2(LQ)*

Table 7. List of deletion strains that genetically interacted with *myo2(LQ)* in two independent replicates of an SGA screen. Strains appear in alphabetical order according to their systematic name.

Negative interactors		Positive interactors	
Systematic name	Standard name	Systematic name	Standard name
YAL048C	GEM1	YBL087C	RPL23A
YBL007C	SLA1	YBL090W	MRP21
YBR179C	FZO1	YBR098W	MMS4
YBR200W	BEM1	YBR284W	YBR284W
YBR246W	RRT2	YBR298C	MAL31
YCL010C	SGF29	YCL009C	ILV6
YCR028C	FEN2	YCL062W	YCL062W
YDL006W	PTC1	YCR076C	FUB1
YDL134C	PPH21	YCR090C	YCR090C
YDR050C	TPI1	YDL129W	YDL129W
YDR136C	YDR136C	YDL182W	LYS20
YDR150W	NUM1	YDL190C	UFD2
YDR162C	NBP2	YDL203C	ACK1
YDR435C	PPM1	YDR011W	SNQ2
YDR470C	UGO1	YDR014W	RAD61
YDR477W	SNF1	YDR015C	YDR015C
YEL036C	ANP1	YDR022C	ATG31
YER068W	MOT2	YDR042C	YDR042C
YGL058W	RAD6	YDR079C-A	TFB5
YGL070C	RPB9	YDR183W	PLP1
YGL119W	COQ8	YDR251W	PAM1
YGL168W	HUR1	YDR306C	YDR306C
YGL211W	NCS6	YDR382W	RPP2B
YGL214W	YGL214W	YDR391C	YDR391C
YGL218W	YGL218W	YDR448W	ADA2
YGR036C	CAX4	YEL067C	YEL067C
YGR078C	PAC10	YFL010W-A	AUA1
YGR089W	NNF2	YFL020C	PAU5
YGR101W	PCP1	YFR038W	IRC5
YGR180C	RNR4	YGL032C	AGA2
YHR129C	ARP1	YGL066W	SGF73
YHR183W	GND1	YGL081W	YGL081W
YHR187W	IKI1	YGL199C	YGL199C
YIL040W	APQ12	YGL208W	SIP2
YIL128W	MET18	YGL226W	MTC3
YIR023W	DAL81	YGR042W	YGR042W
YJL056C	ZAP1	YGR125W	YGR125W
YJL063C	MRPL8	YGR126W	YGR126W
YJL179W	PFD1	YGR244C	LSC2
YJL204C	RCY1	YHL004W	MRP4

Negative interactors		Positive interactors	
Systematic name	Standard name	Systematic name	Standard name
YJL206C	YJL206C	YIL041W	GVP36
YKL002W	DID4	YIR017C	MET28
YKL048C	ELM1	YIR028W	DAL4
YKL136W	YKL136W	YJL012C	VTC4
YKL201C	MNN4	YJL100W	LSB6
YKL213C	DOA1	YJL136W-A	YJL136W-A
YKR004C-A	YKR004C-A	YJL146W	IDS2
YKR054C	DYN1	YJL159W	HSP150
YLL006W	MMM1	YJL215C	YJL215C
YLL040C	VPS13	YJR048W	CYC1
YLL049W	LDB18	YJR053W	BFA1
YLR014C	PPR1	YJR087W	YJR087W
YLR024C	UBR2	YJR091C	JSN1
YLR055C	SPT8	YJR094W-A	RPL43B
YLR182W	SWI6	YJR096W	YJR096W
YLR240W	VPS34	YJR097W	JJJ3
YLR319C	BUD6	YJR135W-A	TIM8
YLR320W	MMS22	YJR151W-A	YJR151W-A
YLR337C	VRP1	YKL065C	YET1
YLR357W	RSC2	YKL093W	MBR1
YLR373C	VID22	YKL106C-A	YKL106C-A
YLR418C	CDC73	YKL137W	CMC1
YML013C-A	YML013C-A	YKL205W	LOS1
YML032C	RAD52	YKR035C	YKR035C
YML112W	CTK3	YLR035C	MLH2
YMR024W	MRPL3	YLR118C	YLR118C
YMR072W	ABF2	YLR125W	YLR125W
YMR116C	ASC1	YLR152C	YLR152C
YMR202W	ERG2	YLR248W	RCK2
YMR294W	JNM1	YLR312C-B	YLR312C-B
YNL025C	SSN8	YLR342W-A	YLR342W-A
YNL170W	YNL170W	YLR435W	TSR2
YNL233W	BNI4	YMR143W	RPS16A
YNL250W	RAD50	YMR269W	TMA23
YNL298W	CLA4	YMR307W	GAS1
YNL304W	YPT11	YNL069C	RPL16B
YNR010W	CSE2	YNL173C	MDG1
YOL081W	IRA2	YNR045W	PET494
YOR035C	SHE4	YNR052C	POP2
YOR039W	CKB2	YNR057C	BIO4
YOR058C	ASE1	YOL012C	HTZ1
YOR106W	VAM3	YOL013C	HRD1
YOR139C	YOR139C	YOL024W	YOL024W
YOR231W	MKK1	YOL027C	MDM38

Negative interactors		Positive interactors	
Systematic name	Standard name	Systematic name	Standard name
<i>YOR246C</i>	<i>ENV9</i>	<i>YOL037C</i>	<i>YOL037C</i>
<i>YOR269W</i>	<i>PAC1</i>	<i>YOL045W</i>	<i>PSK2</i>
<i>YOR299W</i>	<i>BUD7</i>	<i>YOL046C</i>	<i>YOL046C</i>
<i>YOR311C</i>	<i>DGK1</i>	<i>YOL048C</i>	<i>RRT8</i>
<i>YPL002C</i>	<i>SNF8</i>	<i>YOL067C</i>	<i>RTG1</i>
<i>YPL023C</i>	<i>MET12</i>	<i>YOL072W</i>	<i>THP1</i>
<i>YPL057C</i>	<i>SUR1</i>	<i>YOL092W</i>	<i>YPQ1</i>
<i>YPL155C</i>	<i>KIP2</i>	<i>YOR006C</i>	<i>TSR3</i>
<i>YPL174C</i>	<i>NIP100</i>	<i>YOR044W</i>	<i>IRC23</i>
<i>YPL264C</i>	<i>YPL264C</i>	<i>YOR061W</i>	<i>CKA2</i>
		<i>YOR078W</i>	<i>BUD21</i>
		<i>YOR108W</i>	<i>LEU9</i>
		<i>YOR111W</i>	<i>YOR111W</i>
		<i>YOR195W</i>	<i>SLK19</i>
		<i>YOR242C</i>	<i>SSP2</i>
		<i>YOR330C</i>	<i>MIP1</i>
		<i>YOR364W</i>	<i>YOR364W</i>
		<i>YPL022W</i>	<i>RAD1</i>
		<i>YPL139C</i>	<i>UME1</i>
		<i>YPL158C</i>	<i>AIM44</i>
		<i>YPL227C</i>	<i>ALG5</i>
		<i>YPL272C</i>	<i>PBI1</i>

List of publications

Scholz, D., Förtsch, J., Böckler, S., Klecker, T., and Westermann, B.[#] (2013). Analyzing membrane dynamics with live cell fluorescence microscopy with a focus on yeast mitochondria. *Methods Mol Biol* 1033, 275-283. doi: 10.1007/978-1-62703-487-6_17

Böckler, S., and Westermann, B.[#] (2014). Mitochondrial ER contacts are crucial for mitophagy in yeast. *Dev Cell* 28, 450-458. doi: 10.1016/j.devcel.2014.01.012

Klecker, T.^{*}, Böckler, S.^{*}, and Westermann, B.[#] (2014). Making connections: interorganelle contacts orchestrate mitochondrial behavior. *Trends Cell Biol* 24, 537-545. doi: 10.1016/j.tcb.2014.04.004

Böckler, S.[#], and Westermann, B. (2014). ER-mitochondria contacts as sites of mitophagosome formation. *Autophagy* 10, 1346-1347. doi: 10.4161/auto.28981

Ackema, K.B., Hench, J., Böckler, S., Wang, S.C., Sauder, U., Mergentaler, H., Westermann, B., Bard, F., Frank, S., and Spang, A.[#] (2014). The small GTPase Arf1 modulates mitochondrial morphology and function. *EMBO J* 33, 2659-75. doi: 10.15252/embj.201489039

* Equally contributing authors

Corresponding author

DVD

The print-version of this thesis contains an additional DVD. The enclosed DVD is divided into the directories:

.../Mitophagy Screen	contains Table S1
.../myo2(LQ) SGA scores	contains Table S2
.../Thesis	contains a PDF document of this thesis and of the summary in English and German

Table S1. List of strains screened for mitophagy positive cells with corresponding mitophagy rates. Strains were ordered according to their mitophagy rate. Values represent the mean of at least two independent experiments, in which at least 100 cells were scored for red vacuolar fluorescence. Figure 8A is based on these data.

Table S2. List of genetic interaction scores derived from two independent replicates of an SGA screen with *myo2(LQ)* as a query strain. Strains were ordered according to their genetic interaction score. Data were acquired as described in the Materials and Methods section ('Synthetic genetic array' and 'SGA data acquisition'). Figure 23C and D are based on these data.

Erklärung

Hiermit erkläre ich eidesstattlich, dass ich die vorliegende Dissertation selbstständig verfasst und keine anderen als die von mir angegebenen Quellen und Hilfsmittel verwendet habe.

Ich habe die Dissertation nicht bereits zur Erlangung eines akademischen Grades anderweitig eingereicht und habe auch nicht bereits diese oder eine gleichartige Doktorprüfung endgültig nicht bestanden.

Die Hilfe von gewerblichen Promotionsberatern bzw. –vermittlern wurde bisher nicht und wird auch künftig nicht von mir in Anspruch genommen.

Ich erkläre mich damit einverstanden, dass die elektronische Fassung meiner Dissertation unter Wahrung meiner Urheberrechte und des Datenschutzes einer gesonderten Überprüfung hinsichtlich der eigenständigen Anfertigung der Dissertation unterzogen werden kann.

Bayreuth, den 5. Juli 2015

Stefan Böckler